

AD 747806

AD

**USAAMRDL TECHNICAL REPORT 72-44**  
**FAN-IN-FIN ANTITORQUE CONCEPT STUDY**

By  
J. K. Davidson  
C. T. Havey  
H. E. Sherrieb

July 1972

**EUSTIS DIRECTORATE**  
**U. S. ARMY AIR MOBILITY RESEARCH AND DEVELOPMENT LABORATORY**  
**FORT EUSTIS, VIRGINIA**

**CONTRACT DAAJ02-71-C-0060**  
**VOUGHT HELICOPTER INCORPORATED**  
**A SUBSIDIARY OF LTV AEROSPACE CORPORATION**  
**DALLAS, TEXAS**

Approved for public release;  
distribution unlimited.



Reproduced by  
**NATIONAL TECHNICAL  
INFORMATION SERVICE**  
U.S. Department of Commerce  
Springfield VA 22151

**DDC**  
**RECEIVED**  
SEP 5 1972  
**REGISTRY**

B  
115

DISCLAIMERS

The findings in this report are not to be construed as an official Department of the Army position unless so designated by other authorized documents.

When Government drawings, specifications, or other data are used for any purpose other than in connection with a definitely related Government procurement operation, the U. S. Government thereby incurs no responsibility nor any obligation whatsoever; and the fact that the Government may have formulated, furnished, or in any way supplied the said drawings, specifications, or other data is not to be regarded by implication or otherwise as in any manner licensing the holder or any other person or corporation, or conveying any rights or permission, to manufacture, use, or sell any patented invention that may in any way be related thereto.

Trade names cited in this report do not constitute an official endorsement or approval of the use of such commercial hardware or software.

DISPOSITION INSTRUCTIONS

Destroy this report when no longer needed. Do not return it to the originator.

CLASSIFICATION	
US	Conf. Section <input checked="" type="checkbox"/>
?	Ext. Section <input type="checkbox"/>
INT. CONTROL	<input type="checkbox"/>
DISTRIBUTION	
BY	
DISTRIBUTION/AVAILABILITY CODES	
Dist.	AvAIL. and/or SPECIAL
A	

Unclassified

Security Classification

DOCUMENT CONTROL DATA - R & D		
<i>(Security classification of title, body of abstract and indexing annotation must be entered when the overall report is classified)</i>		
1. ORIGINATING ACTIVITY (Corporate author) Vought Helicopter Incorporated A Subsidiary of LTV Aerospace Corporation Dallas, Texas		2a. REPORT SECURITY CLASSIFICATION Unclassified
		2b. GROUP
3. REPORT TITLE FAN-IN-FIN ANTITORQUE CONCEPT STUDY		
4. DESCRIPTIVE NOTES (Type of report and inclusive dates) Final Report		
5. AUTHOR(S) (First name, middle initial, last name) J. K. Davidson C. T. Havey H. E. Sherrieb		
6. REPORT DATE July 1972	7a. TOTAL NO. OF PAGES 107	7b. NO. OF REFS 17
8a. CONTRACT OR GRANT NO. DAAJ02-71-C-0060	9a. ORIGINATOR'S REPORT NUMBER(S) USAA MRDL Technical Report 72-44	
b. PROJECT NO. Task 1F162204AA4201	9b. OTHER REPORT NO(S) (Any other numbers that may be assigned this report) VHI Engineering Report VHI/72R-E-6	
c.		
d.		
10. DISTRIBUTION STATEMENT Approved for public release; distribution unlimited.		
11. SUPPLEMENTARY NOTES	12. SPONSORING MILITARY ACTIVITY Eustis Directorate U. S. Army Air Mobility R&D Laboratory Fort Eustis, Virginia	
13. ABSTRACT <p>A study of the development of the Fenestron fan-in-fin helicopter antitorque device and a survey of applicable data from the literature provided the means to analyze the fan-in-fin concept. The objective was to design and evaluate a ducted fan-in-fin system for a helicopter in the 14,000- to 15,000-lb gross weight and 150-kt to 160-kt speed class.</p> <p>A review and study of fan-in-wing literature and shrouded propeller and fan technology provided the foundation to analyze the Fenestron and to determine the basic fan and fin characteristics. A direct performance comparison of an SA 341 helicopter with Fenestron and conventional antitorque systems was conducted to assess the advantages and penalties of the Fenestron.</p> <p>From the knowledge gained, a ducted fan-in-fin antitorque device was designed for the utility transport helicopter in the specified weight and speed class of the SA 330. A parametric analysis of the fan design parameters showed the performance gains achievable with larger diameter fans. The MIL-H-8501A requirements were considered. A fin design was accomplished taking into account area, lift coefficient, lift curve slope, and effective aspect ratio. A trim flap was found to be desirable to optimize performance at off-design conditions.</p> <p>A preliminary design and layout of the resulting fan-in-fin was carried out. The preliminary design included a structural analysis and a fan blade design. A weight comparison between the actual conventional tail rotor system in the SA 330 and the proposed fan-in-fin system showed no appreciable weight penalty. Performance comparisons between the fan-in-fin and tail rotor showed equal or better performance for the fan-in-fin in both hover and forward flight. An acoustical comparison showed the fan-in-fin with higher noise levels except along the longitudinal axis of the helicopter. The fan-in-fin design showed improved maintainability and reliability over a conventional tail rotor.</p>		

DD FORM 1473 1 NOV 65 REPLACES DD FORM 1473, 1 JAN 64, WHICH IS OBSOLETE FOR ARMY USE.

Unclassified

Security Classification

ia





**DEPARTMENT OF THE ARMY  
U. S. ARMY AIR MOBILITY RESEARCH & DEVELOPMENT LABORATORY  
EUSTIS DIRECTORATE  
FORT EUSTIS, VIRGINIA 23604**

This report has been reviewed by the Eustis Directorate, U. S. Army Air Mobility Research and Development Laboratory and is considered to be technically sound. This program was initiated to evaluate the application of the Fenestron type ducted fan as the antitorque device to helicopters in the 150-knot, 14,000- to 15,000-pound gross weight category. The results of this program are based on the initial flight and wind tunnel test data of the Aerospatiale Fenestron development effort.

The program was conducted under the technical management of Patrick A. Cancro of the Aeromechanics Division of this Directorate.

10

Task 1F162204AA4201  
Contract DAAJ02-71-C-0060  
USAAMRDL Technical Report 72-44  
July 1972

FAN-IN-FIN ANTITORQUE CONCEPT STUDY

Final Report

VHI Engineering Report VHI/72R-E-6

By

J. K. Davidson  
C. T. Havey  
H. E. Sherrieb

Prepared by

Vought Helicopter Incorporated  
A Subsidiary of LTV Aerospace Corporation  
Dallas, Texas

for

EUSTIS DIRECTORATE  
U. S. ARMY AIR MOBILITY  
RESEARCH AND DEVELOPMENT LABORATORY  
FORT EUSTIS, VIRGINIA

Approved for public release;  
distribution unlimited.

11

## SUMMARY

A study of the development of the Fenestron fan-in-fin helicopter antitorque device and a survey of applicable data from the literature provided the means to analyze the fan-in-fin concept. The objective was to design and evaluate a ducted fan-in-fin system for a helicopter in the 14,000-lb to 15,000-lb gross weight and 150-kt to 160-kt speed class.

A review and study of fan-in-wing literature and shrouded propeller and fan technology provided the foundation to analyze the Fenestron and to determine the basic fan and fin characteristics. A direct performance comparison of an SA 341 helicopter with Fenestron and conventional antitorque systems was conducted to assess the advantages and penalties of the Fenestron.

From the knowledge gained, a ducted fan-in-fin antitorque device was designed for the utility transport helicopter in the specified weight and speed class of the SA 330. A parametric analysis of the fan design parameters showed the performance gains achievable with larger diameter fans. The MIL-H-8501A requirements were considered. A fin design was accomplished taking into account area, lift coefficient, lift curve slope, and effective aspect ratio. A trim flap was found to be desirable to optimize performance at off-design conditions.

A preliminary design and layout of the resulting fan-in-fin was carried out. The preliminary design included a structural analysis and a fan blade design. A weight comparison between the actual conventional tail rotor system in the SA 330 and the proposed fan-in-fin system showed no appreciable weight penalty. Performance comparisons between the fan-in-fin and tail rotor showed equal or better performance for the fan-in-fin in both hover and forward flight. An acoustical comparison showed the fan-in-fin with higher noise levels except along the longitudinal axis of the helicopter. The fan-in-fin design showed improved maintainability and reliability over a conventional tail rotor.

## FOREWORD

This report was prepared for the Eustic Directorate, U. S. Army Air Mobility Research and Development Laboratory, Fort Eustis, Virginia, by Vought Helicopter Incorporated, a Subsidiary of LTV Aerospace Corporation, under Contract DAAJ02-71-C-0060 (Task 1F162204AA4201). The work was performed between June 1971 and March 1972.

Aerospatiale of Marignane, France, provided the Fenestron data upon which portions of this study were based. Major technical contributions were made by the following Vought Helicopter employees:

Mr. V. H. Brogdon - Structural Analyst  
Mr. F. B. Johnson - Configuration Design

✓

**Preceding page blank**

TABLE OF CONTENTS

	<u>Page</u>
SUMMARY . . . . .	iii
FOREWORD . . . . .	v
LIST OF ILLUSTRATIONS . . . . .	x
LIST OF TABLES . . . . .	xiv
LIST OF SYMBOLS . . . . .	xv
INTRODUCTION . . . . .	i
REVIEW AND ANALYSIS OF EXISTING DATA . . . . .	3
LITERATURE SEARCH . . . . .	3
Inlet Radius Effects on Fan Performance . . . . .	3
Duct Length Effects on Fan Performance . . . . .	3
Blade Twist Effects on Fan Performance . . . . .	4
Hub-Tip Radius Ratio Effects on Fan Performance . . . . .	6
Fin Characteristics . . . . .	7
Fan-Induced Effects . . . . .	7
ANALYSIS OF THE FENESTRON . . . . .	7
Wind Tunnel Tests . . . . .	9
Static Tests . . . . .	17
Flight Tests . . . . .	17
SA 341 Description . . . . .	18
Hover . . . . .	20
Comparison of the Fenestron Figure of Merit to the State of the Art . . . . .	20
Forward Flight . . . . .	23
Directional Stability and Control . . . . .	30
Weight . . . . .	31
Fenestron Acoustical Comparison Study . . . . .	31
PRELIMINARY DESIGN . . . . .	35
PRELIMINARY DESIGN OBJECTIVE . . . . .	35

**Preceding page blank**

	<u>Page</u>
BASE-LINE AIRCRAFT . . . . .	35
PARAMETRIC ANALYSIS OF FAN DESIGN PARAMETERS . . . . .	39
Fan Thrust Vs. Horsepower and Disc Loading . . . . .	40
Antitorque System Thrust Requirements in Hover . . . . .	41
Fan Diameter Sensitivity in Hover . . . . .	43
Fan Design Selection . . . . .	46
FIN DESIGN . . . . .	48
Philosophy . . . . .	48
Design Requirements . . . . .	49
Area . . . . .	50
Lift Coefficient . . . . .	52
Lift Curve Slope . . . . .	52
Camber and Incidence . . . . .	53
Aspect Ratio . . . . .	53
Horizontal Stabilizer . . . . .	53
POINT DESIGN DESCRIPTION . . . . .	53
Structural Description . . . . .	57
Fan Blade Design . . . . .	58
Fan Gearbox and Power Shaft Extension . . . . .	61
WEIGHT COMPARISON . . . . .	61
SENSITIVITY STUDIES . . . . .	64
Fan Diameter . . . . .	64
Fin Area . . . . .	64
Fin Lift Coefficient . . . . .	64
PERFORMANCE COMPARISONS . . . . .	66
Hover . . . . .	66
Forward Flight . . . . .	66
Mission Performance . . . . .	68
MAINTAINABILITY AND RELIABILITY - FAN-IN-FIN VS. TAIL ROTOR . . . . .	72

	<u>Page</u>
ACOUSTICAL COMPARISON . . . . .	74
CONCLUSIONS . . . . .	75
LITERATURE CITED . . . . .	77
APPENDIXES . . . . .	79
I.    BIBLIOGRAPHY OF LITERATURE ON FAN-IN-FIN RELATED WORK . . . . .	79
II.   PERFORMANCE PREDICTION METHODS . . . . .	84
III.  EXCERPTS FROM AEROSPATIALE NOISE TESTS . . . . .	88
DISTRIBUTION . . . . .	94

LIST OF ILLUSTRATIONS

<u>Figure</u>		<u>Page</u>
1	Inlet Lip Radius Effects on Ducted Propeller Performance . . . . .	4
2	Effect of Duct Length on Ducted Propeller Performance . . . . .	5
3	Approach Velocity Profiles From Reference 5 . . . .	5
4	Modified Twist Effects on Ducted Propeller Performance, Reference 5 . . . . .	6
5	Comparison of Lift Curve Slope From Fan-in-Wing Wind Tunnel Tests and Theory . . . .	8
6	Fenestron Wind Tunnel Model . . . . .	9
7	Side-Force Coefficient Vs. Advance Ratio, Fenestron Wind Tunnel Tests . . . . .	11
8	Side-Force Coefficient Vs. Blade Pitch Angle, Fenestron Wind Tunnel Tests . . . . .	12
9	Power Ratio Vs. Advance Ratio, Fenestron Wind Tunnel Tests . . . . .	13
10	Drag Coefficient Vs. Advance Ratio, Fenestron Wind Tunnel Tests . . . . .	14
11	Fan-Induced Drag, Fenestron Wind Tunnel Tests . . .	15
12	Lift Curve Slope Vs. Advance Ratio, Fenestron Wind Tunnel Tests . . . . .	16
13	Comparison of Lift Curve Slope From Fenestron and Fan-in-Wing Wind Tunnel Tests . . . . .	16
14	Center of Thrust Shift With Advance Ratio, Fenestron Wind Tunnel Tests . . . . .	17
15	SA 341 Gazelle Light Multipurpose Helicopter . . . .	19

LIST OF ILLUSTRATIONS (Continued)

<u>Figure</u>		<u>Page</u>
16	SA 341 With Conventional Tail Rotor . . . . .	21
17	Antitorque Power Comparison in Hover, SL STD . . . . .	22
18	Comparison of the Fenestron to State-of-the-Art Figure of Merit . . . . .	24
19	Comparison of Predicted Power Required and Flight Test Data in Forward Flight, SL STD, SA 341 . . . . .	25
20	Antitorque Power Comparison in Forward Flight, SL STD, GW=3750 Lb . . . . .	25
21	Comparison of Total Power Required for Tail Rotor and Fenestron Systems, SL STD, SA 341, GW= 3750 Lb . . . . .	26
22	SA 341 Antitorque Thrust Requirement in Forward Flight and the Fan Thrust Required for Various Fin Areas, $C_L = \text{Const}$ , SL STD, GW=3750 Lb . . . . .	27
23	SA 341 Fin Thrust Vs. Speed, Showing the Effect of Varying Fin Area . . . . .	29
24	SA 341 Fin Lift Coefficient Vs. Speed From Flight Tests, SL STD, GW=3750 Lb . . . . .	30
25	Fenestron Blade Pitch Required for Hover, SA 341 . . . . .	31
26	Fenestron Blade Pitch in Forward Flight, Climb, and Autorotation, SA 341, GW=3530 Lb . . . . .	32
27	SA 330 Engine Power Available . . . . .	38
28	SA 330 Puma, Utility Tactical Transport . . . . .	37
29	Comparison of Predicted Hover Power Required With Flight Test Data, SA 330 . . . . .	39

LIST OF ILLUSTRATIONS (Continued)

<u>Figure</u>		<u>Page</u>
30	Comparison of Predicted Power Required in Forward Flight With Flight Test Data, SL STD, SA 330 . . . . .	40
31	Comparison of Predicted Power Required in Forward Flight With Flight Test Data, 4000 Ft, 95°F, SA 330 . . . . .	41
32	Parametric Ducted Propeller Referred Static Performance for Blades With 0.3 Design Lift Coefficient, a Hub-Tip Radius Ratio of 0.3 and a Duct Length-to-Diameter Ratio of 0.2. (Referred - Adjusted to SL STD Conditions) . . . . .	42
33	Parametric Ducted Propeller Referred Performance at a 35-Kt Crosswind for Blades With 0.3 Design Lift Coefficient, a Hub-Tip Radius Ratio of 0.3 and a Duct Length-to-Diameter Ratio of 0.2. (Referred - Adjusted to SL STD Conditions) . . . . .	43
34	Comparison of Antitorque Power Required in Hover for Various Fan Diameters, SL STD . . . . .	46
35	Fan Diameter Required To Hover OGE at 4000 Ft, 95°F Vs. Takeoff Gross Weight . . . . .	47
36	Influence of Fan Diameter on OGE Hover Ceilings . . . . .	48
37	SA 330 Fan-in-Fin Estimated Hover Yaw Response Following Full Control Input . . . . .	49
38	Modified SA 330 Antitorque Thrust Required in Forward Flight With Fan and Fin Contributions, SL STD, GW=13,230 Lb . . . . .	51
39	Predicted Fin Lift Characteristics With Speed for the SA 330 Fan-in-Fin Antitorque System, SL STD, GW=13,230 Lb . . . . .	52
40	SA 330 With Fan-in-Fin . . . . .	55
41	SA 330 Fan-in-Fin Design Layout . . . . .	59
42	Maximum Velocity Sensitivity With Fin Area . . . . .	65

LIST OF ILLUSTRATIONS (Continued)

<u>Figure</u>		<u>Page</u>
43	Required Fan Thrust Vs. Speed for Various Fin Lift Coefficients . . . . .	65
44	Maximum Velocity Sensitivity With Fin Lift Coefficient . . . . .	66
45	Comparison of Fan-in-Fin and Tail Rotor Antitorque Power Required in Forward Flight, SL STD, SA 330 . . . . .	67
46	Comparison of Total Power Required for Fan-in-Fin and Tail Rotor Systems . . . . .	68
47	Maximum Speed Comparison for Fan-in-Fin and Tail Rotor Systems . . . . .	69
48	SA 330 Specific Range With Tail Rotor . . . . .	70
49	SA 330 Specific Range With Fan-in-Fin . . . . .	71
50	Best Range Speed Comparison for Fan-in-Fin and Tail Rotor Systems . . . . .	72
51	Comparison of Fan-in-Fin and Tail Rotor Payload-Range Performance . . . . .	73
52	Location of Instrumentation; SA 341-02 (Gazelle). . . . .	89
53	Location of Instrumentation; SA 3180-03 (Alouette II)	90
54	Directional Effects of the SA 341-02 Fenestron at 25M	91
55	Directional Effects of the SA 3180-03 Two-Bladed Rotor at 25M With an Average Frequency of 63 Hz . . . . .	92
56	Comparison of Perceived Noise Levels Between the SA 341-02 (Gazelle)Fenestron and the SA 3180-03 (Alouette II) Two-Bladed Conventional Tail Rotor . . . . .	93

LIST OF TABLES

<u>Table</u>		<u>Page</u>
I	SA 341 Main Rotor and Fenestron Rotor Characteristics . . . . .	18
II	Comparison of SA 341 Antitorque Device Rotor Characteristics . . . . .	22
III	Comparison of SA 341 Antitorque Device Weights . . . . .	33
IV	Fenestron Noise Level Comparison . . . . .	34
V	Fenestron Noise Directivity Comparison . . . . .	34
VI	SA 330 Main Rotor and Tail Rotor Characteristics . . . . .	35
VII	SA 330 Hover Antitorque System Thrust Requirements, SL STD, Forward CG . . . . .	44
VIII	Minimum Required Fan Diameters, SL STD . . . . .	45
IX	Summary of Fan-in-Fin Design Parameters' . . . . .	54
X	Fan Blade Design Parameters . . . . .	58
XI	Blade Station Design Data . . . . .	62
XII	SA 330 Antitorque System Weight Comparison . . . . .	63
XIII	SA 330 Fan-in-Fin Acoustical Comparison . . . . .	74

## LIST OF SYMBOLS

A	area of fan or rotor, sq ft
AR	aspect ratio
b	span of vertical fin, ft
c	chord of fan blade, ft
$C_L$	lift coefficient of fin: $F_y/(1/2)\rho V^2 S$
$C_{L\alpha}$	lift curve slope, per degree
$C_x$	drag coefficient of fin $F_x/(1/2)\rho V^2 A$
$C_y$	side force coefficient: $F_y/(1/2)\rho V^2 A$
$C_{y\beta}$	side force curve slope - equivalent to fin $C_L$ diameter of fan or rotor, ft
D	fan or propeller diameter, ft
Figure of Merit	$(T/1100P)\sqrt{T/\rho A}$
$F_x$	drag of fin
$F_y$	side force, lb
$f_y$	side force coefficient referenced to tip speed: $F_y/(1/2)\rho U^2 A$
L	duct length, ft
$M_n$	torque coefficient: $P/(1/2) AU^3$
n	rotational speed, rps
P	power, hp
q	dynamic pressure, psf
R	radius, ft
r	inlet lip radius, ft

S	fin or wing planform area, ft <sup>2</sup>
T	thrust, lb
U	tip speed, fps
V	freestream velocity, fps
W	weight, lb
X <sub>cp</sub>	center of thrust location, percent fin chord
w <sub>f</sub>	fuel flow, lb/hr
$\beta$	sideslip angle, deg
$\mu$	advance ratio: U/V
$\theta$	blade pitch angle, deg
$\rho$	density at ambient, slugs/ft <sup>3</sup>
$\rho_o$	density at SL STD, slugs/ft <sup>3</sup>
$\sigma$	solidity: fan blade area/fan disc area, density ratio: $\rho/\rho_o$

Sub-subscripts

$\mu$	at forward velocity
O	at static conditions
$\alpha$	at angle of attack
$\beta$	at sideslip angle

## INTRODUCTION

The fan-in-fin antitorque device has been shown to offer improvements over the conventional tail rotor on single main rotor helicopters. Studies in References 1 and 2 selected this concept as giving improvements in the areas of high-speed dynamics, vulnerability to damage, safety, and noise. Uncertainties in the estimation of performance and handling qualities remained. It is the objective of this report to further study the application of the fan-in-fin concept for future Army aircraft using information gained from a literature survey and an analysis of wind tunnel and flight test data from the development of the Fenestron ducted fan antitorque system.

The problem of matching a fan designed for hover with a fin designed for a high-speed condition is complex. Weight and power requirements must be minimized without undue performance penalties. To reduce power required in hover, a larger diameter fan is desired. To alleviate the penalties of fan-induced effects, such as fan-induced drag, it is desirable to unload the fan in forward flight.

Tail aspect ratio, lift curve slope, and end-plate effects taking into account a fan thrusting within a duct through the fin must be estimated for the resulting fin-fan combination. Fin characteristics and directional stability can then be determined. Fan and duct performance must be evaluated for a condition where the duct and fan axis is normal to the free stream flow as well as for static conditions. Fan thrust and power can then be obtained. Fan-induced lift and drag are also important in determining the overall performance of the system.

The Fenestron developed by Aerospatiale demonstrated the fan-in-fin antitorque system for the SA 341, a light, high-speed helicopter currently in production. A review and study of fan-in-wing literature and ducted propeller and fan technology provided the foundation to analyze the data from the Fenestron development and to determine the basic fan and fin characteristics.

The results of this evaluation were applied to a preliminary design of a Fenestron-type antitorque system for a helicopter in the 150-kt, 14,000- to 15,000-lb category. Specifically, a fan-in-fin was sized to take the place of the conventional tail rotor on the SA 330 Puma, a tactical transport having a maximum gross weight of 14,110 lb. Design studies and performance comparisons were carried out to obtain the most favorable combination of fan and fin characteristics. Compliance with MIL-H-8501A control requirements was an objective.

The predicted performance of the ducted fan aircraft was generated and compared to the conventional SA 330. In addition, system weight, noise, and control complexity were studied. Thus, through a realistic application of fan-in-fin technology, the potential of this antitorque device is assessed for future advanced aircraft.

## REVIEW AND ANALYSIS OF EXISTING DATA

### LITERATURE SEARCH

A literature search was conducted to survey existing data that would pertain to the ducted fan antitorque concept. Ducted propeller (fan) data and fan-in-wing results were determined to be most applicable. A bibliography of the references reviewed is given in Appendix I.

#### Inlet Radius Effects on Fan Performance

Inlet radius effects on jet engine static performance are generally well known, in that a small inlet radius usually causes separation of the flow from the inlet surface. The resulting effect is a reduction in pressure recovery and a loss in performance. With a jet engine installation, the first stage of rotating machinery is usually at least three-fourths of a diameter downstream from the inlet lip, which allows the flow to re-attach to the inlet wall. This then reduces the effect of flow separation mainly to the loss in total pressure recovery.

In a ducted fan, the proximity of the rotating component is usually immediately downstream from the inlet radius. Therefore, the separated flow associated with a small inlet radius is felt by the rotating component, which affects its performance and may affect its structural integrity.

During this literature search, References 3 and 4 presented data relating the effect of inlet lip radius on figure of merit. Figure 1 presents these data. The trend indicated by Reference 3 on this figure is that performance deteriorates at a significant rate below a lip radius-to-diameter ratio of 0.05 to 0.06. Reference 4 gives no zero radius-to-diameter ratio data, however, it is reasonable to assume the trend would be similar.

#### Duct Length Effects on Fan Performance

The basic duct effect is to eliminate slipstream contraction aft of the propeller and thereby increase the amount of air passing through the propeller. In some experimental data, significant losses in unit thrust were observed when the duct was shortened. Other data did not reflect this effect. The data in Figure 2 presents what is felt to be the conservative approach as presented in Reference 1 and actual test data of Reference 3 which has been demonstrated as achievable. It is probable that the disc loading has an effect on this and could be shown as a series

of lines between the data of Reference 3 and the line of Reference 1. This is based on approximately 200 lb/sq ft disc loading for the test unit on which Reference 1 data is based and a disc loading of approximately 20 lb/sq ft for the test unit on which Reference 3 is based. Unfortunately, no known data was available for other disc loadings within that span to verify this probability.

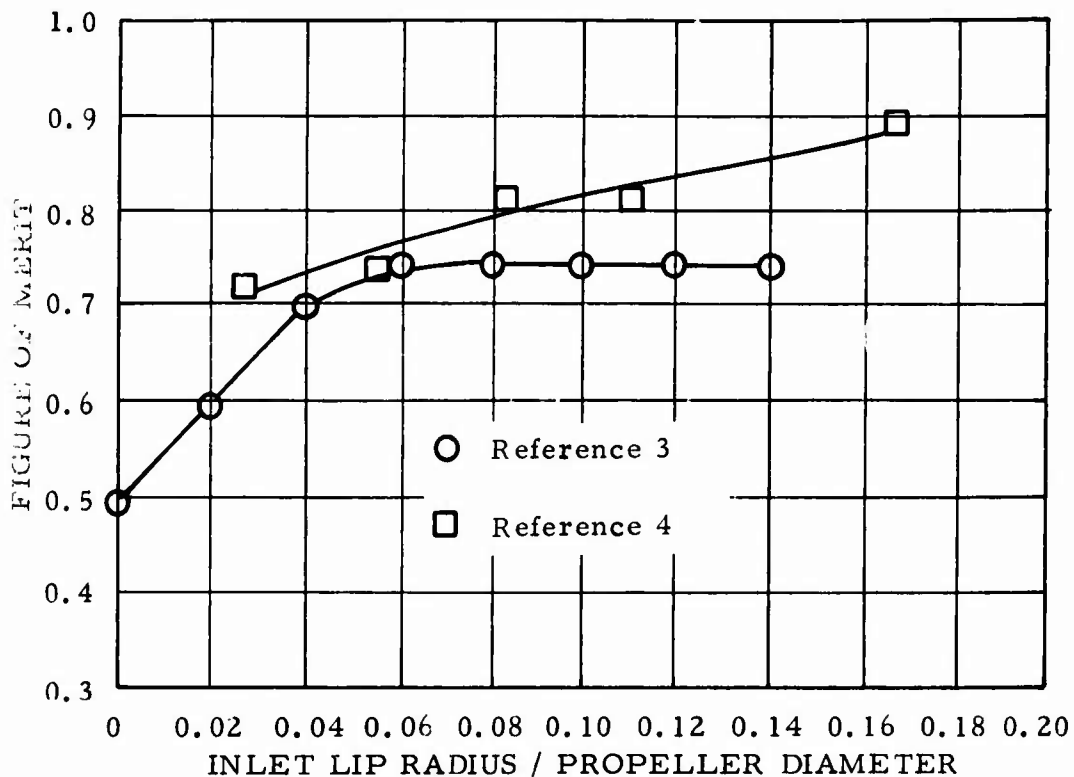


Figure 1. Inlet Lip Radius Effects on Ducted Propeller Performance.

Blade Twist Effects on Fan Performance

Reference 5 provided data showing the effect of twist modification. The standard configuration was designed for a constant inflow velocity distribution. The modified twist blades were of constant chord with the tip twisted to a higher pitch angle than the standard configuration. Figure 3 presents the inlet velocity profile for the standard and modified twist blades. Obviously the modified twist increased the amount of energy imparted to the air at the blade tip (the inner surface of the duct).

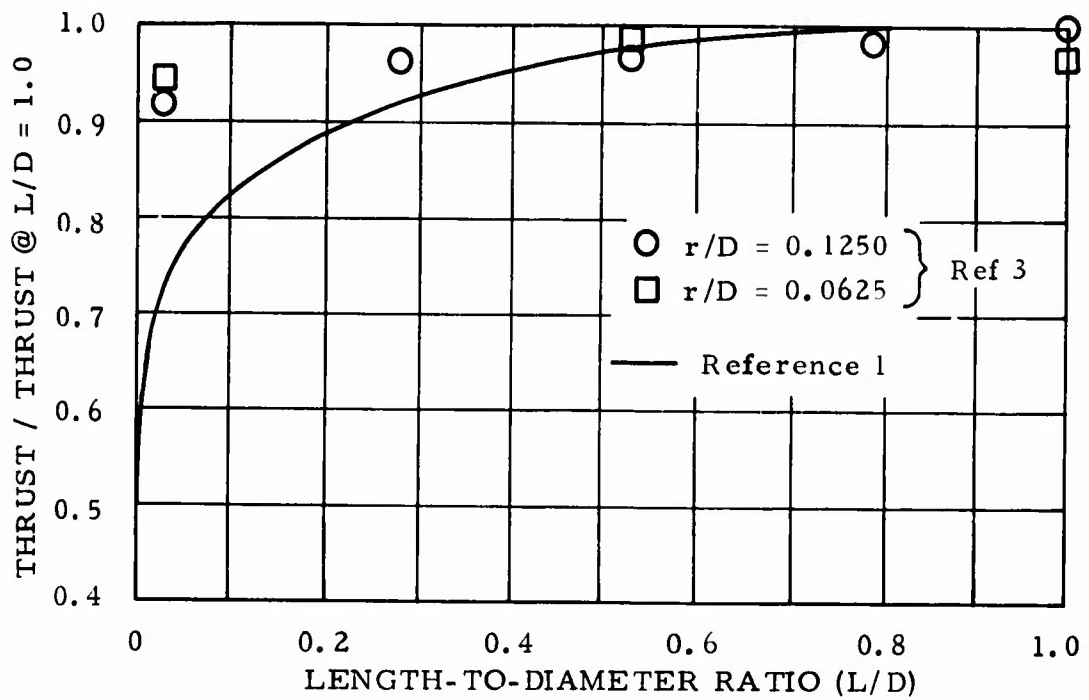


Figure 2. Effect of Duct Length on Ducted Propeller Performance.

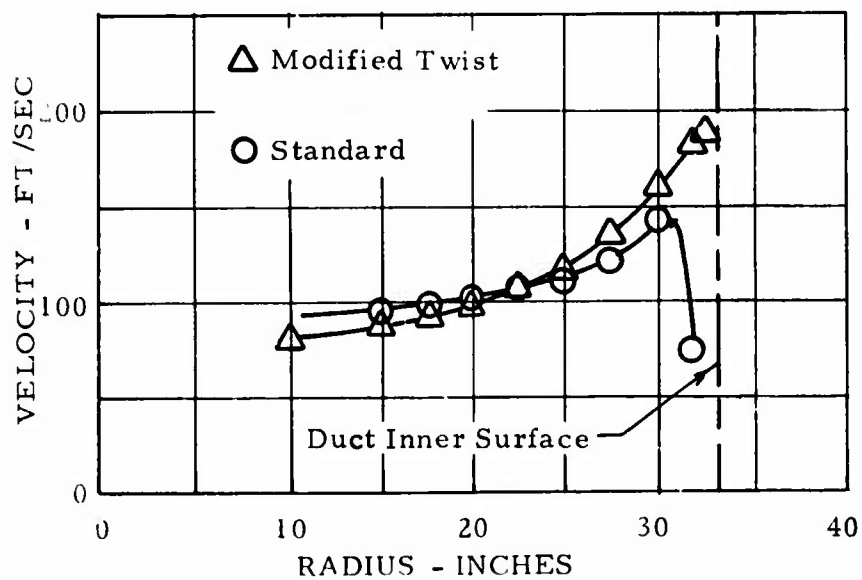


Figure 3. Approach Velocity Profiles From Reference 5.

Figure 4 further illustrates the overall performance effects of the modified twist. The increased tip-induced velocity causes a significant increase in duct thrust.

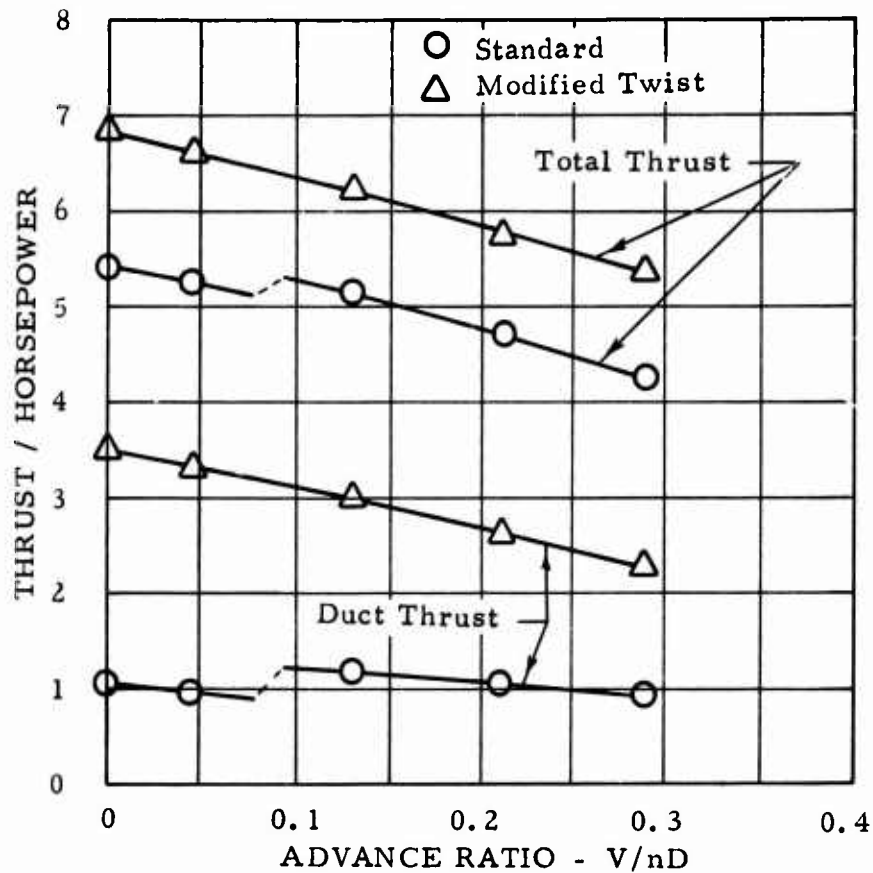


Figure 4. Modified Twist Effects on Ducted Propeller Performance, Reference 5.

#### Hub-Tip Radius Ratio Effects on Fan Performance

The higher disc loadings associated with turbojets, turbofans, etc., show specific trends of specific airflow vs. hub-tip radius ratio. This is possible since the induced velocities into the annular area between the hub and tip approach sonic speeds. One of the recent areas of investigation has been the blade root (hub) performance on configurations using low hub-tip radius ratios (less than 0.4) to achieve acceptable work per pound of air in relation to the outer portions of the blade.

With the low to moderate disc loadings considered in this study for a fan-in-fin antitorque device, the hub-tip radius ratio parameter has little if any significance. There is no meaningful data available in the

literature surveyed. This is understandable since the inflow velocities are substantially below sonic; in fact, they are significantly below speeds usually associated with compressibility losses. It is probable that where the effects of hub-tip radius ratio have been investigated, the results will be inconsequential because other parameters such as solidity, blade camber, etc., have much stronger effects. Generally the hub-tip radius ratio on this class of rotating machinery is set based on required root (hub) blade solidities and/or blade retention considerations.

### Fin Characteristics

Measurement of lift curve slope,  $C_{L\alpha}$ , from several fan-in-wing models in References 7, 8, 9, and 10 shows good agreement with lifting surface theory as shown in Figure 5. The curve labelled Lifting Surface Theory represents the expression

$$C_{L\alpha} = 2\pi AR / (AR + 2) \left[ (AR + 4) / (AR + 2) \right]$$

Good agreement is also shown with an experimentally determined curve from NACA TN 775 (Reference 6), which is commonly used for estimating the effective aspect ratio of vertical tail surfaces. The excellent agreement between the fan-in-wing data and theory is due to the fan-in-wing model's being either full span or perfectly end-plated. Thus, the model geometric aspect ratio and effective aspect ratio are equal in value.

### Fan-Induced Effects

The influence of fan operation on the fin characteristics has been studied for the fan-in-wing concept. A summary of experimental data in Reference 11 shows increased lift with speed due to fan-induced effects. It is indicated that increasing the fan area to wing area ratio reduces the induced lift. Lift curve slope was shown to remain approximately constant with increases in fan thrust in References 7 and 10. The center of lift for a fan-in-fin has also been demonstrated to shift forward of the fan axis.

The drag contribution due to fan airflow has been shown to be significant. This fan-induced drag increases with increase in speed and fan thrust.

### ANALYSIS OF THE FENESTRON

The Fenestron rotor-fin antitorque device for the SA 341 has evolved through wind tunnel tests, rig tests, and prototype flight tests to the

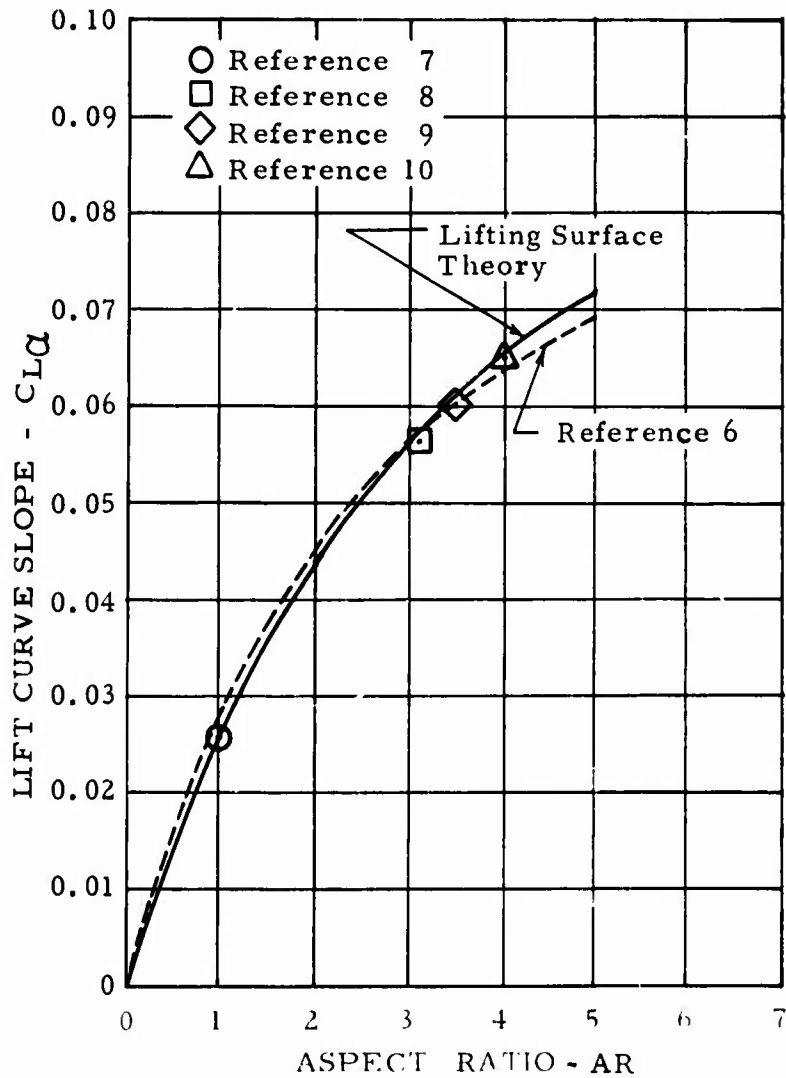


Figure 5. Comparison of Lift Curve Slope From Fan-in-Wing Wind Tunnel Tests and Theory.

production configuration. The wind tunnel tests determined the aerodynamic characteristics of the design over the flight envelope. The rig tests proved out the full-scale configuration prior to installation on a helicopter, and the prototype flight tests refined the design. The Fenestron was analyzed from the Aerospatiale (Sud Aviation) reports listed in Appendix I.

#### Wind Tunnel Tests

The first wind tunnel tests of the Fenestron were conducted with a rotor that had been developed in earlier static tests. Figure 6 describes the wind tunnel model. The model rotor diameter is 43 percent of the full-

Tip Speed 471 ft./sec  
 Blade Airfoil 16 Series  
 Duct Dia. 0.985 ft  
 Duct Length 0.410 ft  
 Diffuser Angle 7 deg.  
 Inlet Radius 0.082 ft

Rotor Dia. 0.978 ft  
 Hub Dia. 0.382 ft  
 No. of Blades 5  
 Blade Chord 0.1475 ft  
 Solidity (Rotor) 0.4775  
 RPM 9130

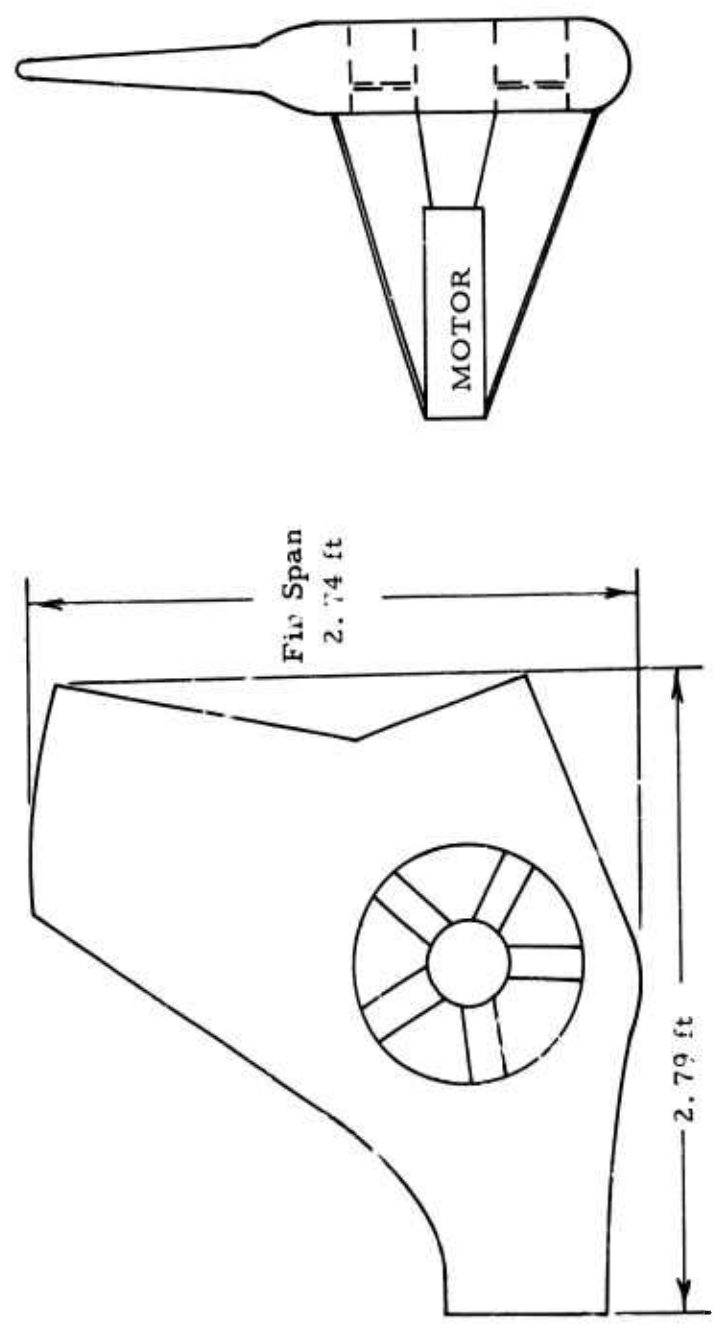


Figure 6. Fenestron Wind Tunnel Model.

scale diameter. The model fin has a symmetrical untwisted section and is 2.74 feet in span. A variable-frequency, three-phase, synchronous motor was used to drive the rotor. This motor was attached to the model on the inlet side of the Fenestron, and due to its close proximity and possible disturbing influence, the test results may be conservative.

Drag, lateral forces, yawing moments, and power were measured from static conditions to a Fenestron rotor advance ratio of 0.35 for blade pitch angles of  $-20^{\circ}$  to  $+30^{\circ}$ . The entire operational envelope was investigated by obtaining measurements at pitch angles from  $-10^{\circ}$  to  $+7^{\circ}$  and yaw angles from  $-8^{\circ}$  to  $+8^{\circ}$ . A one-seventh scale model of the SA 341 was also tested with and without a tail fin. This model was unpowered.

Side-force test results are shown in Figure 7. At 0 degrees blade pitch, there is approximately zero thrust over the speed range. Thus the increase in side force is due to fan thrust. Side-force coefficient as a function of blade pitch angles for different speeds is given in Figure 8. There was no indication of stall due to lip separation over the range investigated.

The power required to obtain a given thrust at low advance ratios is shown in Figure 9 to increase above the power required to obtain the same thrust in hover. The power increases to a maximum at about  $\mu = 0.10$  and then decreases with increase in advance ratio. It can be seen that the same thrust can be obtained at the higher advance ratios for less than one-half the power required in static conditions. Or for a given power, the thrust increases with speed.

The drag of the fan-in-fin is shown to increase with blade pitch in Figure 10. This fan-induced drag caused by the increase in flow through the fan is shown in Figure 11 as a function of the increase in side force. The positive values represent negative blade angle setting with resulting thrust in the torque direction.

The slope of the side-force curve with fin angle of attack was determined for a blade pitch of zero degrees. The variation of this slope referenced to fin planform area is shown in Figure 12 versus speed. A fin planform area of 4.87 sq ft was defined as the fin area aft of a line extending vertically downward from the point of intersection of the boom and the fin leading edge.

A comparison of the lift curve slope with fan thrusting and the fan at zero thrust in Figure 13 indicates that an end-plating effect (similar to the way the horizontal tail of a fixed wing airplane end-plates a vertical tail) is created by the fan thrust. The increase in lift curve slope with fan thrust can be attributed to end-plating because this effect was not

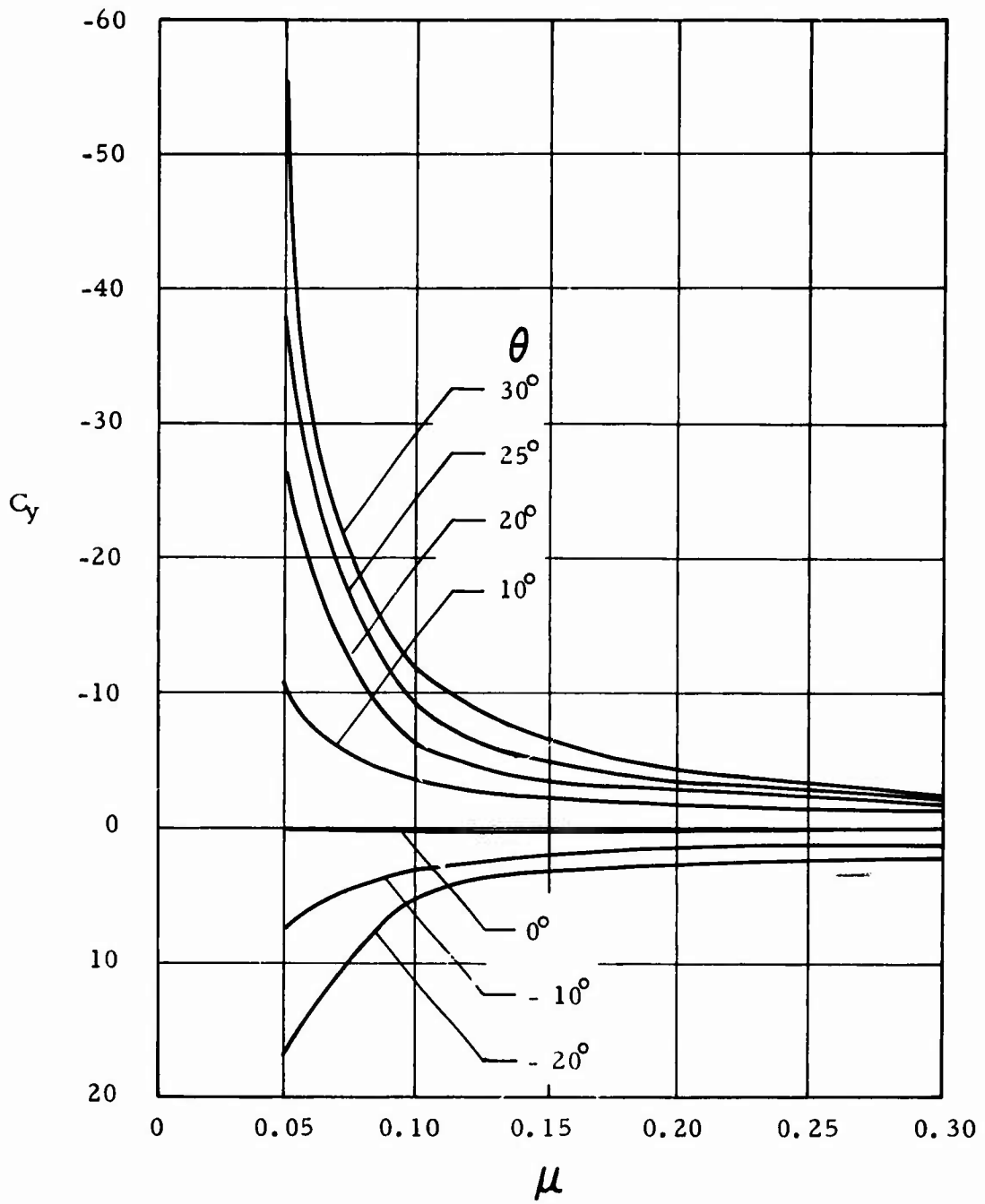


Figure 7. Side-Force Coefficient Vs. Advance Ratio, Fenestron Wind Tunnel Tests.

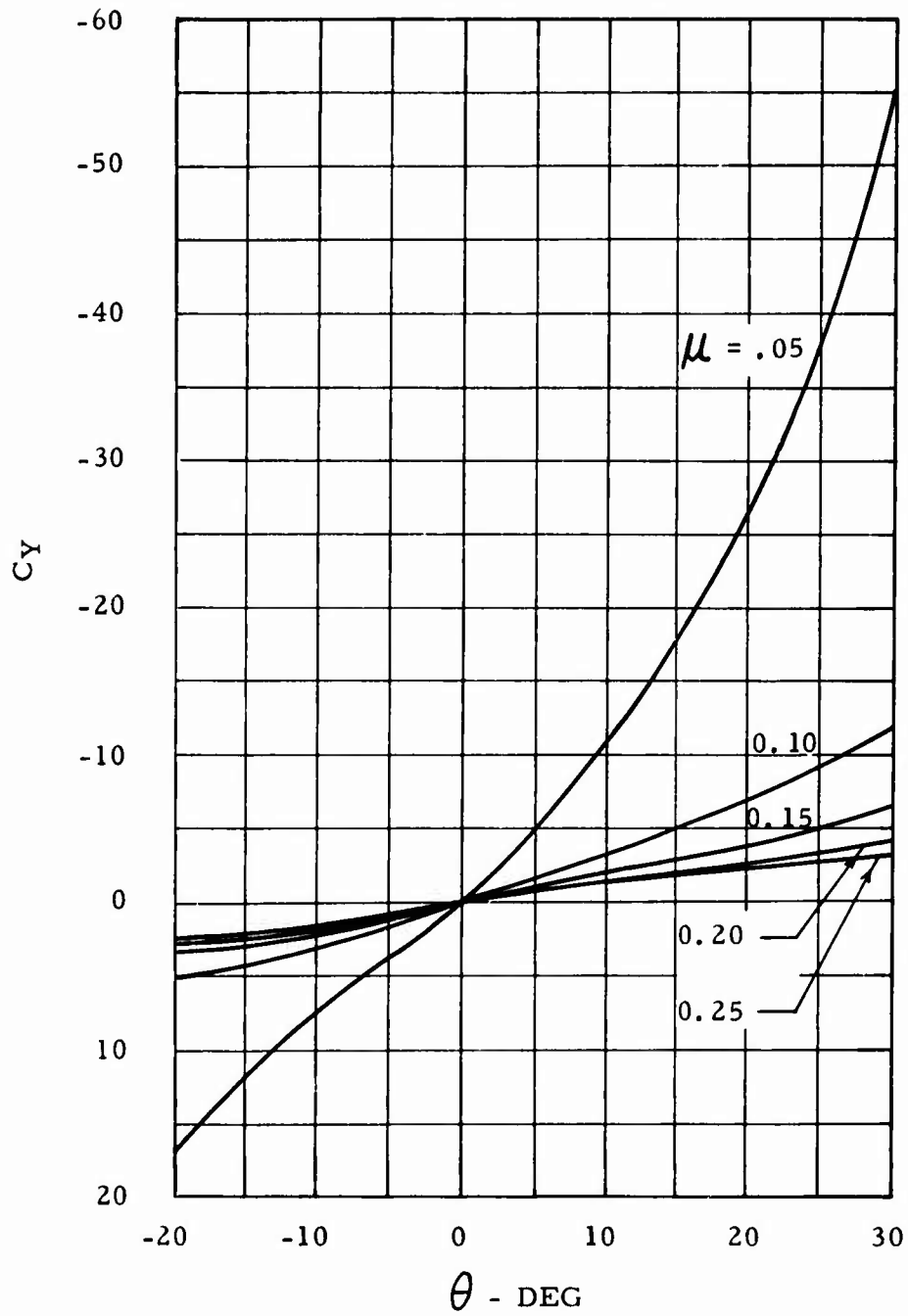


Figure 8. Side-Force Coefficient Vs. Blade Pitch Angle, Fenestron Wind Tunnel Tests.

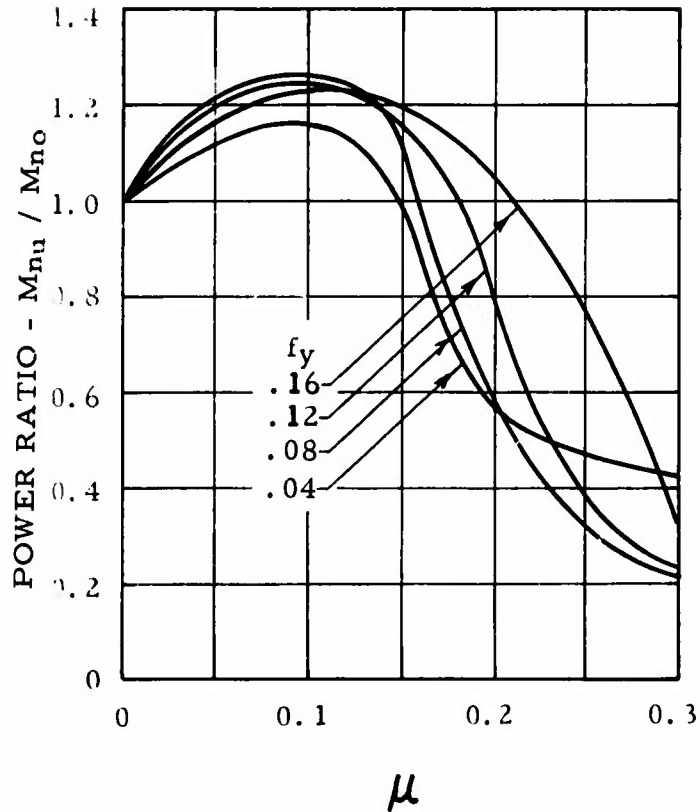


Figure 9. Power Ratio Vs. Advance Ratio, Fenestron Wind Tunnel Tests.

apparent in the perfectly end-plated or full span fan-in-wing model tests. A data point from the one-seventh scale SA 341 model also indicates that end plating is not evident without the fan thrusting. These data are shown only to graphically demonstrate the end-plating effects and do not represent a correlation with theory.

The results in Figure 14 show that the thrust center moves forward of the fan center towards the vehicle nose, with increase in advance ratio reaching a maximum and then returning to the area of the fan center at the higher advance ratios. The forward movement of the thrust center would effectively reduce the moment arm for this antitorque device and thus require greater power to provide the antitorque moment. It would therefore be desirable to use the fin for antitorque force as much as possible.

Also the model was tested with fore and aft pitch. The influence of model pitch on the side thrust and power was small except that pitch-up at the

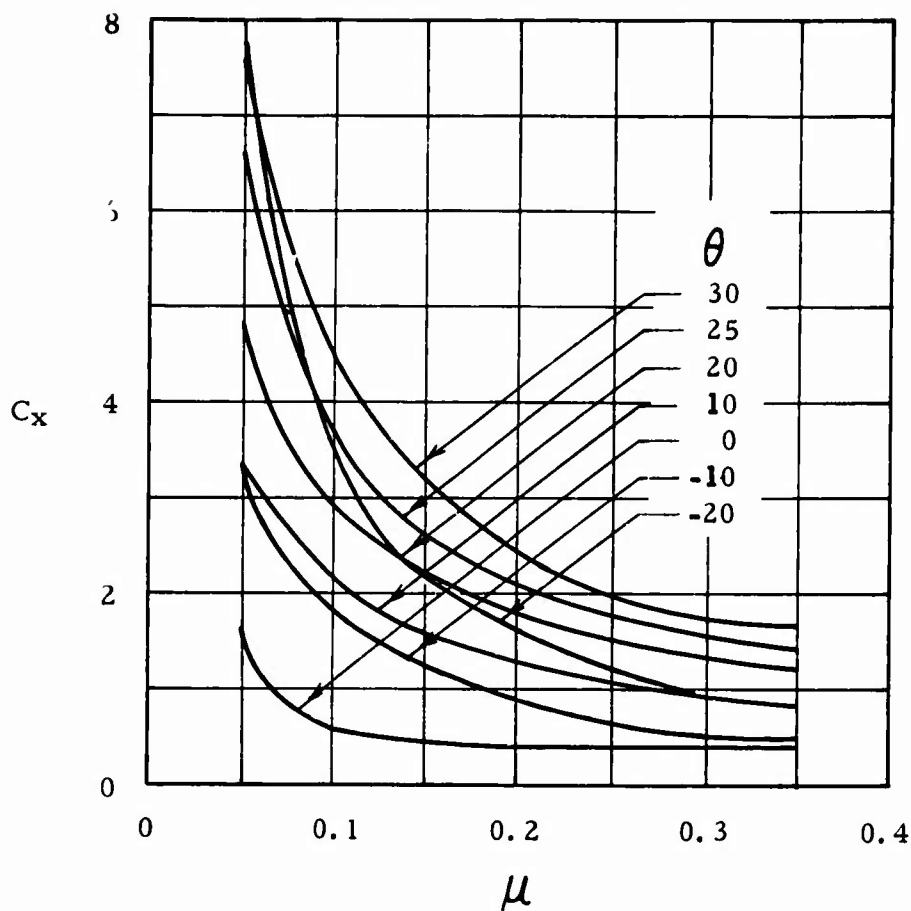


Figure 10. Drag Coefficient Vs. Advance Ratio, Fenestron Wind Tunnel Tests.

higher speeds required slightly more power than at zero pitch. A second series of wind tunnel tests were conducted on a 00XY (uncambered section with thickness of XY percent) rotor blade profile and sharp-edged and rounded-edged diffuser exits. The test results showed that the 00XY blades were slightly more efficient than the 16 series blades in the main torque direction and the 16 series blades slightly more efficient with speed in the antitorque direction. The 16 series blades were selected because of their more favorable contribution in the antitorque region.

A diffuser exit with rounded edges of 15 mm radius was tested to determine reverse thrust (torque direction) effects. There was an increase in torque direction thrust and the drag of the Fenestron-fin unit was reduced. However, the thrust (antitorque direction) was significantly reduced, therefore the rounded edges were not incorporated.

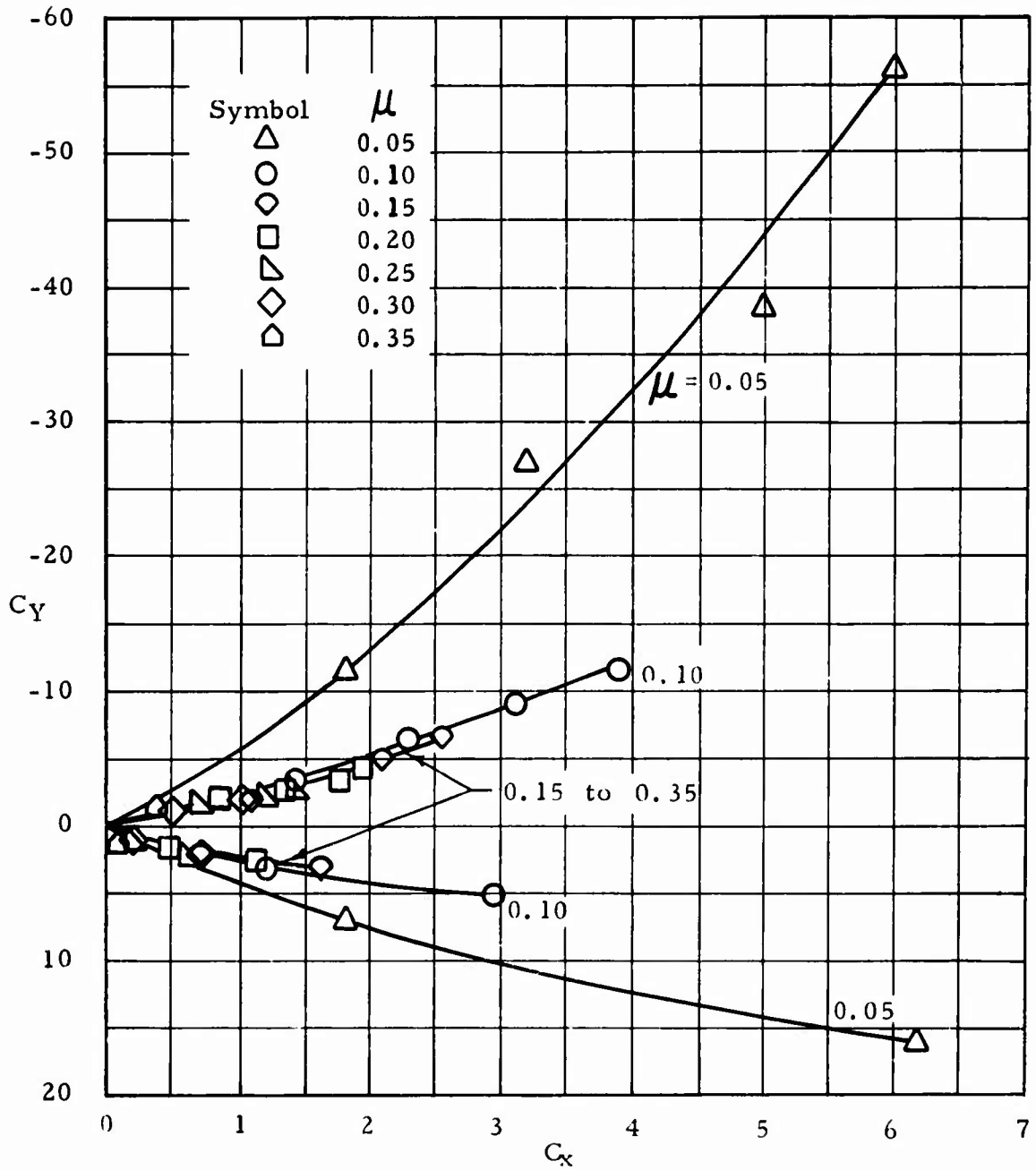


Figure 11. Fan-Induced Drag, Fenestron Wind Tunnel Tests.

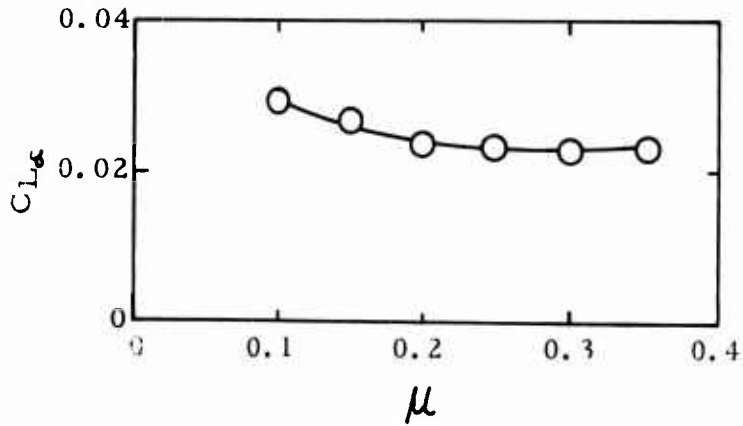


Figure 12. Lift Curve Slope Vs. Advance Ratio, Fenestron Wind Tunnel Tests.

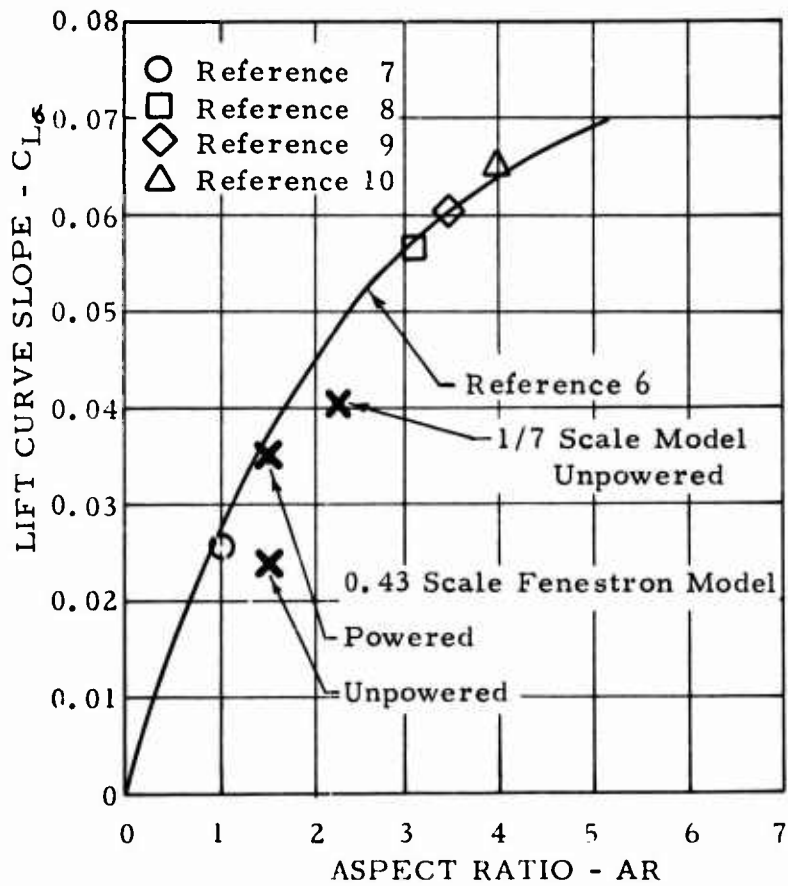


Figure 13. Comparison of Lift Curve Slope From Fenestron and Fan-in-Wing Wind Tunnel Tests.

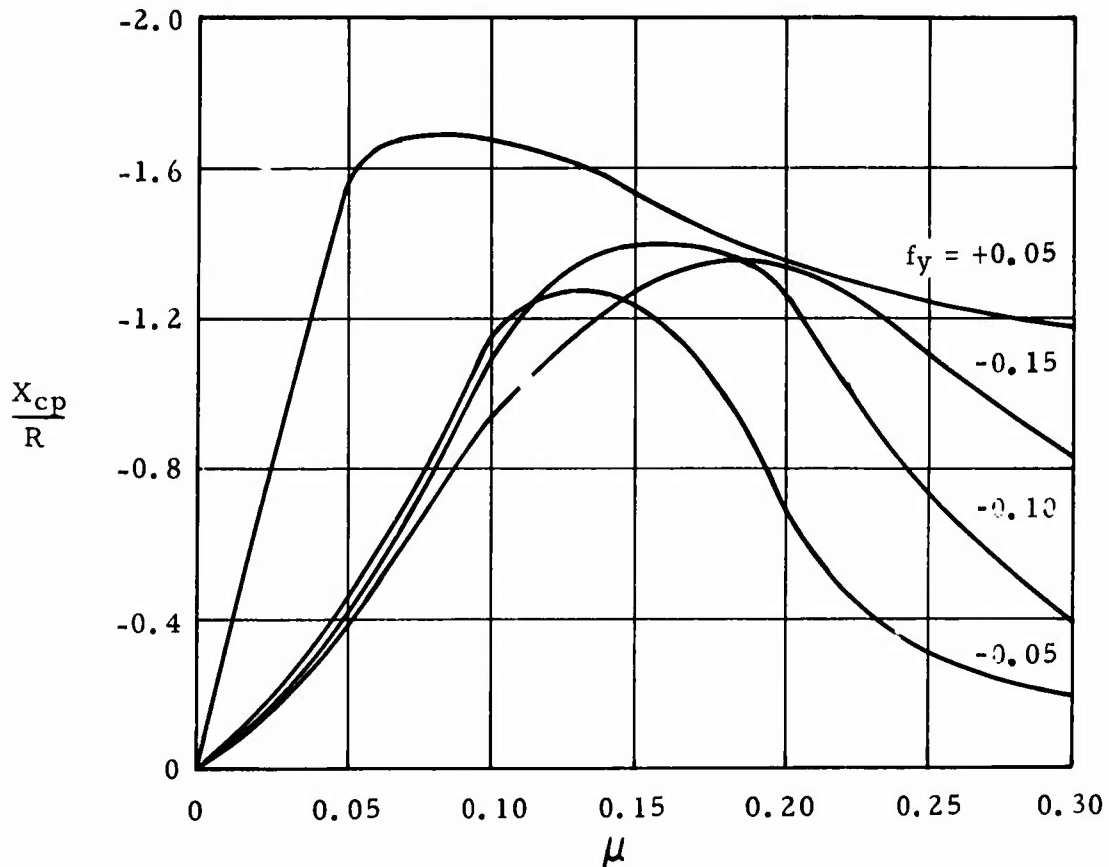


Figure 14. Center of Thrust Shift With Advance Ratio, Fenestron Wind Tunnel Tests.

#### Static Tests

A full-scale version of the Fenestron was constructed and mounted on an SA 341 tail boom. It was connected to all the drive shafting, the main gearbox and an engine, and static tests were conducted. Thrust was measured by a strain-gaged bar attached to the tail boom, and a torque-meter measured the power input into the Fenestron gearbox. These tests confirmed the static wind tunnel tests. Faired and unfaired hub support arms were tested, and faired arms were shown to be beneficial

#### Flight Tests

Flight test data of the 341 in hover and forward flight have been analyzed to determine the fan and fin characteristics. Comparisons were made between the performance of the Fenestron and the conventional tail rotor

flown on the same ship. Although both antitorque devices were installed on the same vehicle, the nature of the initial experimental program in developing a new helicopter produced little data on the performance of the tail rotor. Thus, it has been necessary to estimate the tail rotor performance. Power prediction methods described in Appendix II have been used in the data analysis.

SA 341 Description

The SA 341 "Gazelle" is a light, multipurpose, high-speed helicopter featuring a ducted fan antitorque device called the Fenestron. It is the only production helicopter employing this type of antitorque concept. The 341, shown schematically in Figure 15, has a maximum weight of 3750 lb and is powered by a Turbomeca Astazou III turbine engine rated at 592 hp. The general characteristics of the Fenestron and semiarticulated main rotor are given in Table I. It should be noted that the main rotor rotates in a clockwise direction as viewed from above.

The Fenestron rotor consists of 13 aluminum alloy di-forged blades with NACA 16 series airfoil cross section. The blades, having only a pitch hinge, are mounted on self-lubricating bearings and are attached to the hub by means of laminated metal strips. Power is transmitted to the rotor through a gearbox in the hub integral with the fan assembly. Blade pitch is controlled by means of the rudder pedals through a hydraulic servo unit mounted on the gearbox.

TABLE I. SA 341 MAIN ROTOR AND FENESTRON ROTOR CHARACTERISTICS		
	Main Rotor	Fenestron Rotor
Diameter - ft	34.45	2.3
Chord - ft	0.983	0.128
No. of Blades	3	13
Rotational Speed - rpm	378	5774

The SA 341 fin is in three parts: a lower section which is symmetrical in the freestream direction and serves as a crushable tail skid, a fan section which is streamwise asymmetrical but of unknown effective camber, and an upper fin which has 4 percent camber and a thickness

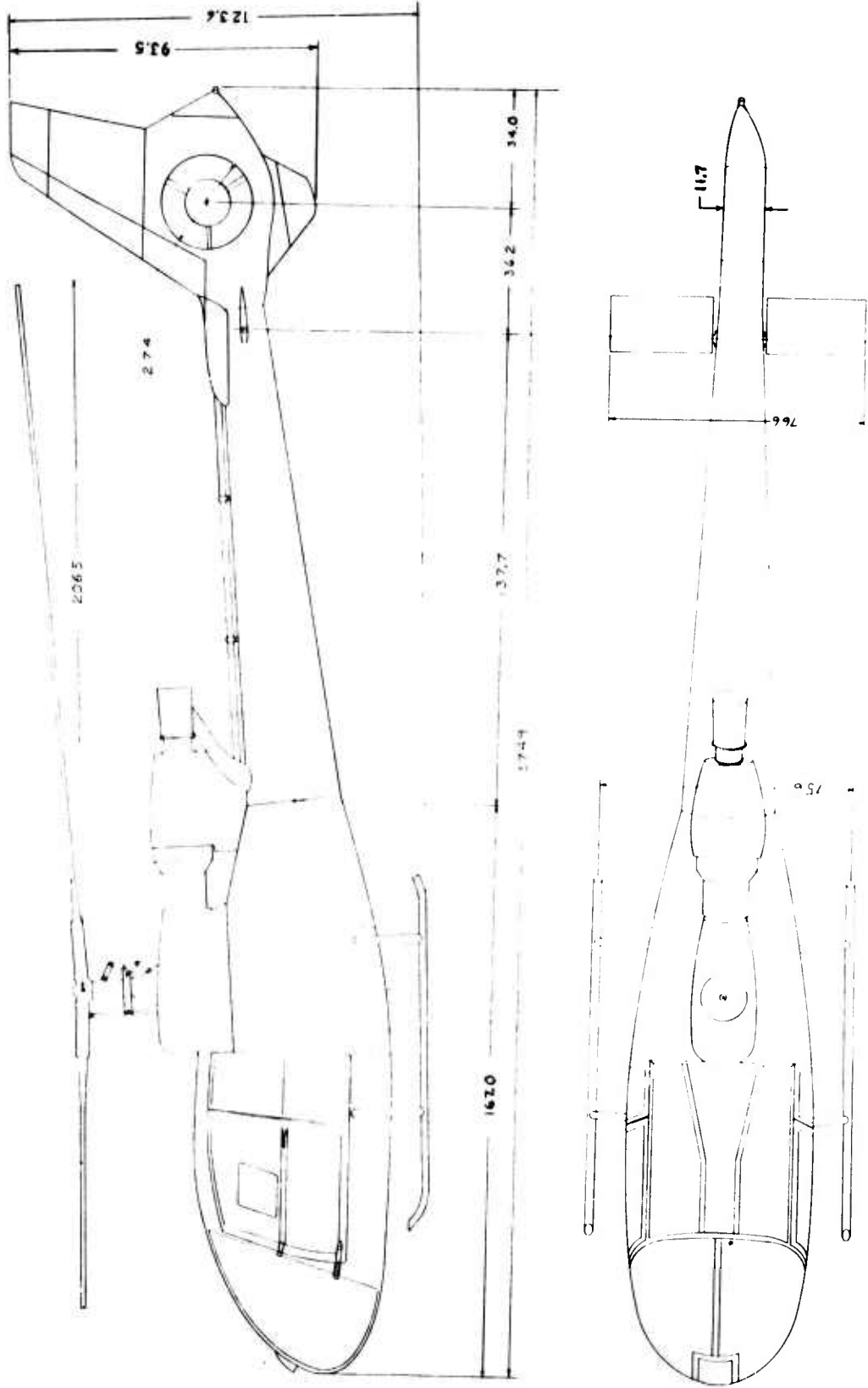


Figure 15. SA 341 Gazelle Light Multipurpose Helicopter.

ratio ranging from 18 percent at the fan structural joint to 12 percent at the tip. The overall vertical fin is set at 2 degrees angle of incidence in the antitorque direction. A total fin planform area of 26.3 sq ft is defined as the area aft of a vertical line extending from the point of intersection of the fin leading edge and tail boom.

To provide conventional tail rotor data for comparison with the Fenestron results, data were extracted from records of the SA 341 development program. Figure 16 shows the prototype configuration selected. This configuration was the same as the SA 341 except for small vertical fins on the horizontal tail plane and the conventional tail rotor. The vertical fins on the horizontal tail plane were found to be noncontributing and were not put on the SA 341. The characteristics of the conventional tail rotor are presented in Table II and are compared to the Fenestron.

### Hover

Fenestron power measured in hover ratioed to the total power required is shown in Figure 17 for a range of weights. The same ratio is shown for the conventional tail rotor. The fan with a disc loading of about 60 lb/sq ft for a gross weight of 3750 lb requires more power than the conventional tail rotor having a disc loading of approximately 8 lb/sq ft.

### Comparison of the Fenestron Figure of Merit to the State of the Art

The Fenestron development was oriented toward achieving a given level of performance without too much regard to the efficiency. The basic design of the SA 341 allowed this to occur since in most areas of the operational envelope it has excess power available. The result is that the existing Fenestron requires significantly more power than a tail rotor requires to do the same job.

One of the obvious reasons for the increased power required is the Fenestron size. Theoretically the addition of a shroud or duct around an existing propeller or rotor increases its static thrust by a factor of two. The SA 341 tail rotor was approximately 6.3 ft in diameter. Therefore, assuming the static efficiency to be constant, a ducted fan (propeller) would require one-half the area or a 4.5-ft diameter for the same power requirement. The 2.3-ft diameter of the Fenestron will require approximately twice the power because of disc loading effects on power loading, lb thrust/hp.

The additional power requirement over and above the disc loading effects of the Fenestron is due to nonoptimum blade and duct geometry. An indication of the degree to which the existing Fenestron could be improved

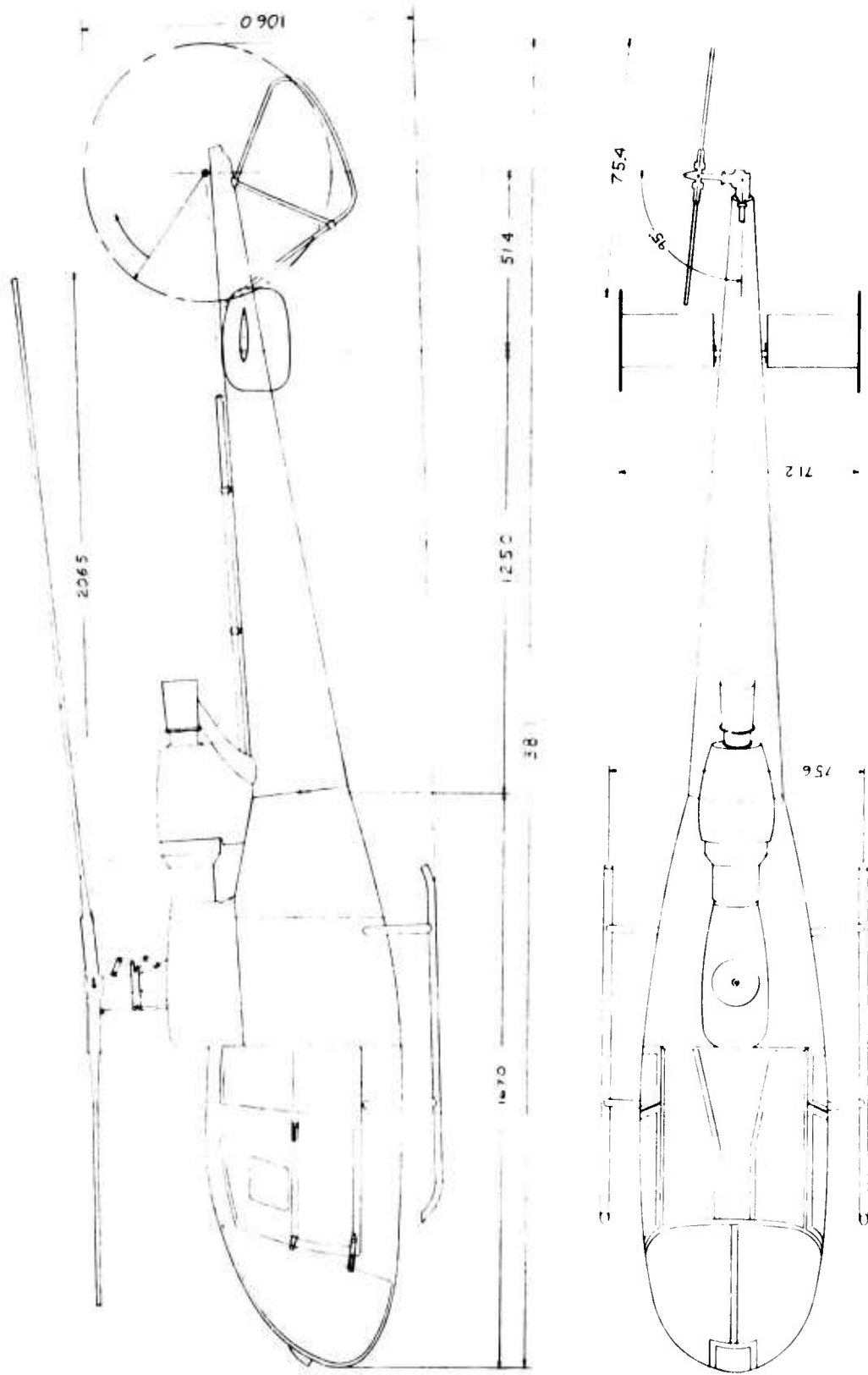


Figure 16. SA 341 With Conventional Tail Rotor.

TABLE II. COMPARISON OF ANTITORQUE DEVICE ROTOR CHARACTERISTICS		
	SA 340 Tail Rotor	SA 341 Fenestron Rotor
Diameter - ft	6.28	2.3
Chord - ft	0.517	0.128
No. of Blades	2	13
Rotational Speed - rpm	2053	5774

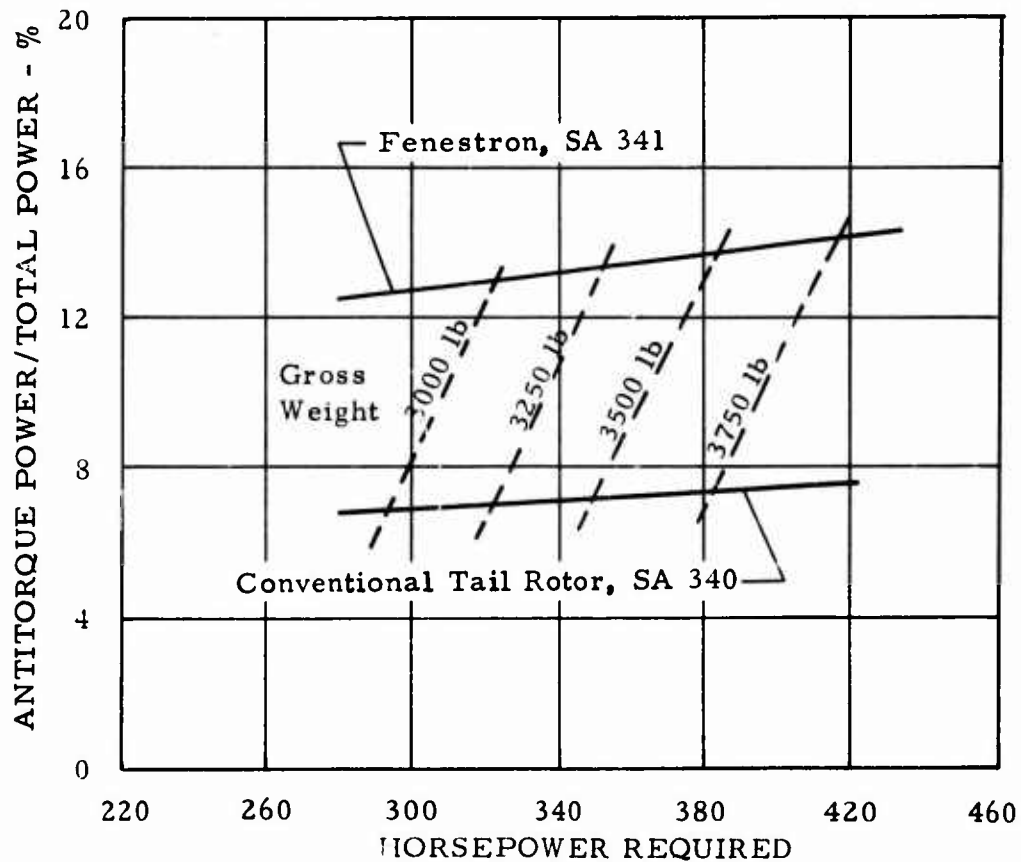


Figure 17. Antitorque Power Comparison in Hover, SL STD.

is shown in Figure 18. The state-of-the-art line includes the short duct effects discussed in the literature survey and presented in Figure 2. Since the use of a reasonably low disc loading is indicated (approximately 60 psf), the state of the art shown is considered to be conservative.

Rationalization of the decrement in performance shown is as follows:

- The tip clearance is excessive. Therefore, duct velocities are not as high as they should be to produce the normal duct forces.
- The blade twist is not optimum. The indicated induced velocities near the tip of the blades tend to fall off. This in combination with the tip clearance makes the duct forces low and also significantly reduces total blade forces.
- The blade camber is too low. Significant gains are indicated by using a cambered airfoil section for the blading. Examination of the existing Fenestron blading indicates that little or no camber is being used.

The opinion resulting from this study is that if all the items listed were corrected, the performance of the Fenestron would be increased approximately to the level indicated by the state-of-the-art line.

#### Forward Flight

The total power required for the SA 341 in forward flight was determined by the methods outlined in Appendix II. Main rotor power and the anti-torque thrust were computed. The Fenestron fan contribution to anti-torque thrust and power required was estimated from test data. The power increments due to fin- and fan-induced drag and mechanical losses were estimated. Good agreement with flight test data is shown in Figure 19. The predicted power required is approximately 3 percent higher at a given speed than flight test data would indicate. This results in a predicted speed about 1.5 percent lower for a given power than can be obtained from flight tests. Thus for this application the prediction methods are conservative.

The power required for the SA 341 with conventional tail rotor was estimated in a similar manner. A comparison of the antitorque power required versus speed in Figure 20 shows the power savings of the Fenestron. However, these savings are not totally reflected in the total power because of the fan- and fin-induced drag requires additional main rotor power. A comparison of the total power required for the two systems shows a small decrease in power required by the Fenestron

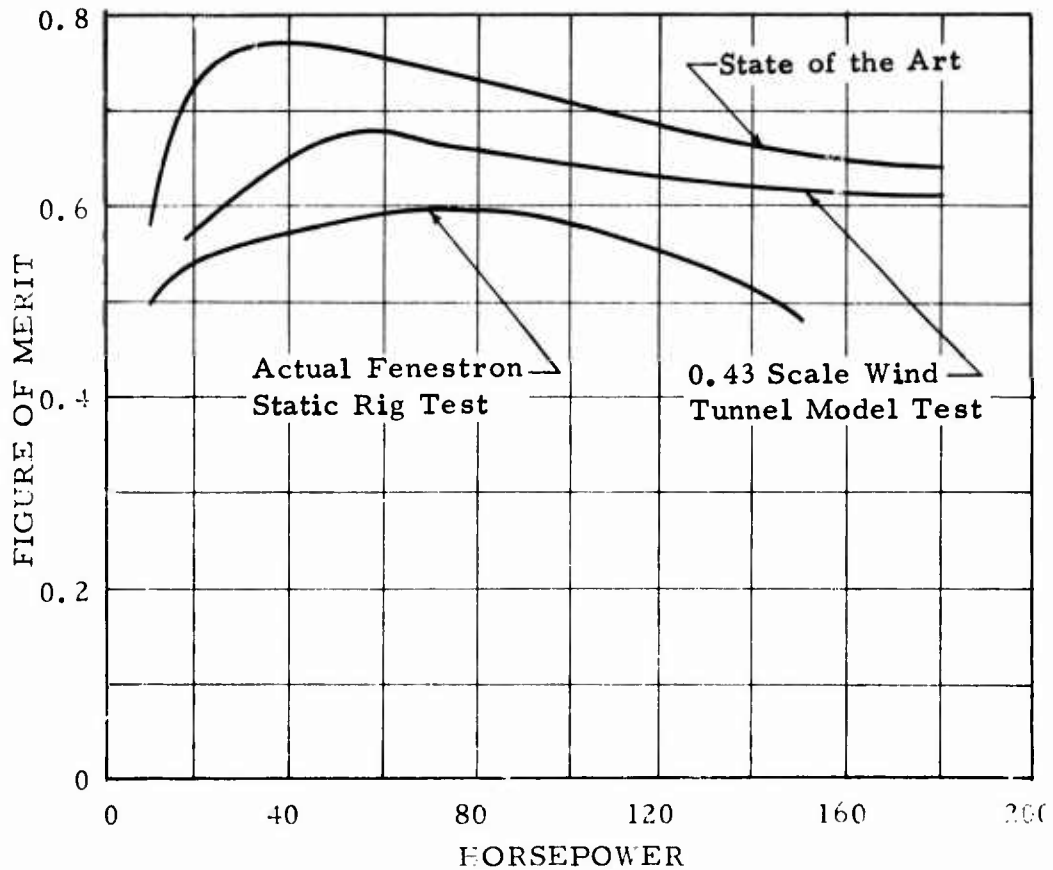


Figure 18. Comparison of the Fenestron to State-of-the-Art Figure of Merit.

system at the higher speeds in Figure 21. An increase in maximum speed of 2 kt or about 1.5 percent is noted at maximum continuous power.

A 6-kt increase in speed can be estimated by comparing predicted 340 data with 341 flight test data. It should be noted that the maximum stress measured in the blade root blend radius of the Fenestron fan was 1450 psi. The stress level of the conventional tail rotor blades was not measured.

Figure 22 shows the antitorque thrust required for the SA 341 at a weight of 3750 lb through its normal speed range. The required fan contribution, labelled (1), is derived from flight test results. The fan thrust is shown to diminish as the speed increases due to the fin's assuming the anti-torque load requirement for the helicopter. The fin contribution is then the difference between the thrust required and the fan thrust. The fin thrust is shown in Figure 23.

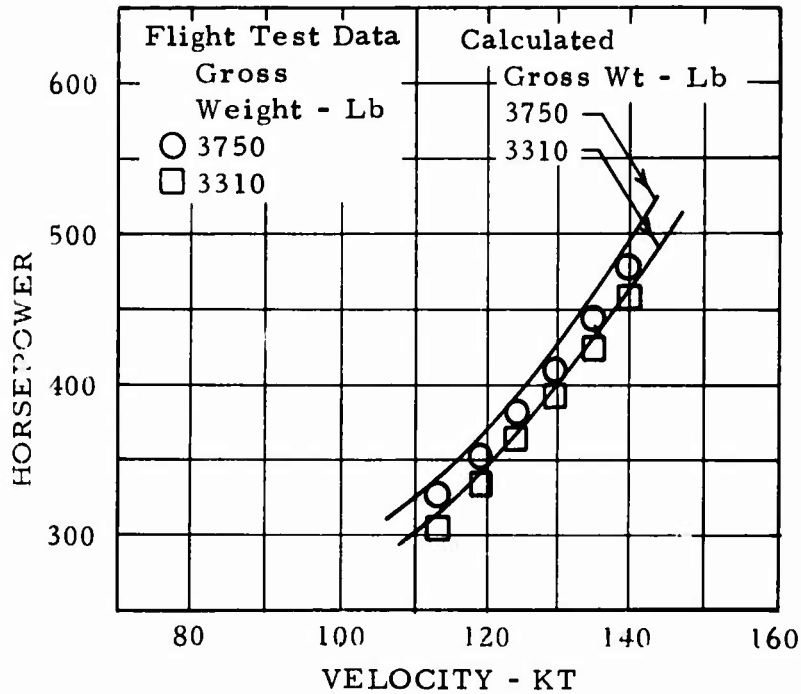


Figure 19. Comparison of Predicted Power Required and Flight Test Data in Forward Flight, SL STD, SA 341.

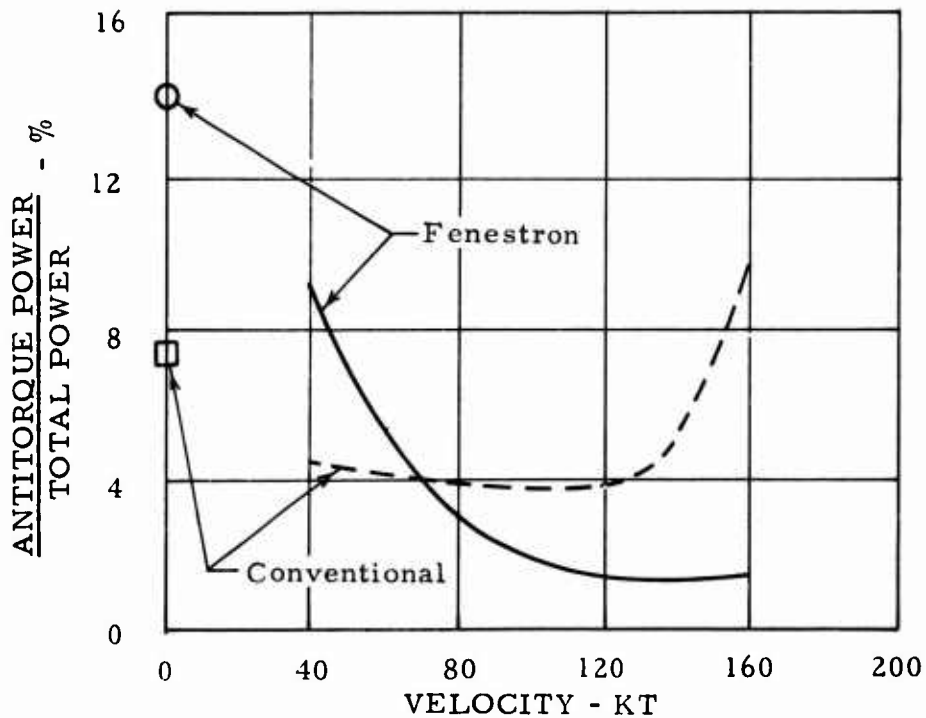


Figure 20. Antitorque Power Comparison in Forward Flight, SL STD, GW=3750 Lb.

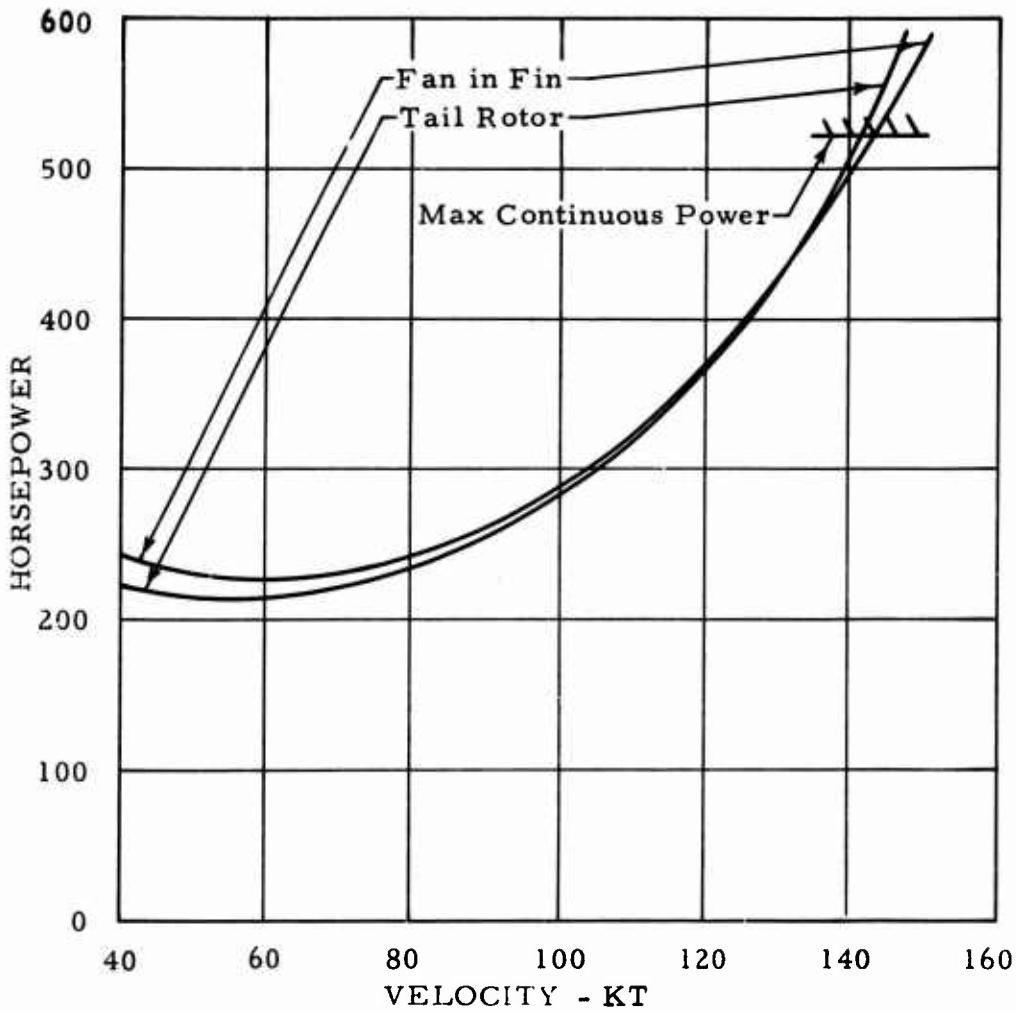


Figure 21. Comparison of Total Power Required for Tail Rotor and Fenestron Systems, SL STD, SA 341, GW=3750 Lb.

The fan thrust required for an SA 341 antitorque system having fins of different total areas is shown in Figure 22. These results were adapted from fan-in-wing model tests (References 7 and 10). The corresponding fin thrust contributions are shown in Figure 23.

Considering both Figures 22 and 23, it can be seen that the SA 341 fan-in-fin system functions well. The fin allows the fan to be unloaded to a small, essentially constant thrust level at cruise speed. This small fan thrust level is desirable since its effect is to close the fan duct and prevent any incipient flow condition from developing that could adversely affect the pressure distribution on the vertical fin surfaces.

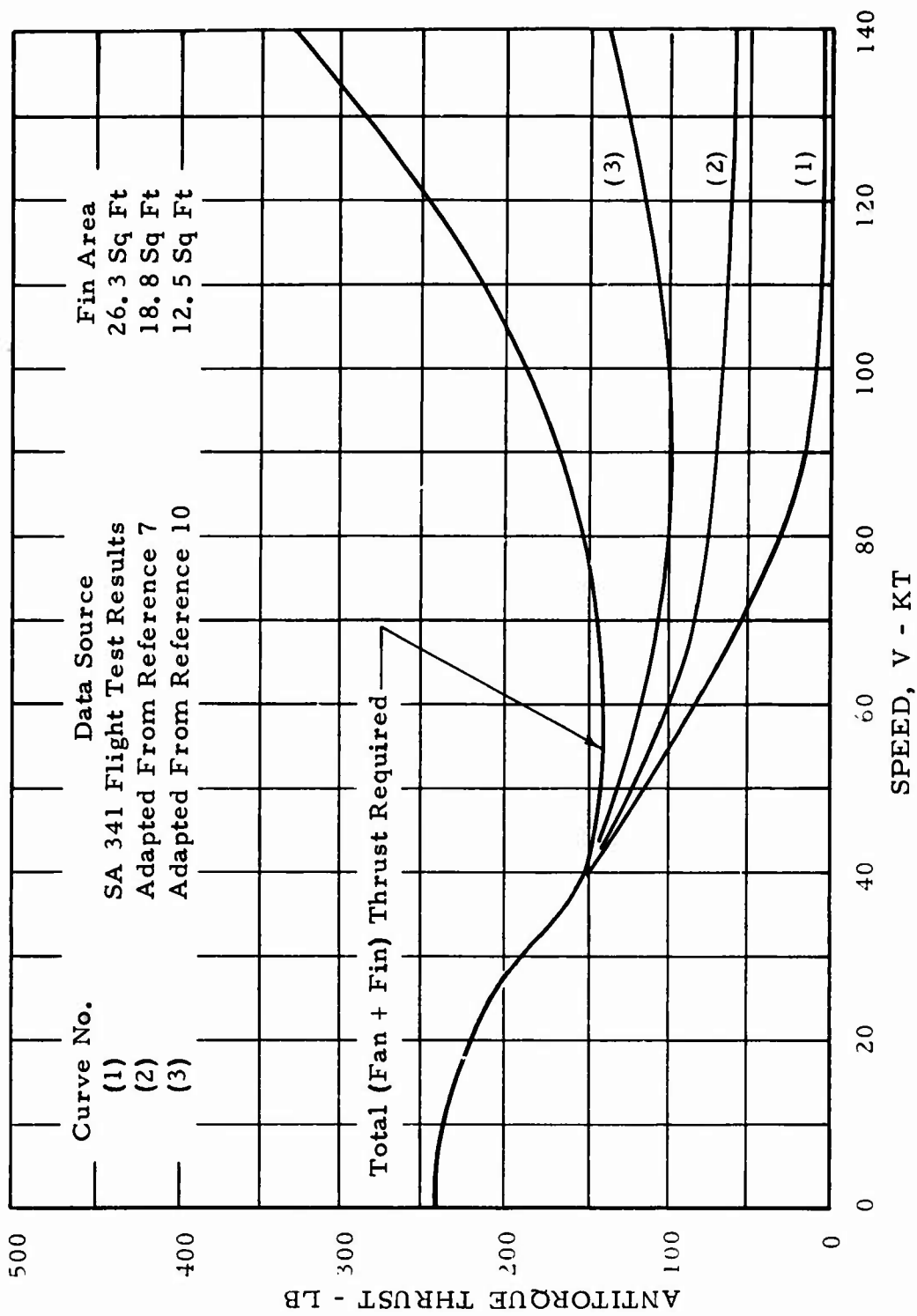


Figure 22. SA 341 Antitorque Thrust Requirement in Forward Flight and the Fan Thrust Required for Various Fin Areas,  $C_L = \text{Const}$ , SL STD,  $GW=3750$  Lb.

One area in which fan-in-fin performance can be improved is evident in curve (1) of Figure 23. It is seen that the fin contributes little antitorque thrust in the low-speed region. In fact, the fin contribution is not measurable below 40 kt. This phenomenon is probably caused by adverse interactions of the fan efflux, the main rotor downwash and the freestream flow, but further experimental testing will be required to develop an understanding for improvement. An improvement in low-speed fin thrust can be obtained by employing an adjustable trim flap on the upper fin trailing edge. Trim flap size as applied for antitorque purposes in this study is approximately one-third span in length and one-third chord in width. Such a trim flap would increase the upper fin effectiveness and produce a fin thrust curve more in character with the fan-in-wing results, curves (2) and (3), of Figure 23. This would allow the fan to be unloaded at a lower speed. In addition, an adjustable trim flap on the upper fin could be used to trim the helicopter for off-design speed and gross weight conditions and during autorotational approaches with the antitorque fan inoperative. While the upper fin is only a part of the overall vertical surface, a trim flap on this portion should help to increase the aerodynamic lift of the fan-in-fin system when operating in the low-speed range.

The fin lift coefficient of the Fenestron antitorque system for trimmed forward flight is shown in Figure 24. This plot was calculated from the fin thrust (Curve (1) in Figure 23) obtained from flight test results. The curve of lift coefficient versus speed shows how sharply the fan-in-fin aerodynamic lift diminishes in the low-speed range below 70 kt. In the speed range of 60 to 140 kt, the fan is only nominally lifting. The fin  $C_L$  for trimmed cruise flight is seen to be approximately 0.185. The angle for zero sideward fin lift was determined to be 3.5 degrees. Thus, a meaningful value of lift curve slope can be estimated as 0.053 per degree for the fin. An effective aspect ratio of 2.7 can be determined from lifting surface theory. This is a higher value than the geometric aspect ratio of 2.31. Thus it is assumed that for this trimmed cruise condition, the low fan thrust provides enough end-plating to make the fin act similar to a vertical tail for a fixed-wing aircraft which is end-plated by a horizontal stabilizer.

A forward shift (toward the nose and along the longitudinal axis) of the Fenestron thrust was noted over a specific speed range. Wind tunnel test data showed a maximum shift at approximately 55 kt, which resulted in an 8-percent effective decrease in moment arm length. Overall vehicle effects at that speed would be a 9-percent increase in required antitorque thrust, which would require an additional 1 percent in total power. At lower speeds the shift is shown to be less pronounced, and at higher speeds the fan is sufficiently unloaded that this forward shift

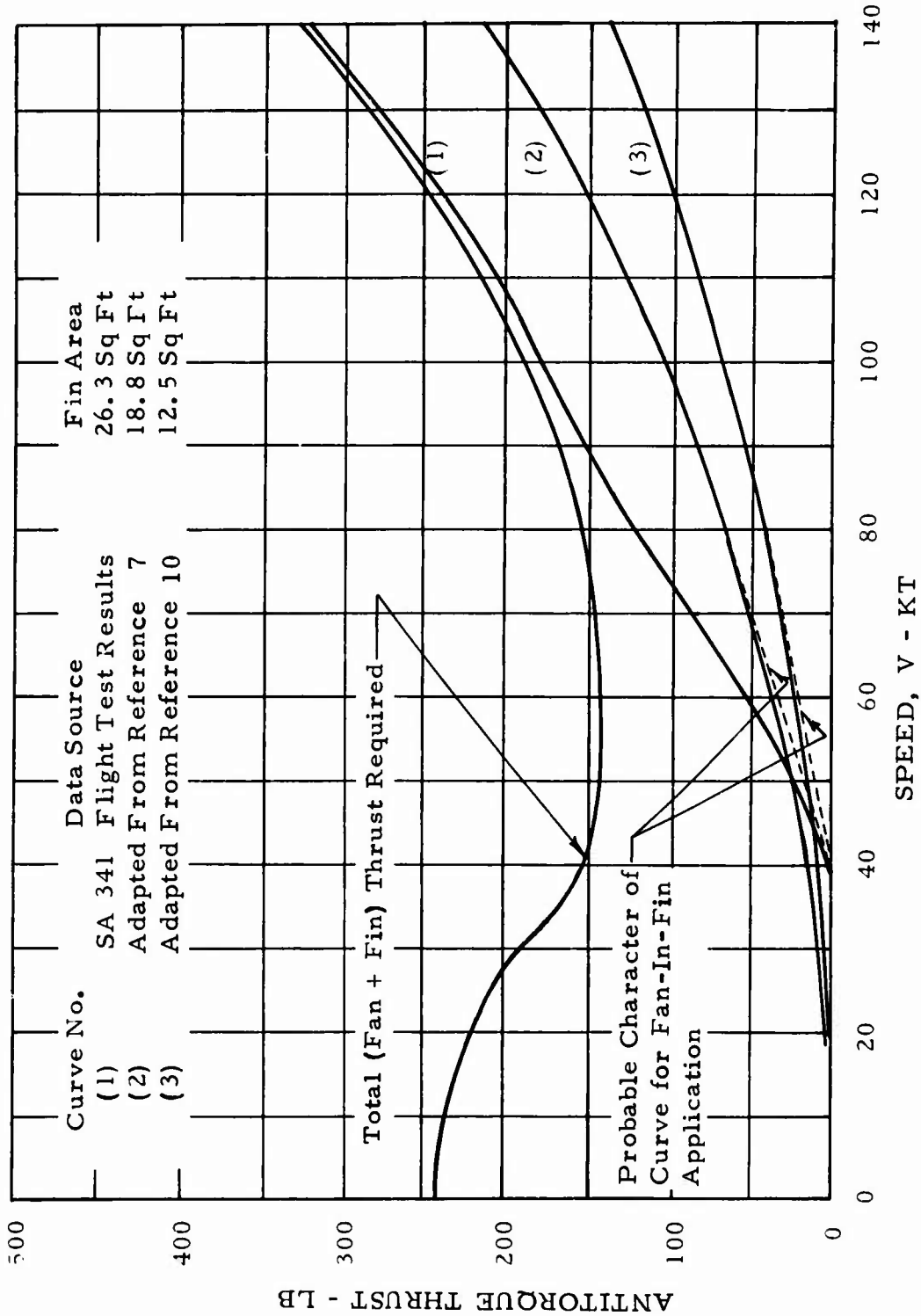


Figure 23. SA 341 Fin Thrust Vs. Speed, Showing the Effect of Varying Fin Area.

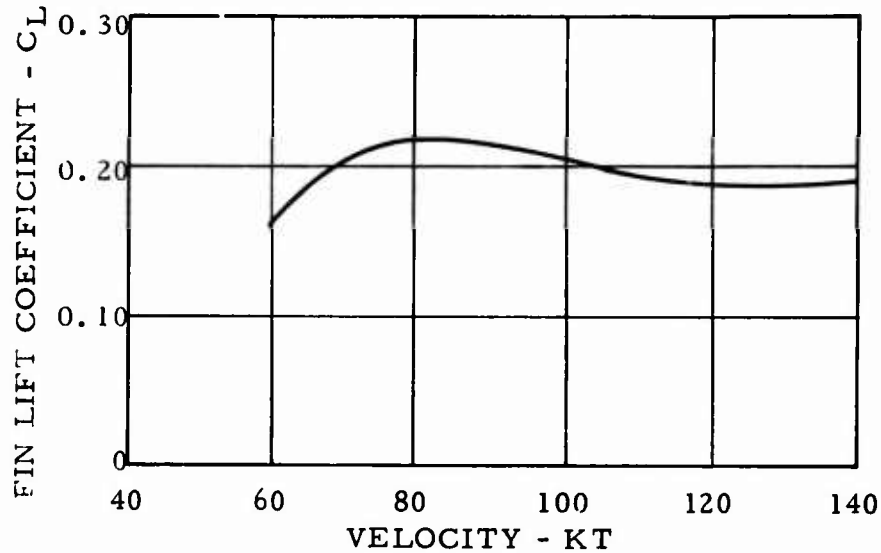


Figure 24. SA 341 Fin Lift Coefficient Vs. Speed  
From Flight Tests, SL STD, GW=3750 Lb.

effect is minimized. Thus there is a corresponding decrease in anti-torque thrust required and total power. Taking this effect into account, the performance of the SA 341 was not changed significantly.

#### Directional Stability and Control

The SA 341, as shown in Figure 25, has sufficient blade pitch margins to provide adequate yaw control in hover. Approximately 35 percent more control is available for the case of a 30-kt side wind at sea level at a weight of 3530 lb. Of interest is the 20 percent control margin available for a 20-kt side wind at a density altitude of 9200 ft and maximum gross weight of 3750 lb.

Blade pitch versus sideslip angle in Figure 26 shows positive directional stability at 65 kt and at 120 kt, although there is a region at 120 kt where the stability is reduced. This has been explained as a case where the blade pitch position corresponds to null thrust on the rotor and the air-flow through the duct is changing direction in an incipient manner. Thus it is desirable to have the fan positively loaded at all times in forward flight to avoid this null region. Positive stability is also shown for climbing flight and autorotation at 65 kt. Blade pitch travel margins are noted to be adequate for control in these cases. The fan null-thrust condition has been avoided in Aerospatiale tests. This condition is recognized as a problem and should be investigated.

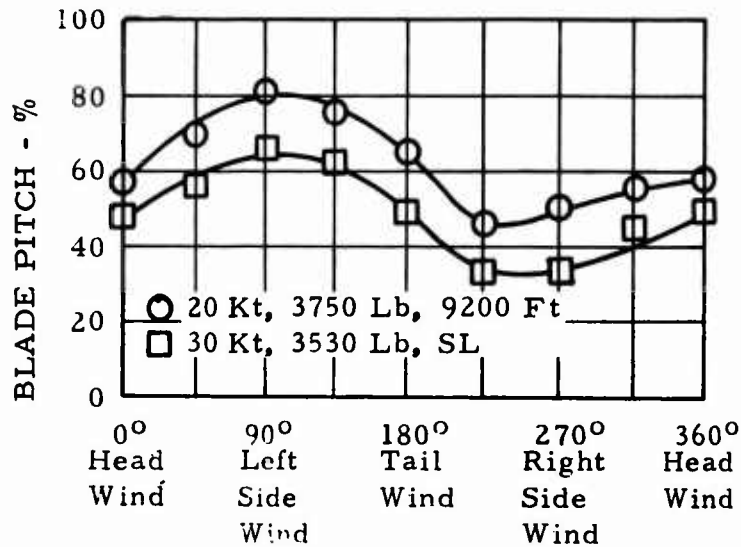


Figure 25. Fenestron Blade Pitch Required for Hover, SA 341.

### Weight

A weight breakdown of the conventional tail rotor and Fenestron used in the SA 340 and 341 respectively is given in Table III.

A weight penalty of 16.5 lb is noted for the Fenestron. However, the conventional system for this size helicopter does not have a pylon, an intermediate gearbox, or servo controls as is the case with larger vehicles.

### Fenestron Acoustical Comparison Study

The fan-in-fin antitorque device is acoustically compared to the conventional tail rotor on two aircraft. The SA 318, Alouette II, two-bladed tail rotor, which is the same as the tail rotor installed on the SA 340, is compared to the SA 341 Fenestron.

Tests conducted by Aerospatiale compared the noise levels of the SA 318 (Alouette II) tail rotor to the SA 341 Fenestron fan-in-fin. This comparison is made since both helicopters are of the same weight and power class and require almost identical antitorque thrust levels. The results are documented in Reference 14 (excerpts from Reference 14 are presented in Appendix III).

The calculated fan-in-fin noise levels are based on Reference 12, which

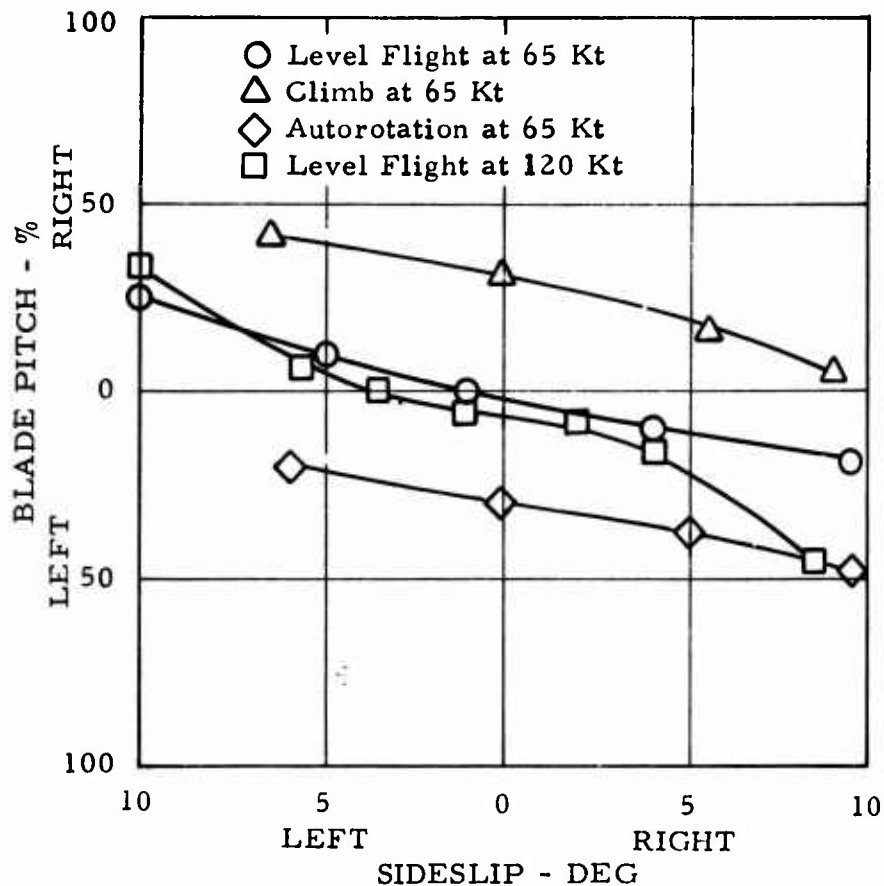


Figure 26. SA 341 Fenestron Blade Pitch in Forward Flight, Climb, and Autorotation, Wt=3530 Lb.

is the procedure developed by Hamilton Standard for predicting propfan noise. Conventional tail rotor noise levels were estimated using Reference 13.

The calculated noise levels are based on the assumption of spherical spreading of sound. Ground-cover attenuation is neglected because frequency - times - distance is low for the major harmonics. The atmospheric absorption was also found to be negligible for the low frequencies of the tail rotor and for the short distances used in the comparison.

Table IV shows the parameters used to predict the maximum noise levels for the two types of antitorque devices. The table also shows the results of ground tests obtained from Reference 14 for the lightweight helicopters. In general, it can be concluded that fan-in-fin maximum

TABLE III. COMPARISON OF ANTITORQUE DEVICE WEIGHTS		
	SA 340 With Conventional Tail Rotor - lb	SA 341 With Fenestron Rotor - lb
Airframe, including:	71.0	92.6
Tail boom		
Tail fin		
Stabilizer		
Protective guard or shoe		
Transmission, including:	28.6	26.4
Tail rotor gearbox		
Tail rotor drive inst.		
Controls, including:	3.3	7.0
Control linkage		
Servo units and lines (for SA 341)		
Rotor, including:	18.7	12.1
Hub		
Blades		
TOTAL	<u>121.6</u>	<u>138.1</u>

noise levels are slightly higher than comparable tail rotors if directivity is not considered.

Table V is a comparison of the directivity between the SA 318 tail rotor and the SA 341 fan-in-fin. It shows that the tail rotor is relatively insensitive to direction but vice versa for the fan-in-fin. The data in this table was obtained from Reference 14. Excerpts from Reference 14 and other French data is presented in Appendix III.

TABLE IV. FENESTRON NOISE LEVEL COMPARISON		
	SA 318 Tail Rotor	SA 341 Fan-in-Fin
PNL @ 25M (82 ft) - PNdb	78	87
Test PNL @ 25M	78	87
PNL @ 50M (164 ft) - PNdb	72	81
Test PNL @ 50M	72	75
Tip Speed - fps	670	690
Antitorque Power - hp	28	60
Diameter - ft	6.3	2.3
No. Blades	2	13
Thrust - lb	236	240

TABLE V. FENESTRON NOISE DIRECTIVITY COMPARISON			
	SOUND PRESSURE LEVEL (db re 0.0002 $\mu$ bar) AZIMUTH*		
	0°	44°	96°
SA 318 Tail Rotor	78	78	77
SA 341 Fan-in-Fin	78	84	75
* 0 azimuth aft			

## PRELIMINARY DESIGN

### PRELIMINARY DESIGN OBJECTIVE

The objective of the preliminary design task was to design a fan-in-fin antitorque device for the SA 330 "Puma." Information obtained from the analysis of existing data was used to define a fin size and fan disc loading combination. A preliminary design of the resulting fan/fin combination was accomplished. The predicted performance of the ducted fan aircraft was generated and compared to the actual performance of the conventional SA 330.

### BASE-LINE AIRCRAFT

The SA 330 "Puma," a utility tactical transport having a maximum gross weight of 14,110 lb, was selected as the base-line conventional system to study the application of a ducted propeller antitorque device. The SA 330, shown in Figure 28, features a single four-bladed articulated main rotor and a five-bladed pusher type tail rotor, described in Table VI. The main rotor rotates in a clockwise direction when viewed from above.

	Main Rotor	Tail Rotor
Diameter - ft	49.26	10.24
No. of Blades	4	5
Solidity Ratio	0.09	0.19
Rotational Speed - rpm	265	1279
Articulation	Full	Flapping

The SA 330 is powered by two Turbomeca Turmo III C-4 free turbine engines. The two engines are connected to a main gearbox through which power is transmitted to the main rotor and to the tail rotor by means of a tail drive shaft, an intermediate gearbox, and a tail gearbox. Installed

engine performance is given in Figure 27.

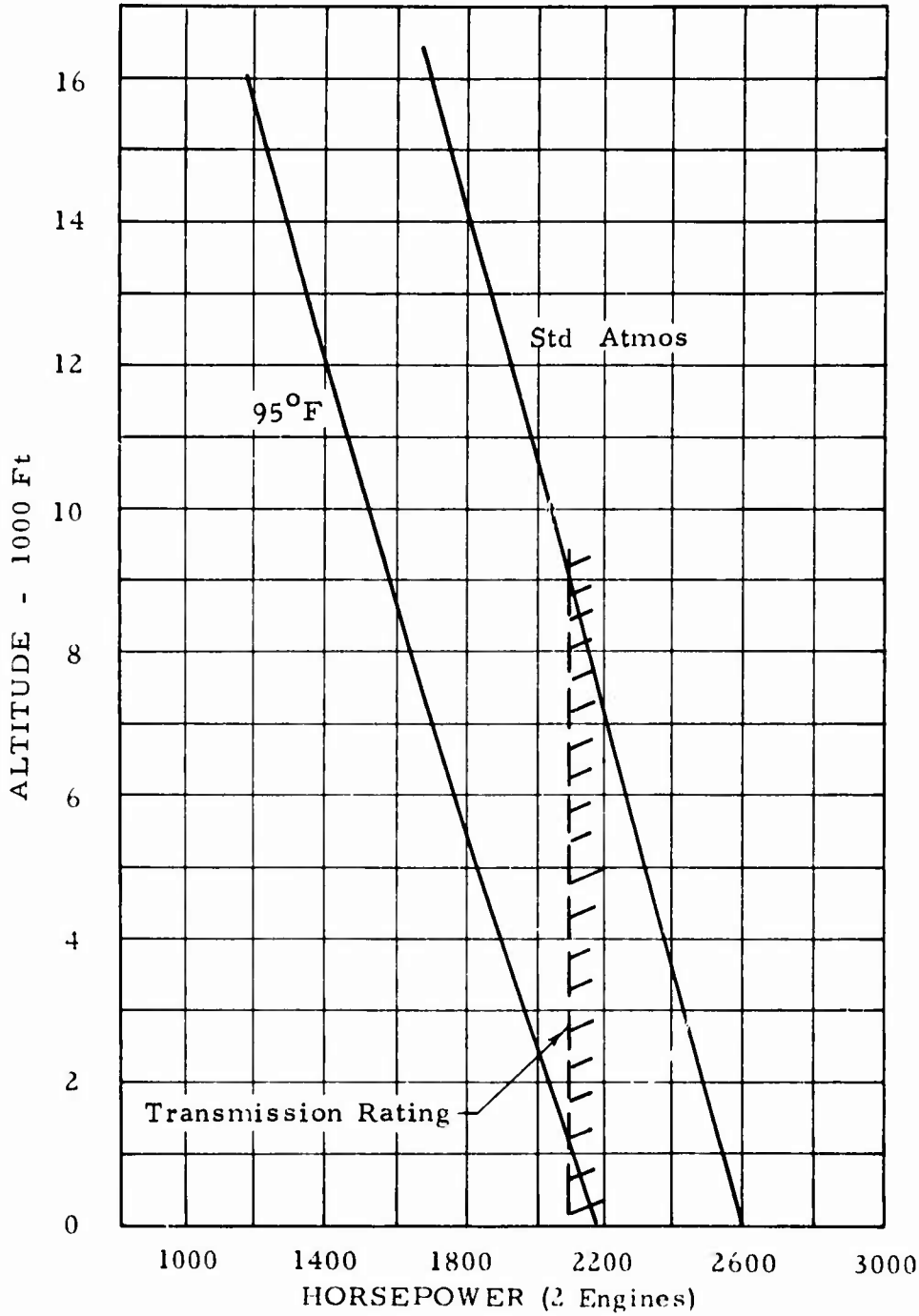


Figure 27. SA 330 Engine Power Available.

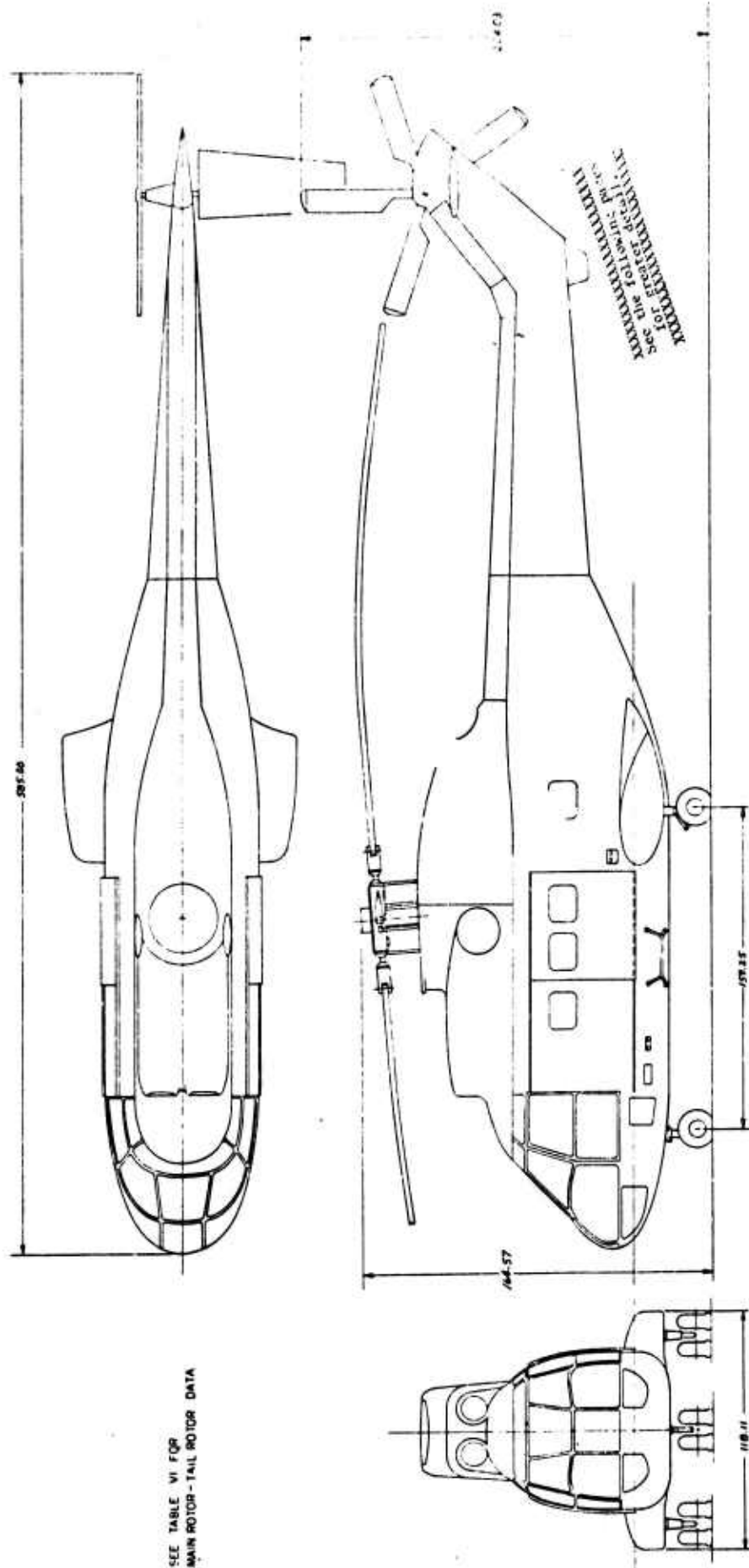


Figure 28. SA 330 Puma, Utility Tactical Transport.

37.3

37.2

37.1

A

SEE TABLE VI FOR  
MAIN ROTOR - TAIL ROTOR DATA

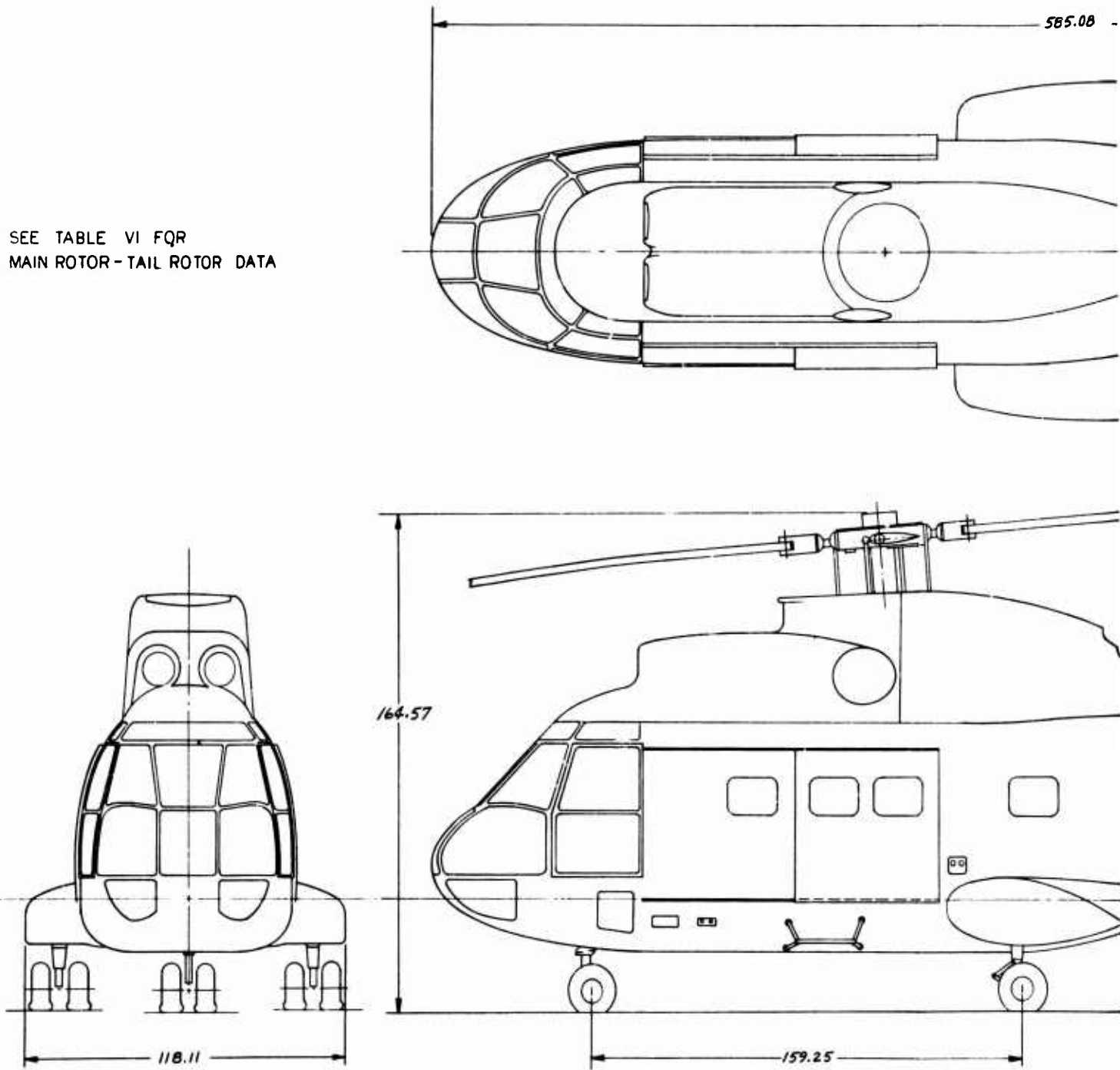
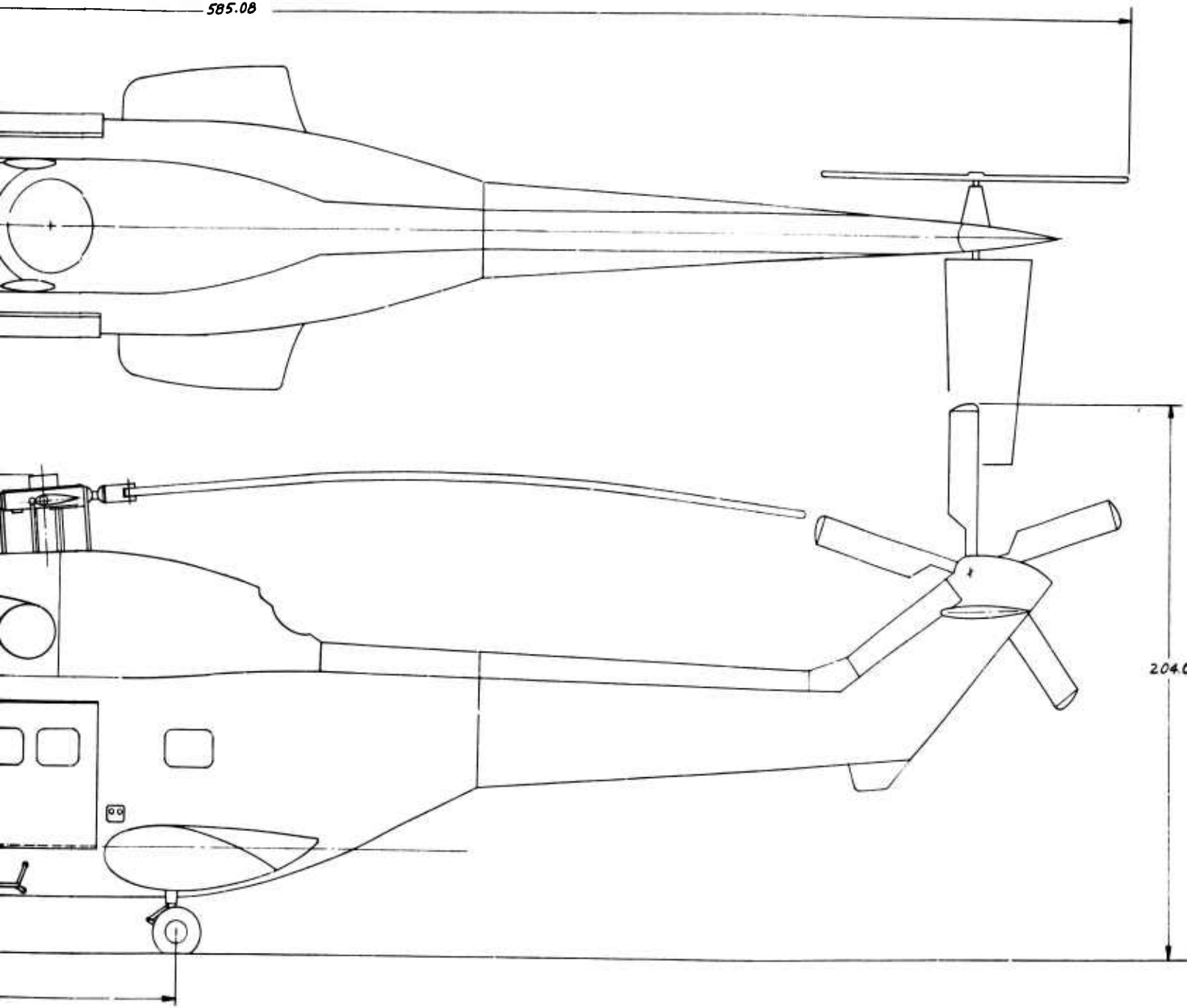


Figure 28. SA 330 Puma, Utility Tactical Transport.

B

585.08



37.2

37.3

The power required to hover OGE was estimated by the methods outlined in Appendix II as the sum of the main rotor power, tail rotor power, and power due to accessories and mechanical losses. The antitorque thrust was determined from the main rotor torque. Fin interference effects are taken into account in determining the tail rotor thrust in hover. It is estimated from Figure 5 of Reference 15 that fin force reduces the tail rotor thrust achievable by 10 percent for the SA 330 pusher tail rotor. Thus, the net tail rotor thrust required was 1.11 times the antitorque thrust. In forward flight, fin interference effects were considered to be minimal. Accessory power and power due to mechanical losses are estimated to be 5 percent of the total power required. Hover power required for various gross weights at SL STD and 4000 ft, 95°F is shown in Figure 29 and power required in forward flight in Figures 30 and 31. A comparison of the described power prediction methods and flight test data shows good agreement, thus verifying this approach.

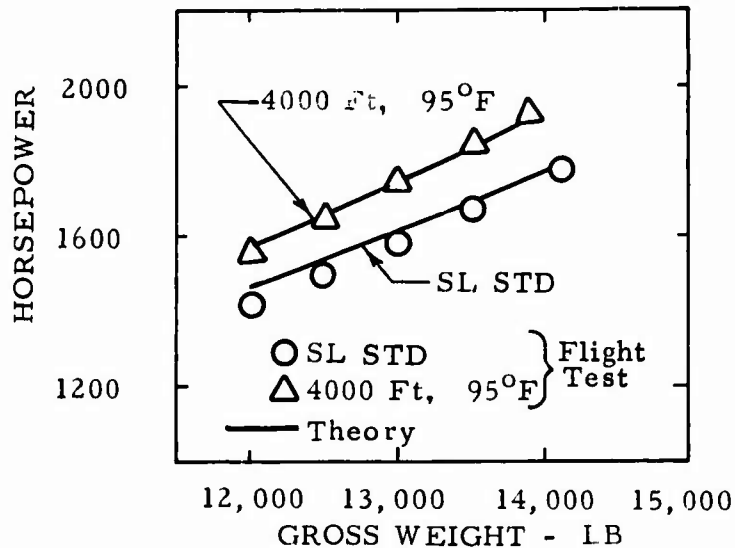


Figure 29. Comparison of Predicted Hover Power Required With Flight Test Data, SA 330.

### PARAMETRIC ANALYSIS OF FAN DESIGN PARAMETERS

Parametric fan performance was generated to study the design parameters and to establish sizing criteria. The methods used are discussed in the following paragraphs.

**Preceding page blank**

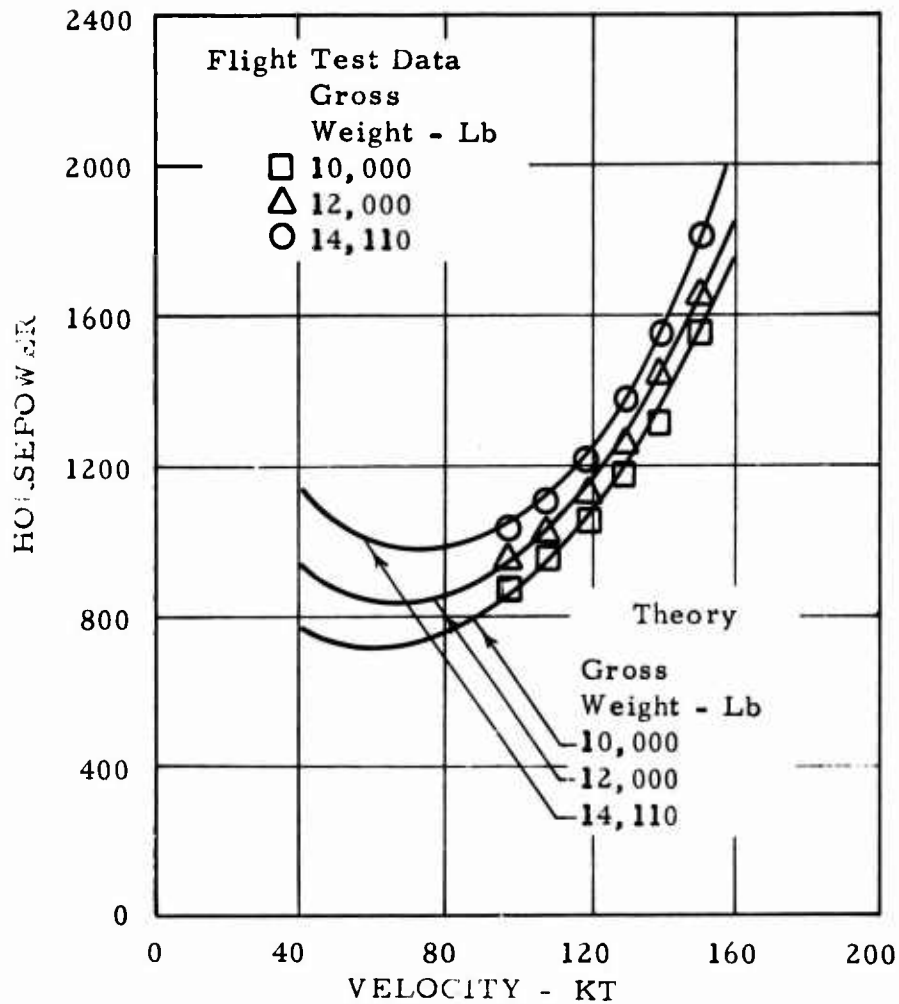


Figure 30. Comparison of Predicted Power Required in Forward Flight With Flight Test Data, SL STD, SA 330.

Fan Thrust Vs. Horsepower and Disc Loading

Parametric ducted propeller performance was generated for the purpose of sizing a propeller for a fan-in-fin configuration at static conditions. Data from Reference 16 was used to generate an achievable envelope for a given blade camber and hub-tip radius ratio, while activity factor (solidity) was allowed to vary. The resulting envelope was then used to obtain the parametric performance shown in Figure 32.

Similar methods were employed to obtain a limited parametric performance at a cross-wind speed of 35 kt, which is presented in Figure 33. This parametric plot allowed further refinement of initial sizing and assured the capability to meet side-wind requirements.

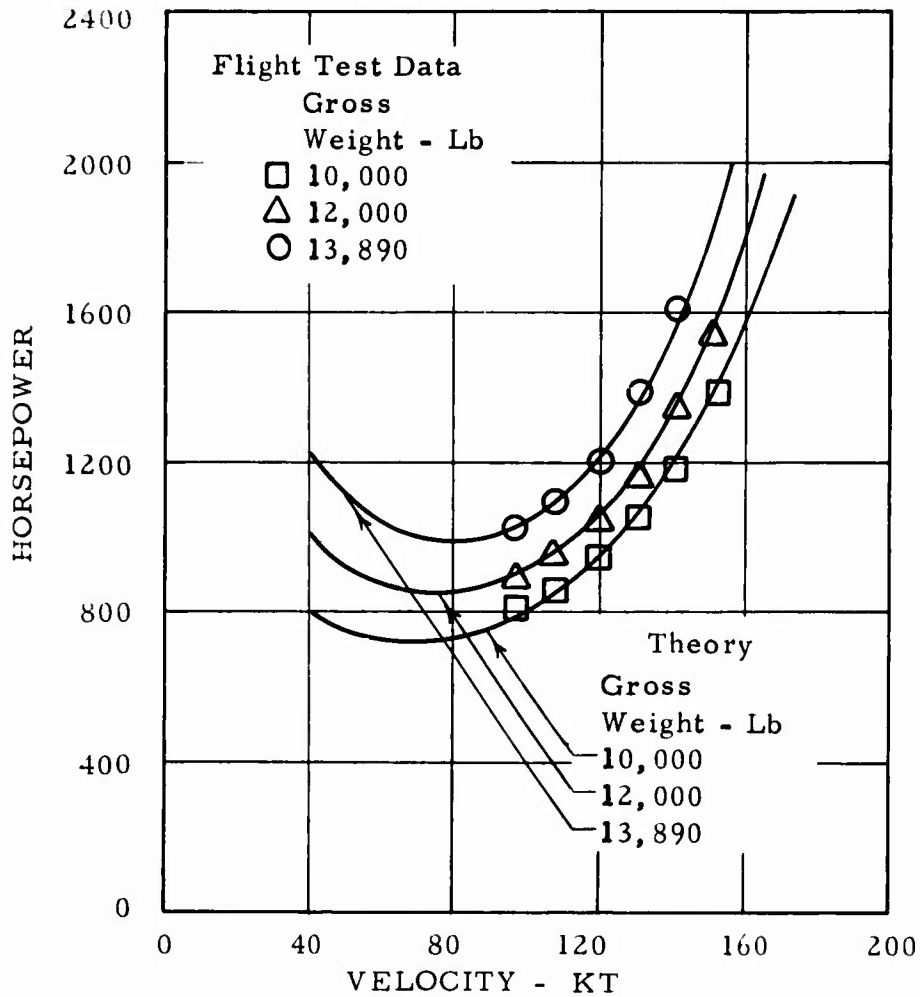


Figure 31. Comparison of Predicted Power Required in Forward Flight With Flight Test Data, 4000 Ft, 95°F, SA 330.

Both of these figures reflect basic state-of-the-art data modified by the thrust correction factor presented in Figure 2.

#### Antitorque System Thrust Requirements in Hover

The thrust required in hover from an antitorque device is the lateral yawing thrust necessary to balance the main rotor torque plus the thrust necessary for yaw control and side-wind trim. For hover control in still air, paragraph 3.3.5 of MIL-H-8501A specifies a yaw displacement of at least  $30/(W + 1000)^{1/3}$  degrees after 1 second at the maximum overload gross weight. Paragraph 3.3.6 requires a yaw angular displacement of  $110/(W + 1000)^{1/3}$  degrees after 1 second for control while hovering in a 35-kt adverse side wind at the maximum weight. For the SA 330,

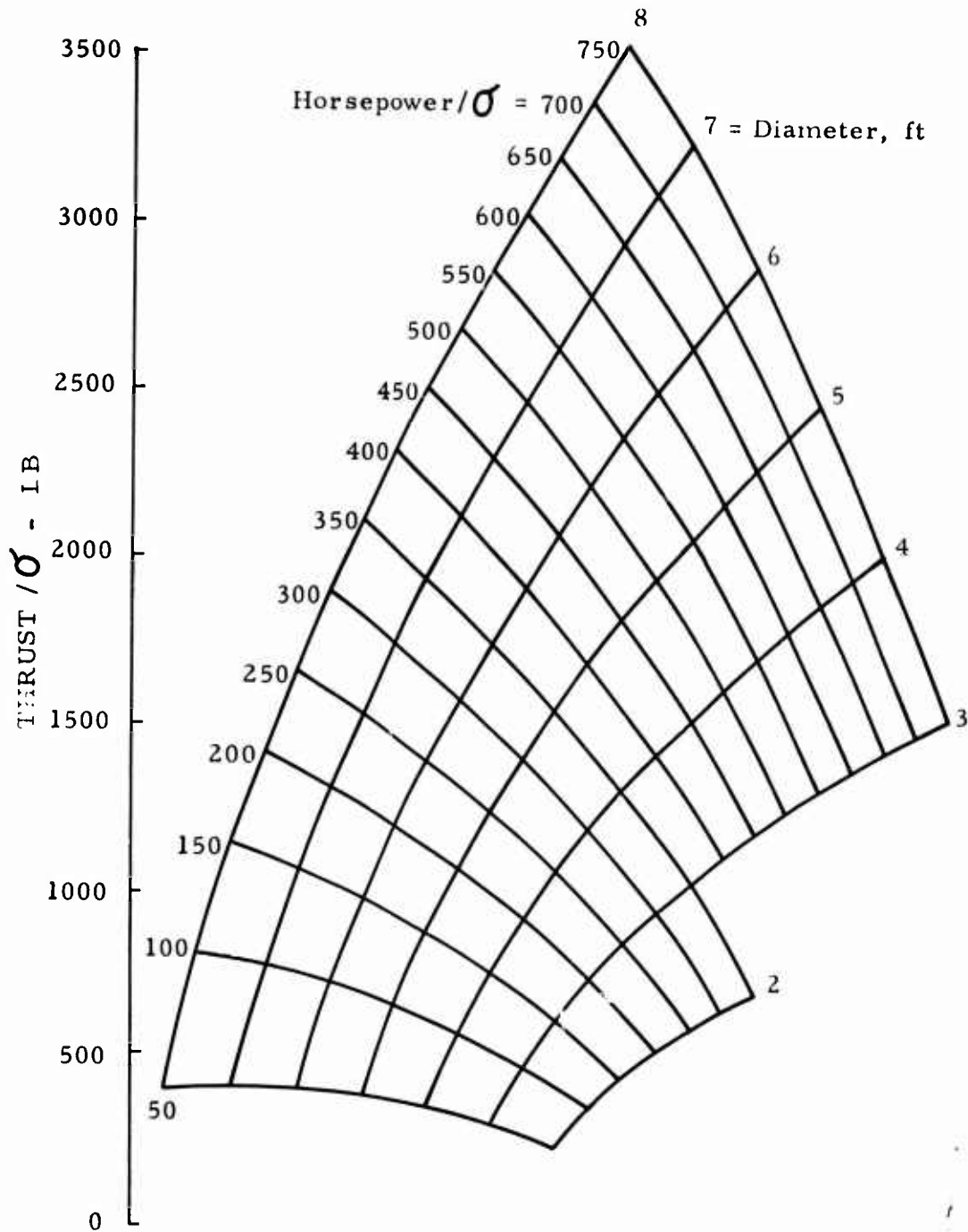


Figure 32. Parametric Ducted Propeller Referred\* Static Performance for Blades With 0.3 Design Lift Coefficient, a Hub-Tip Radius Ratio of 0.3, and a Duct Length-to-Diameter Ratio of 0.2. (\*Referred - Adjusted to SL STD Conditions).

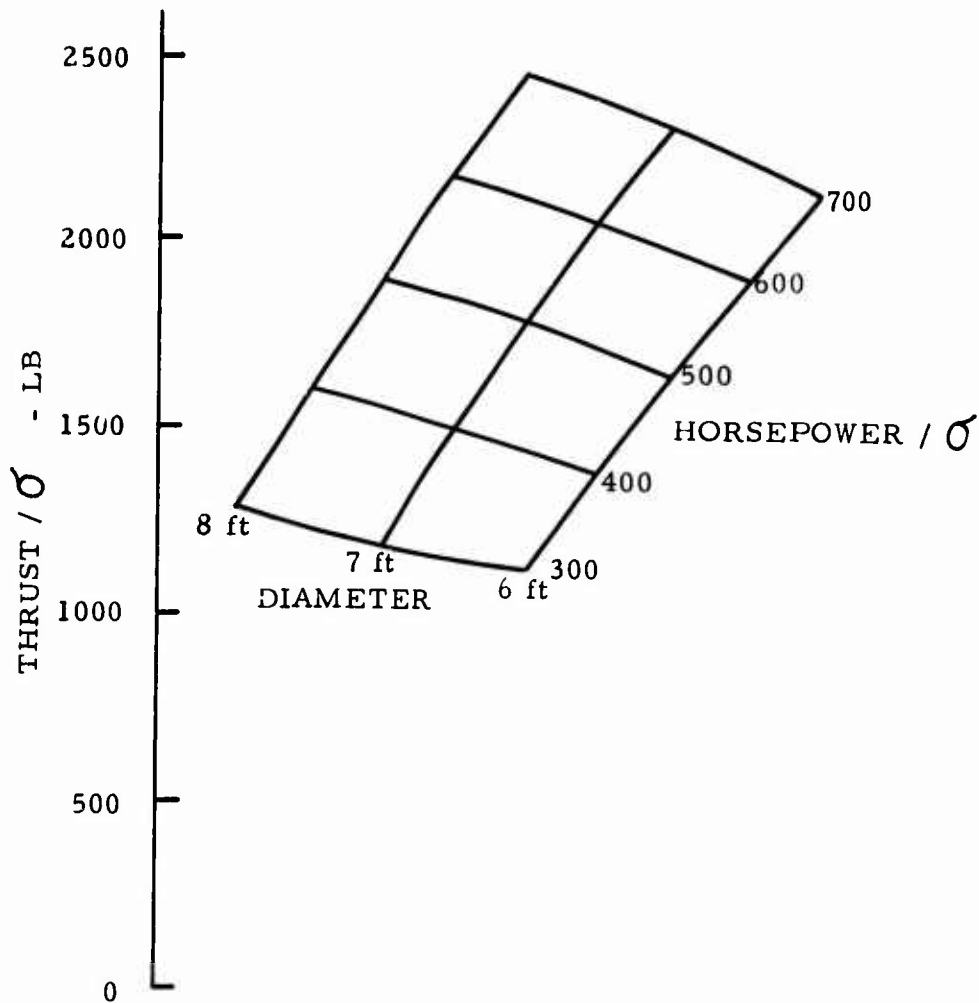


Figure 33. Parametric Ducted Propeller Referred\* Performance at a 35-kt Crosswind for Blades With 0.3 Design Lift Coefficient, a Hub-Tip Radius Ratio of 0.3, and a Duct Length-to-Diameter Ratio of 0.2. (\*Referred - Adjusted to SL STD Conditions).

at the maximum certified weight of 14,110 lb, an angular acceleration of  $0.648 \text{ rad/sec}^2$  is needed to meet the criteria of paragraph 3.3.5 and a  $2.016 \text{ rad/sec}^2$  acceleration in the case of a 35-kt side wind. Table VII gives the resulting sea level standard day thrust requirements for the SA 330 in hover at a forward cg position. A side study showed the forward cg position to be the most critical requirement for the SA 330.

#### Fan Diameter Sensitivity in Hover

To evaluate the influence of the MIL-H-8501A control requirements and the effect on performance requirements of hot-day conditions at altitude,

TABLE VII. SA 330 HOVER CONVENTIONAL ANTITORQUE SYSTEM THRUST REQUIREMENTS, SL STD, FORWARD CG		
THRUST REQUIREMENT	THRUST REQUIRED	
	0-KT WIND (Paragraph 3.3.5)	35-KT SIDE WIND (Paragraph 3.3.6)
Antitorque	1023	825
Yaw Control	495	165
Side-Wind Trim	-	504
Total	1518	1494

a study of fan diameter sensitivity with helicopter gross weight was carried out. Hover performance for the SA 330 was generated at a sea level standard day and at 4000 ft, 95°F day for three conditions:

1. 0-kt wind
2. 0-kt wind and yaw requirement of paragraph 3.3.5, MIL-H-8501A
3. 35-kt side wind and yaw requirement of paragraph 3.3.6, MIL-H-8501A

For each of these conditions, the antitorque thrust plus the maneuver thrust required was determined for a range of weights from 12,000 lb to 14,110 lb. The maximum power available to the antitorque device at the selected weights was assumed to be the total engine power available minus the main rotor power and power due to mechanical losses. Thus for each gross weight and thrust requirement, a fan could be uniquely sized from Figure 32 or from Figure 33 for a 35-kt side wind. The resulting fan diameters are then the minimum size needed to meet each requirement. Table VIII shows the minimum fan diameters required for a modified SA 330 at sea level, standard day conditions. Also shown for comparison at each condition is a fan diameter which will produce the required thrust for the same power that is absorbed by the conventional 10.24-ft-diameter tail rotor. It can be noted that a 6.4-ft-diameter fan sized to give equal performance to the conventional tail rotor at zero wind is larger than the fan diameter required to meet the most severe sizing requirement of a 35-kt side wind with a yaw maneuver using all available antitorque power.

TABLE VIII. MINIMUM REQUIRED FAN DIAMETERS FOR A MODIFIED SA 330, SL STD					
WIND	YAW ACCEL REQUIREMENT	THRUST REQUIRED (lb)	FAN DIA (ft)	TAIL ROTOR POWER REQ. (hp)	EQUIV. FAN DIA (ft)
0 kt	NO	1023	2.7	152	6.4
0 kt	YES	1518	4.1	258	6.7
35 kt Side Wind	YES	1494	6.2	363	8.0

The sensitivity of antitorque power required with fan diameter to hover OGE at sea level is presented as a function of total power required in Figure 34 for different takeoff gross weights. The 6.4-ft-diameter fan is shown to require the same power as the 10.24-ft-diameter conventional tail rotor presently installed on the SA 330. The effect of smaller diameter fans is shown to be an increase in total power required. At 14,110 lb, the increase in total power is 1.5 percent for a 5.5-ft-diameter fan and 3.3 percent for a 4.5-ft-diameter fan.

The increase in power required for smaller fans results in performance penalties such as a decrease in payload for a given power. Limited to the power required to hover with a tail rotor at a weight of 14,110 lb, it is estimated that the takeoff weight would drop to 13,950 lb with a 5.5-ft fan and to 13,700 lb with a 4.5-ft fan, a loss in payload of 160 lb and 410 lb respectively.

Figure 35 gives the minimum fan diameter required with gross weight for the SA 330 in hover OGE at 4,000 ft on a 95°F day. This figure shows that an increase in gross weight indicates a need for a larger antitorque fan. Larger gross weights require more main rotor power which increases the torque and decreases the power that is available for antitorque purposes. Thus, for a helicopter with a given total power, a good way to increase antitorque fan thrust with a minimum increase in fan power, is to increase the fan size. If the fan is sized to a minimum diameter that increases with the decreasing available antitorque power, the upper limit on fan size will be dictated by weight and structural considerations. Within these constraints there is a minimum fan size associated with each gross weight. Increasing the fan diameter from 4 ft to 5 ft results in a 2.4-percent increase in the gross weight hover capability at 4,000 ft, 95°F and a 4.9-percent

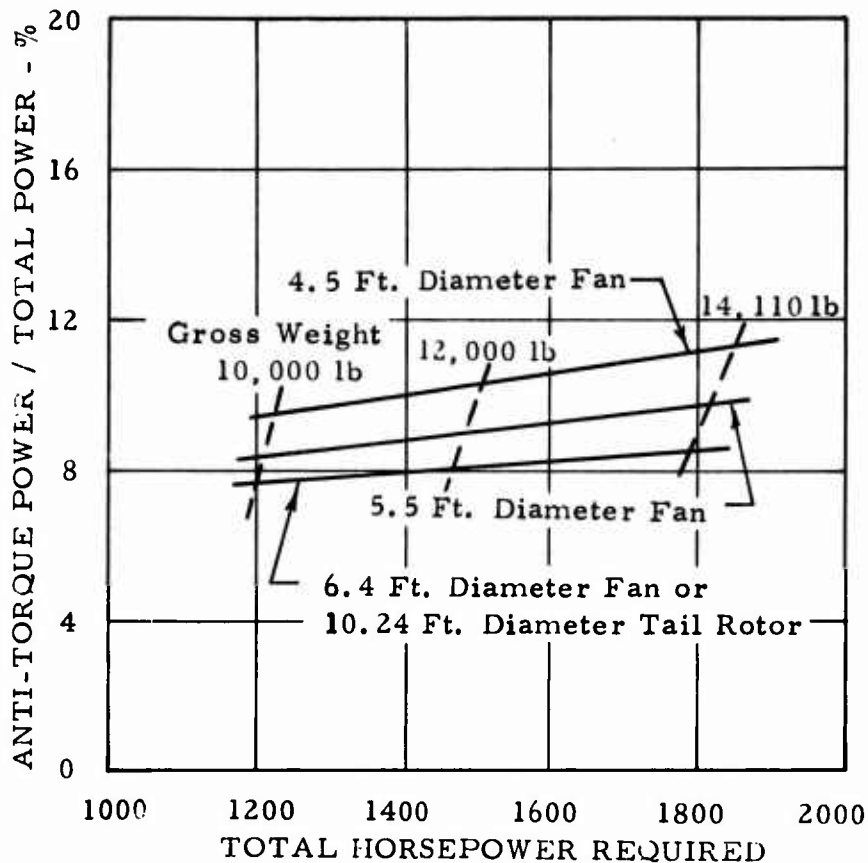


Figure 34. Comparison of Antitorque Power Required in Hover for Various Fan Diameters, SL STD

increase in the gross weight hover capability with the zero wind yaw requirements.

The influence of fan size on OGE hover ceilings, defined by power required and power available, is shown in Figure 36. A 1-ft increase in fan diameter is shown to increase the hover ceiling approximately 500 ft.

#### Fan Design Selection

The fan selection with respect to diameter was initially estimated by momentum theory considerations. It can be shown that the addition of a circular duct around a propeller increases its thrust by a factor of two. Therefore, assuming an existing rotor to be adequate, a ducted propeller (fan) would provide equivalent static performance with one-half the disc area of the tail rotor. Applying this rationalization to the SA 330, the existing 10.24-ft-diameter tail rotor could be replaced by a ducted propeller

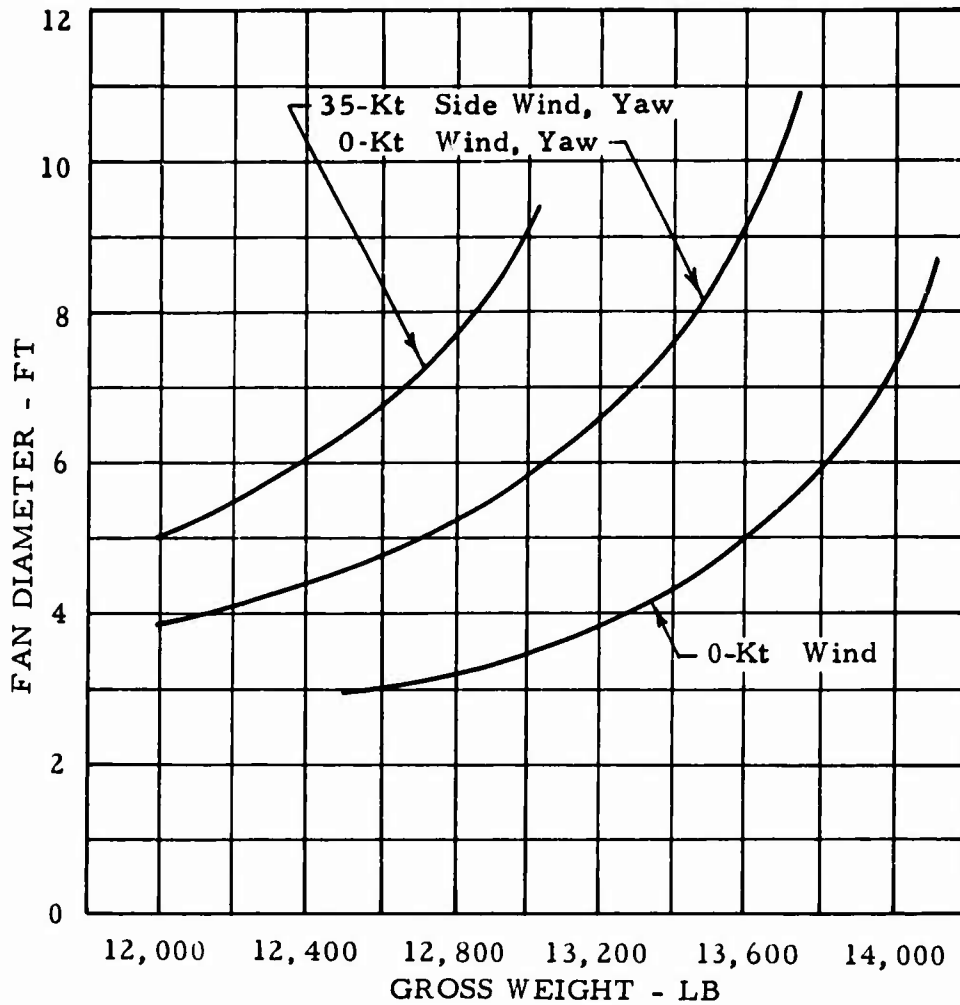


Figure 35. Fan Diameter Required To Hover OGE at 4,000 Ft, 95°F Vs. Takeoff Gross Weight.

7.24 ft in diameter ( $10.24 / \sqrt{2} = 7.24$ ). From the standpoint of the figure of merit (static efficiency), the addition of the circular duct drastically reduces tip losses. Also, the use of cambered airfoil sections, the addition of blade twist, and the use of optimized exit diffusion increases the figure of merit. Any increase in the figure of merit therefore further reduces the size required to yield performance equivalent to a conventional tail rotor.

The 6.4-ft-diameter fan has been selected as the design point for this application. The selection was based on its capability for no-wind, hovering performance, equivalent to the 10.24-ft-diameter conventional tail rotor, its ability to achieve the yaw requirements of MIL-H-8501A,

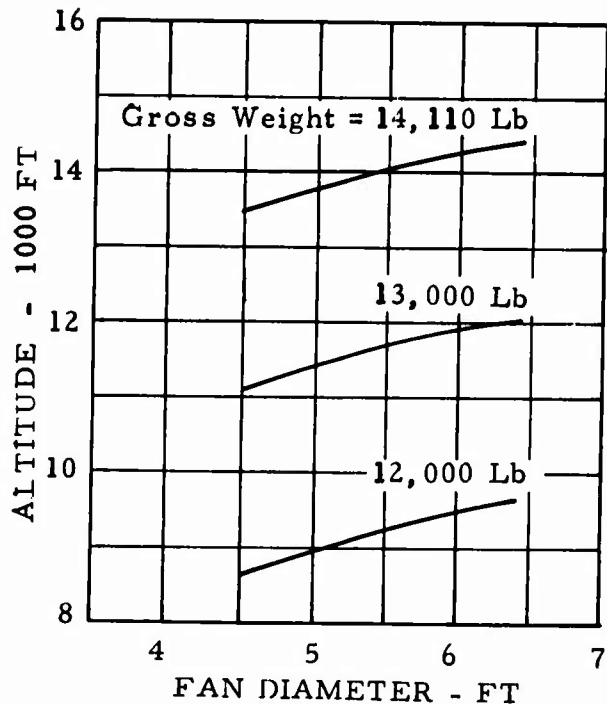


Figure 36. Influence of Fan Diameter on OGE Hover Ceilings.

and its good performance at the 4,000 ft, 95°F condition.

To evaluate the yaw control for this size fan in hover, the yaw angular displacement after 1 second following a full pedal input was estimated. The yaw equation of motion including the basic helicopter damping was solved. It was assumed that a 0.2-second ramp control input would give full fan thrust; this assumption was based on what Aerospatiale gives as a valid figure for the fan response of the SA 341. Figure 37 presents the resulting yaw angular displacement after 1 second as a function of hover gross weight and density altitude.

### FIN DESIGN

A vertical fin was sized for the SA 330 to provide optimum operation of the fan-in-fin system in forward flight. The following paragraphs present the philosophy and rationale on which the fin design was based.

#### Philosophy

A decision to employ a fan-in-fin antitorque device in place of a conventional helicopter tail rotor places an emphasis on antitorque systems

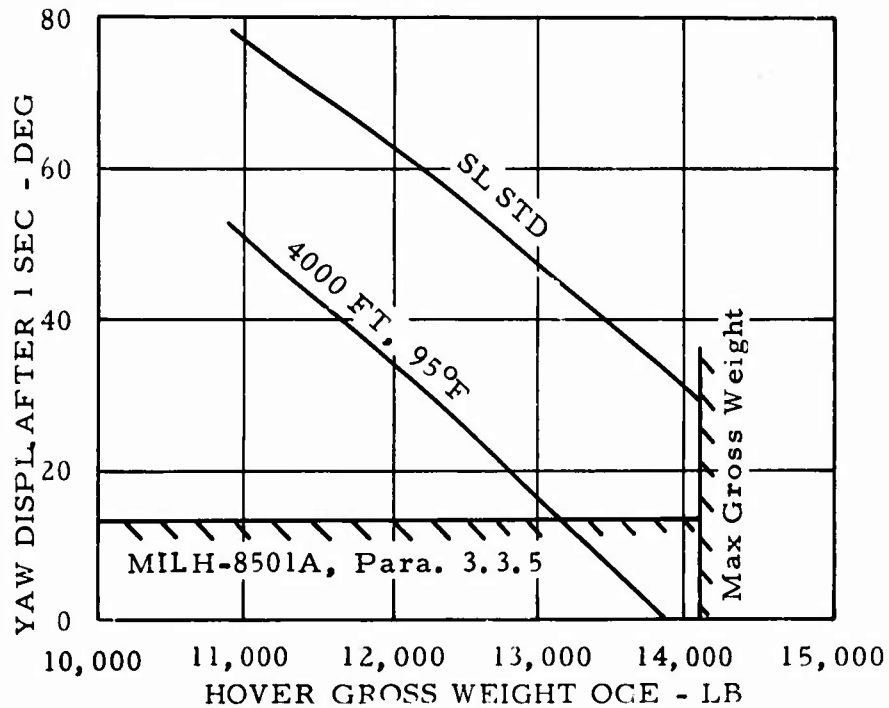


Figure 37. SA 330 Fan-in-Fin Estimated Hover Yaw Response Following Full Control Input.

that is new to helicopter design. The fin can only be designed to a specific gross weight and speed condition. Since nearly all of the helicopter operation will not coincide with the fin design point and since it is desirable in cruise flight to keep the fan thrusting at a low, constant level, a trimmable fin is attractive. Safety in autorotation is also provided by this approach. Thus, an initial consideration in developing the optimum antitorque fin was a means of providing this trim capability. A relatively large (one-third chord, one-third span) trailing-edge flap, mounted on the upper fin and deflectable both right and left, was chosen to provide this capability.

#### Design Requirements

Consideration is given to the selection of the gross weight and cruise speed combination to be used as a design point. Because fuel burn-off affects the antitorque thrust required, an operating gross weight less than the maximum weight of 14,110 lb was chosen. Considering the fuel burn-off, a helicopter gross weight of 13,230 lb was selected as a representative average weight for a typical transport mission.

Figure 38 presents the total antitorque thrust requirement and individual fan and fin contributions to this requirement for the SA 330 helicopter equipped with a fan-in-fin antitorque system in place of its conventional tail rotor. The total antitorque requirement for a gross weight of 13,230 lb at SL STD conditions was predicted with the previously discussed analytical method (see Figures 30 and 31) used to predict and correlate with the flight test data for the SA 330. The curve showing the fan contribution was predicted by the direct application of trends and percentage thrust from the flight test results of the SA 341. The fin contribution to total antitorque thrust is the difference between the total requirement and the fan contribution. This curve becomes the criterion for the overall size of a fin similar to that of the SA 341 and having similar lift characteristics.

A design speed was selected to cover a range of operating speeds below the maximum speed obtainable. Thus a range of trimmed cruise speeds can be achieved with a minimum of drag penalties due to the deflection of a trim device. An additional consideration was that the speed be in a range where a low and constant fan level can be assured. A fin design speed of 120 kt was then selected.

### Area

Several practical aspects were considered in selecting the fin size. Structural design, weight, and the size of the fan to be accommodated were the most important considerations. Directional stability was a secondary factor since flight experience with the SA 341 has demonstrated that the fan-in-fin system provided more stability than a conventional tail rotor. Some guidance in fin sizing was available because the fan was sized independently of all but the weight consideration. Fan-in-wing experimental data was used for guidance on relative fan and fin sizes. The fin lift coefficient of the SA 341 (Figure 24) at the selected design speed was used to calculate an initial fin size. The ratio of independently sized fan area to the calculated fin area was computed. The effect of this ratio on fin lift was estimated from fan-in-wing results from Reference 8. A possible 17-percent degradation in fin lift was indicated for the design speed. Applying this degradation to the assumed 341 lift coefficient, a new fin area was calculated. This area was then used with the known fin antitorque requirements to generate the SA 330 fin lift characteristics. This fin size was examined for compatibility with the fan by conducting a structural design and analysis and estimating the system weight. When compatibility of fan and fin was assured, the fin area was considered final. A fin area of 92 sq ft, which includes the lower crushable portion, the fan portion, and the upper fin with trim flap, was thus determined for the SA 330.

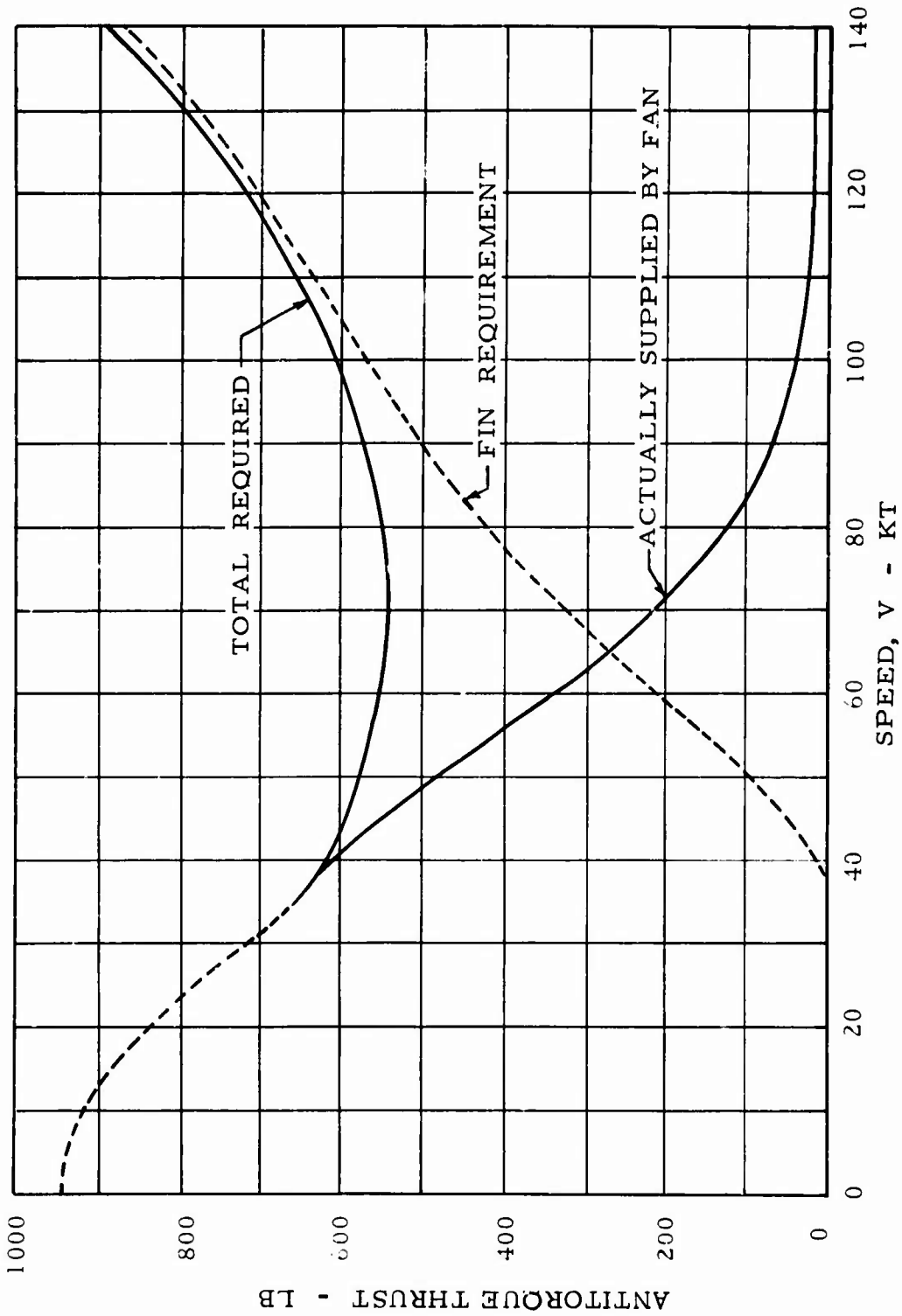


Figure 38. Modified SA 330 Antitorque Thrust Required in Forward Flight With Fan and Fin Contributions, SL STD, GW=13,230 Lb.

### Lift Coefficient

Converting the antitorque fin thrust required from Figure 38 to coefficient form, a curve of fin lift coefficient ( $C_L = \text{Fin Thrust}/qS$ ) versus speed is obtained in Figure 39. It can be noted that this curve has the same characteristics shown for the SA 341 in Figure 24. For the fin design speed of 120 kt, a fin lift coefficient of 0.153 is selected for the SA 330 design.

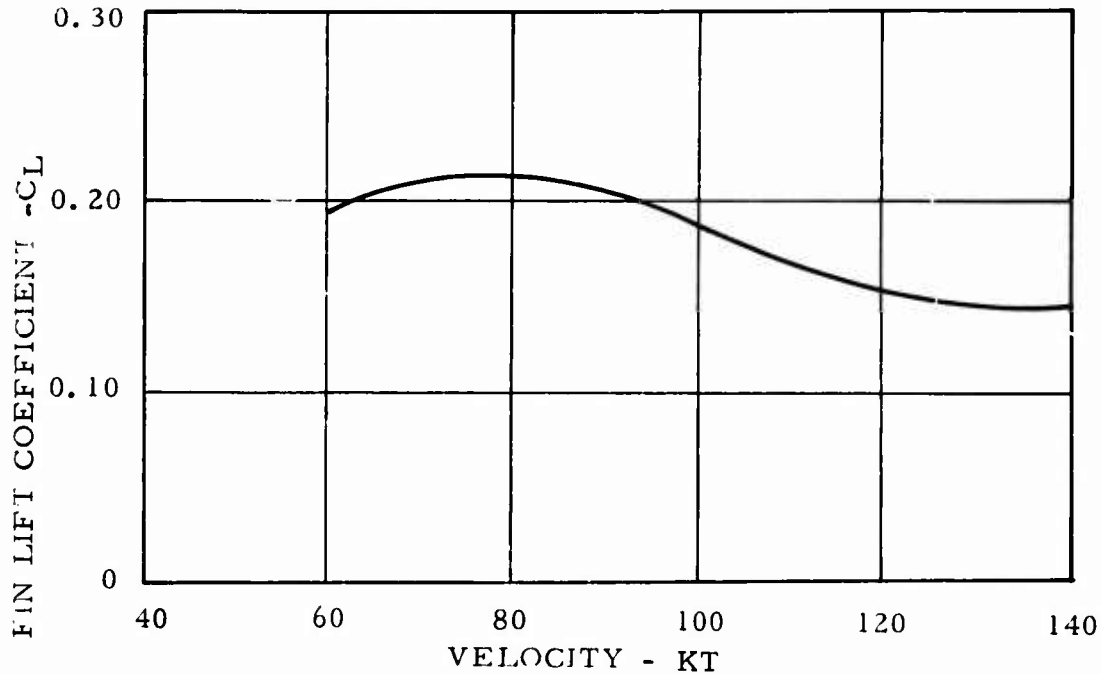


Figure 39. Predicted Fin Lift Characteristics With Speed for the SA 330 Fan-in-Fin Antitorque System, SL STD, GW=13,230 Lb.

### Lift Curve Slope

A lift curve slope of 0.053 per degree was obtained from SA 341 flight test results. The SA 330 fin was designed geometrically similar to the SA 341 fin with a similarly positioned fan providing the same end-plating effect in order to justify the use of the same lift curve slope. This should be a valid technique since both vehicles have similar shapes. Wind tunnel test results were not as applicable since in the case of the Fenestron model there was no helicopter tail boom or main rotor simulation. In the case of the 1/7 scale SA 341 model, there was no tail fan simulation giving end-plating effects.

### Camber and Incidence

The upper fin portion and the lower crushable tail skid were designed as symmetrical, noncambered panels. This selection was made because of the use of a trim flap which introduces effective camber in either direction. It was not desirable to add the effects of built-in camber in studying the basic technology. Thus, the only asymmetrical portion of the fin was the part that must accommodate the fan and its duct. The effective camber of this part of the fin may be determined from wind tunnel tests.

For a symmetrical (zero camber) fin, the cruise design lift must be attained by giving the fin the proper incidence angle. The cruise design lift coefficient has been determined to be  $C_L = 0.153$  at 120 kt, and the fin  $C_{L\alpha}$  has been established at a value of 0.053. These parameters combine to determine a fin incidence angle of 2.89 degrees; both the upper fin portion and the lower crushable skid should be set at this angle of incidence.

### Aspect Ratio

To preserve geometric similarity, it was desirable to set the SA 330 fin aspect ratio as near as possible to the SA 341 aspect ratio. The geometric aspect ratio was reduced from the SA341 value of 2.31 to 2.13 by establishing a fin span of 14 ft based on considerations of fin position relative to the main rotor. By placing the fin in a position similar to the SA 341 and its main rotor, the freestream flow and the SA 330 main rotor downwash should combine to form a similar flow field. Thus, significant changes in  $C_{L\alpha}$  and effective aspect ratio are not expected.

### Horizontal Stabilizer

A horizontal stabilizer was designed for a location on the helicopter tail boom ahead of the fan-in-fin. The existing 15-sq ft, single-panel, pylon-mounted horizontal stabilizer was replaced by an 18-sq ft, double-panel (9-sq ft on each side of the tail boom) surface having constant-chord, inverted airfoil section of 2 percent camber at zero incidence; a NACA 23012 would be adequate. The new area was determined in proportion to the shortened moment arm. The chord and span were selected to minimize interference with fan inlet flow and difficulty in ground handling.

### POINT DESIGN DESCRIPTION

The resulting point design and modified SA 330 are shown in Figure 40. A summary of the resulting parameters for the fan-in-fin point design is presented in Table IX. These parameters analytically describe the configuration and the limitations of the fan-in-fin design.

TABLE IX. SUMMARY OF FAN-IN-FIN DESIGN PARAMETERS

Fin Total Area	92 sq ft
Geometric Aspect Ratio	2.13
Fin Span	168 in.
Fin Thrust Load	1150 lb @ 156 kt
Fin Drag Load	110 lb @ 156 kt
Trim Flap Area	10.25 sq ft
Trim Flap Deflection	$\pm 30$ deg
Trim Flap Load (max design)	190 lb @ $\delta = 30^\circ$ 100 kt
Trim Hinge Moment (max design)	2292 in. -lb @ $\delta = 30^\circ$ 100 kt
Fan Diameter	6.4 ft
Hub-Tip Radius Ratio	.3
Fan Speed	2542 rpm
Fan Tip Speed	850 ft/sec
Number of Blades	13
Fan Blade Loading	77 lb/blade
Fan Thrust, Positive	2,000 lb
Fan Thrust, Reverse	1,000 lb
Fan Direction of Rotation	C. C. W. (facing inlet)
Fan Gearbox Power Rating	437 hp
Input Drive Shaft Speed	4888 rpm
Antitorque Moment Arm	360.36 in.
Ground Clearance Angle	8 deg



A

SEE TABLE IX FOR  
SUMMARY OF DESIGN PARAMETERS

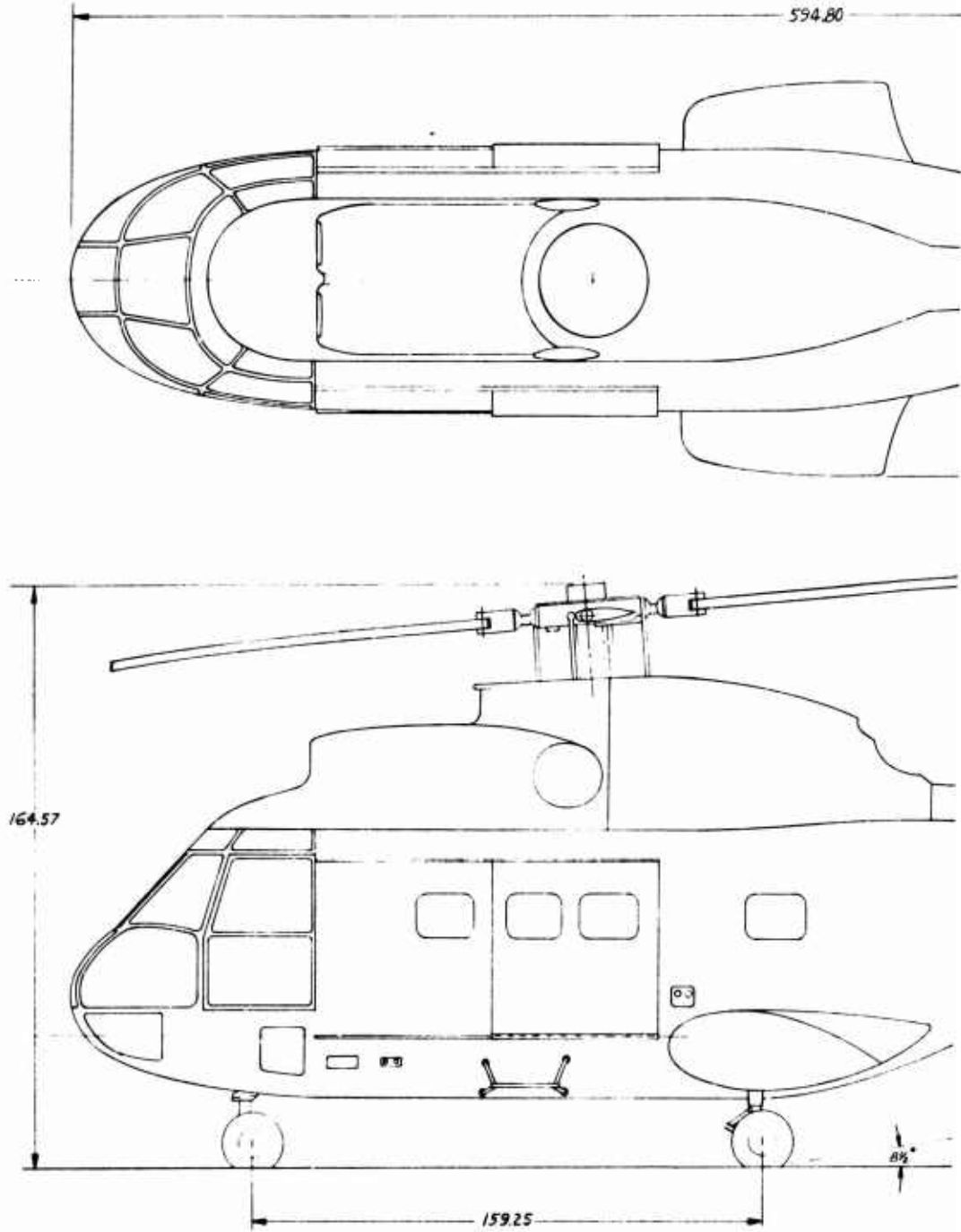
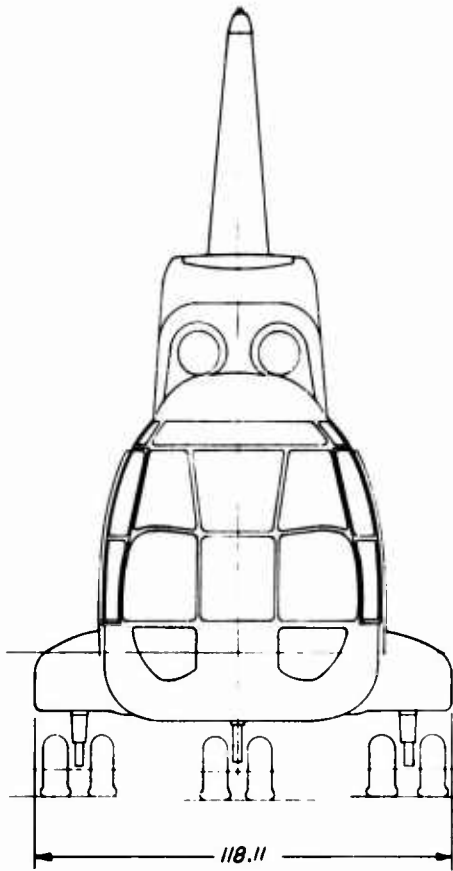
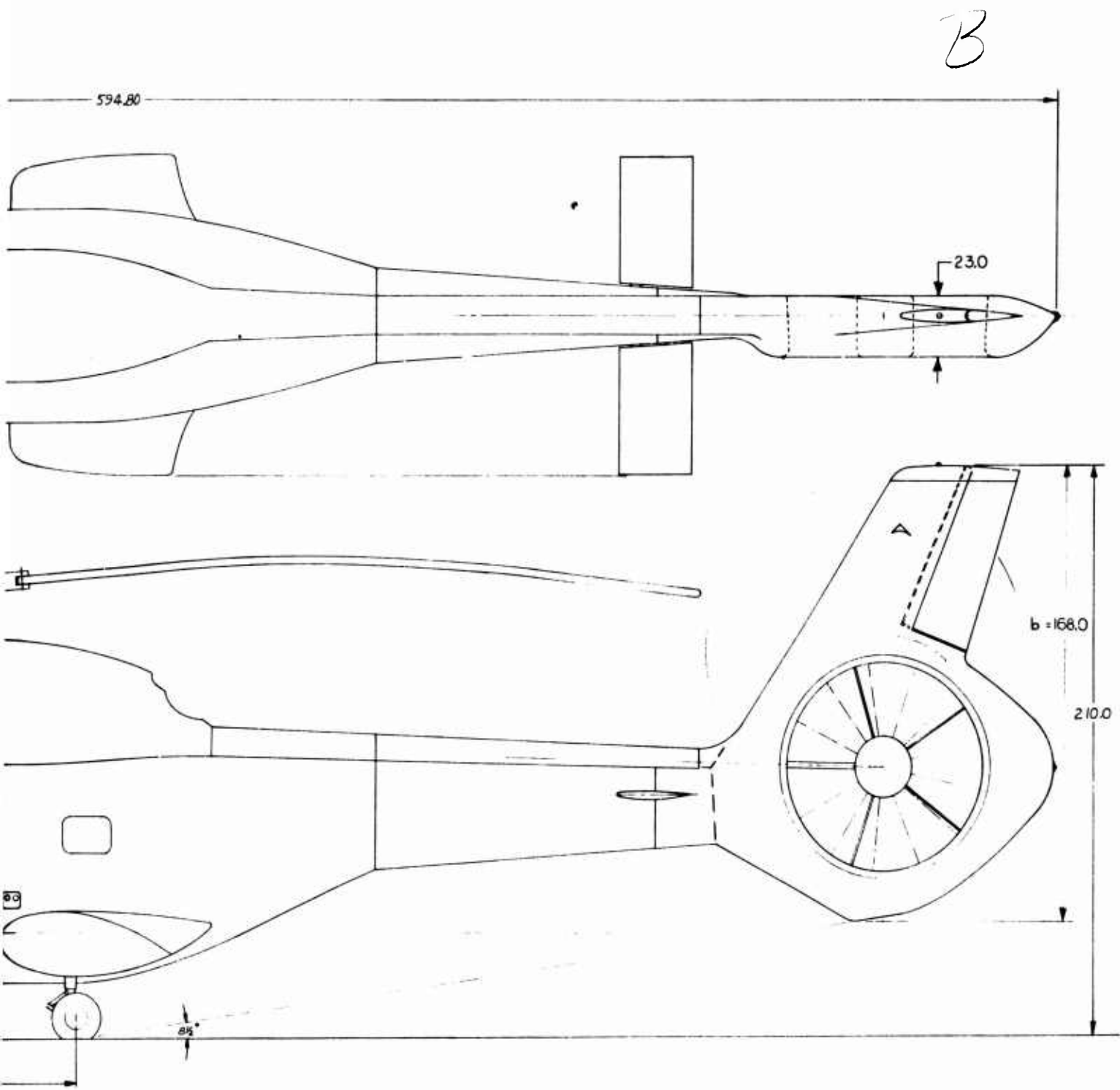


Figure 40. SA 330 With Fan-in-Fin.

55.2



55.2

55.3

## Structural Description

The preliminary design layout of the fan-in-fin on the SA 330 Puma is shown in Figure 41. The fin has an area of approximately 92 sq ft and a geometric aspect ratio of 2.13. The fin incorporates an in-flight adjustable trim flap hinged to the fin rear spar. A 13-bladed, 6.4-ft-diameter fan is mounted in the base of the fin in a duct with a length of 23 in. The fin is attached to the existing tail boom aft of the frame at station 471.65 by means of a splice plate.

The fan-in-fin structure and the interface with the SA 330 tail boom were designed to provide direct load paths with a minimum of compound panels. Aerodynamic contours are provided by means of fiberglass fairings. This configuration keeps tooling and subsequent manufacturing costs to a minimum.

The upper fin is tapered in both thickness and planform. It is a cantilevered, two-cell, four-flanged structure resisting bending and torsion caused by aerodynamic loading. The forward spar is continuous from the fiberglass tip fairing down to the tail boom. The forward spar and the leading-edge skin form a closed cell carrying the major portion of the loads from the upper fin to the boom. The aft spar closes off the second cell of the upper fin. The four spar flanges transmit most of the bending moments produced in the fin. Horizontal ribs are located in the structure to act as panel breakers.

The trim flap is hinged to the aft spar. It is a single-cell, two-flanged, tapered structure with intermediate ribs. The flap can be displaced  $\pm 30$  degrees by an electrical actuator located inside the lower end of the flap. The flap has a planform area of approximately 10 sq ft.

The fan support structure is made up of an integral torus ring of rectangular cross section. The fan duct and gearbox support struts are attached to this ring. Loads in the torus ring are beamed directly to the tail boom by the skins and stringers. The entire lower portion of the fin around the duct is covered by fiberglass aerodynamic fairings. A fiberglass foam-filled crushable tail skid allowing 8 degrees of aircraft rotation is located below the fan.

The tail boom splice is located just aft of an existing frame. The splice plate provides a continuous load path for stresses in the skin and stringers on both sides of the splice.

The horizontal stabilizer is located forward of the splice. It has an area of approximately 18 sq ft. The tail boom skin is strengthened by

**Preceding page blank**

doublers in the area where the support fittings are located. The stabilizer assembly consists of a continuous support tube extending through the boom. Ribs are attached to the tube, and a continuous skin is wrapped around and joined at the trailing edge.

All drive shaft components and hanger bearing supports of the SA 330 are utilized except for the short shaft extending forward of the fan gearbox. This shaft is supported at the forward end by a hanger bearing at the location of the SA 330 intermediate gearbox. The input shaft has a flexible coupling on the forward end and a spline coupling at the gearbox.

Fan Blade Design

Yaw control requirements at maximum gross weight and 4000 ft altitude, 95°F constituted the critical power and thrust combination chosen as the basis for the fan blade design. Physical size was established in the preliminary design effort. Blade aerodynamic characteristics were chosen based on parametric work done in other studies. A summary of all the design criteria is presented in Table X.

TABLE X. FAN BLADE DESIGN PARAMETERS	
Fan Diameter	6.4 ft
Fan Referred* Thrust Required	1966 lb
Fan Referred Power Available	400 hp
Airfoil Section	NACA 16 Series
Section Design Lift Coefficient	0.3
Number of Blades	13
Hub/Tip Radius Ratio	0.3
RPM	2542
* Referred - Adjusted to SL STD conditions	

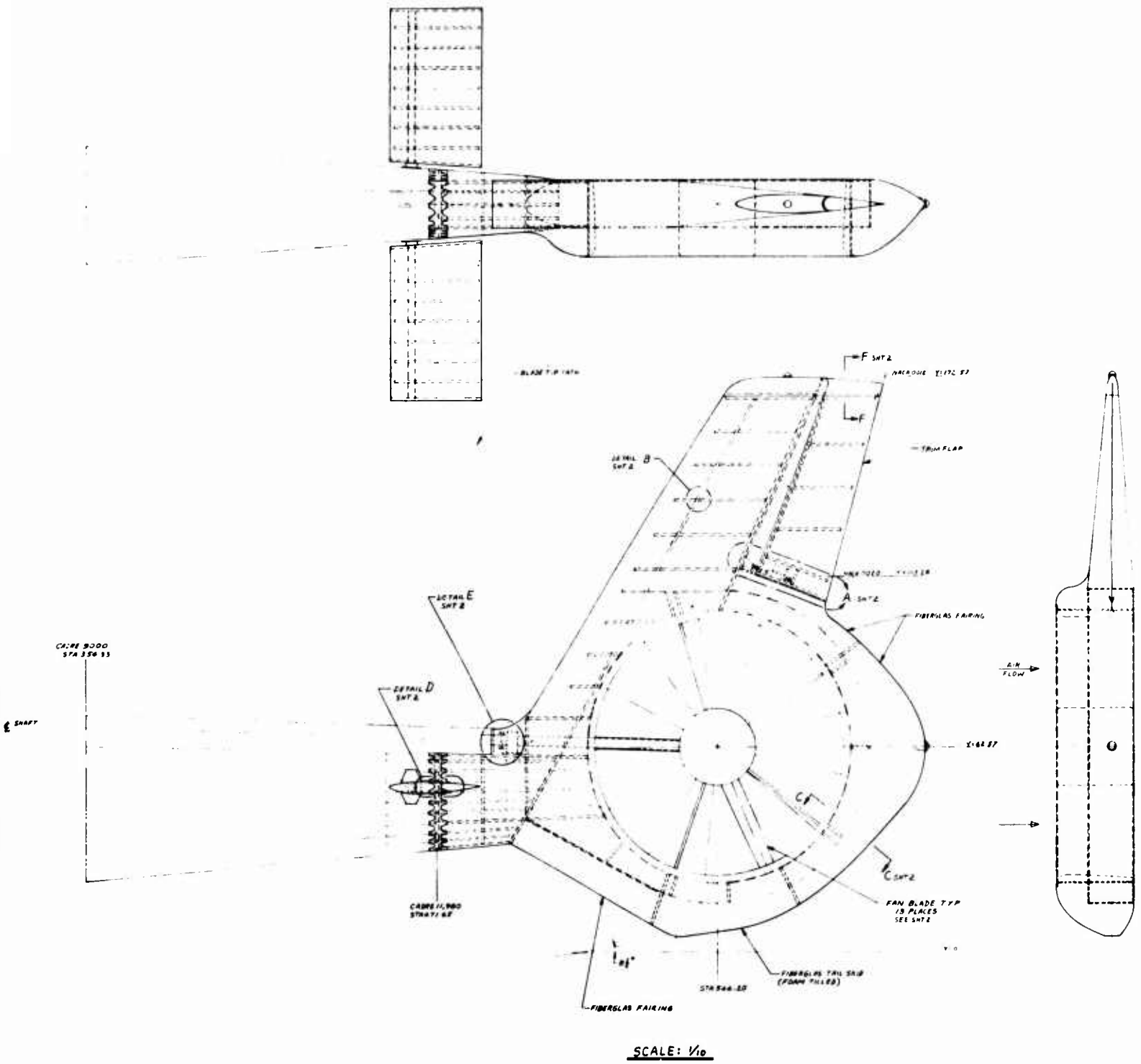


Figure 41. SA 330 Fan-in-Fin Design Layout.

The number of blades, the same as used on the Fenestron, was selected to maintain the system integrity in the event of the loss of a blade and to prevent blade/strut interference. The hub-tip radius ratio was established primarily from the practical considerations of blade retention, actuation, and the size and space requirements of an integrated gear drive system. Aerodynamic blade chord requirements indicate that the hub-tip radius ratio of 0.3 is the minimum possible to maintain reverse thrust capabilities.

The design method used is an adaptation of work done by C. N. Patterson as presented in Reference 17. This method assumes a uniform inflow velocity to all radial stations of the blade. Adhering strictly to this procedure, the resulting blade planform has a rather wide base and very narrow tip. Therefore, the planform is modified to give a uniform chord distribution over approximately one-half the length with a slight taper toward the tip. Blade station design data are presented in Table XI.

#### Fan Gearbox and Power Shaft Extension

The fan gearbox power train reduces the input shaft speed of 4888 rpm to 2542 rpm through a single bevel gear reduction. The fan hub accommodates 13 solid aluminum blades which are retained by a laminated steel strap. Blade bending loads are reacted through a plastic bearing insert at the root of the blade. The blade pitch control head is actuated by a nonrotating shaft powered by a bolt-on hydraulic actuator. To provide the necessary actuating power, 2500-psi hydraulic power lines are available in the fin area.

A shaft extension was required from the existing tail rotor drive shaft to the fan gearbox. A bearing hanger was installed in the area of the existing angle gearbox. The shaft extension attaches to the existing shaft using a flexible coupling. The interface with the gearbox was a spline which allows minor misalignment using a spherical guide. The control complexity of the fan-in-fin system is approximately equivalent to the conventional tail rotor systems. Control actuating forces for both systems are likewise similar since the thrust required and horsepower available are essentially the same. Since the articulated rotor is replaced by a variable-pitch propeller system, control response may be improved by the elimination of the flapping portion of this articulation system.

#### WEIGHT COMPARISON

A comparison of weights of the basic SA 330 and fan-in-fin antitorque and directional control systems, has been accomplished. Skin gages

TABLE XI. BLADE STATION DESIGN DATA

		BLADE STATION							
		.3	.4	.5	.6	.7	.8	.9	1.0
Thickness Ratio		.173	.116	.084	.067	.056	.05	.044	.037
Station Blade Angle, deg	43.24	31.71	24.87	20.48	17.22	14.76	12.85	11.30	
Blade Chord, ft	.460	.460	.452	.434	.412	.394	.380	.361	

for the fan-in-fin were determined by preliminary stress analysis. The fan and gearbox weight estimate was based on statistical trends for prop-fans developed by Hamilton Standard. SA 330 weight estimates were determined from actual complete boom structural weight.

Table XII presents actual weights for the basic SA 330 and estimated weights for the fan-in-fin modification. These weights refer to structure, controls, etc., aft of the manufacturing break between the tail boom and vertical pylon assemblies. The results indicate a slight increase in structural weight (11 lb) of the fan-in-fin system when compared to the conventional tail rotor system. This nominal weight increase indicates that it may be possible to design a fan-in-fin configuration with no weight penalty or even with a weight saving if lightweight advanced blading is used on the fan.

TABLE XII. SA 330 ANTITORQUE SYSTEM WEIGHT COMPARISON		
COMPONENTS	ACTUAL BASIC SA 330 (lb)	ESTIMATED FAN- IN-FIN SA 330 (lb)
Vertical Pylon, Fairings, and Gearbox Support	86	-
Lower Fin Protection	12	-
Horizontal Stabilizer and Attachments	28	27
Tail Rotor Gearbox and Rotor Head	152	-
Blades (5)	31	-
Inclined Shaft	24	-
Intermediate Gearbox	37	-
Control Linkage	6	-
Servos	12	9
Hydraulic Unit	9	-
Fan, Gearbox, Controls, Shroud, etc.	-	225
Fin and Trim-Flap	-	98
Electromechanical Trim Jack, Wiring, etc.	-	4
Fan Support Ring	-	33
Drive Shaft Extension and Coupling	-	12
Total subassembly weight	397	408

## SENSITIVITY STUDIES

Sensitivity studies were carried out on critical fan and fin design parameters at SL STD conditions to determine the influence each variable had on forward-flight performance. Maximum speed, determined by the transmission-limited power available, takes into account the total power required by the system and serves as a basis for comparison. The point design was the baseline in each study, and all point design parameters were held constant except for the parameter being studied.

### Fan Diameter

The effect of fan diameter on maximum-speed performance was found to be negligible over a range of fan diameters from 4.5 ft to 6.5 ft. Although the thrust loading and fan-induced drag increased as fan diameter decreased, the fan thrust required was reduced by the action of the fin with speed. Thus, the effect of higher disc loading due to reduction of fan diameter was minimized, and the resulting small increase in total power required did not significantly alter the overall performance.

### Fin Area

A range of planform areas from 80 sq ft to 120 sq ft was studied. It was assumed that the fin would remain geometrically similar and that a lift coefficient of 0.153 could be achieved by proper selection of fin angle-of-incidence and camber. The fan thrust required was reduced as fin area and the resulting fin contribution to antitorque thrust increased. Assuming that the fan was positively loaded at all times to alleviate the effect of the fan and fin working against each other, the fin thrust in excess of the antitorque requirement can be reduced for optimum operation by means of a trim flap or other such device. The drag penalty and resulting power increase due to the use of a trim flap is much less than when the fan was operated in the reverse thrust direction. Figure 42 shows how the maximum speed (for the SA 330) in level flight varies with increasing vertical fin area. The design point shown in Figure 42 shows that the 92 sq ft fin permits a maximum cruise speed within 2 kt of the maximum cruise speed possible. To increase the fin area would cause an undesirable weight increase for a very small gain in speed performance.

### Fin Lift Coefficient

The fin lift coefficient obtained by fin angle of incidence or camber was investigated over a range of  $C_L=0.17$  to 0.10 for a fin area of 92 sq ft. As lift coefficient decreased, fan thrust required was shown to increase greatly (see Figure 43). Figure 44 shows the variation of cruise speed performance with the  $C_L$  of the 92 sq ft fin. Since this curve represents

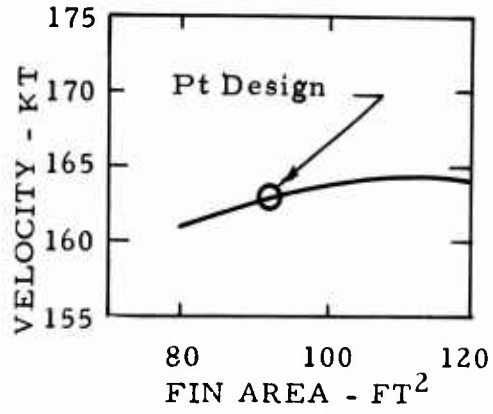


Figure 42. Maximum Velocity Sensitivity With Fin Area.

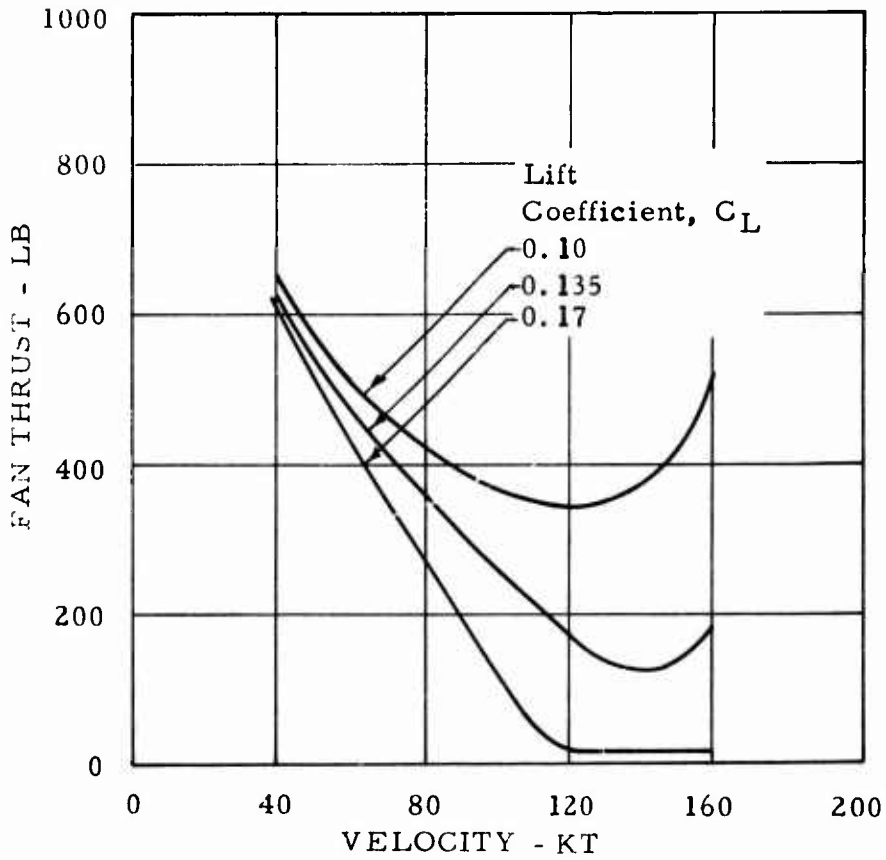


Figure 43. Required Fan Thrust Vs. Speed for Various Fin Lift Coefficients.

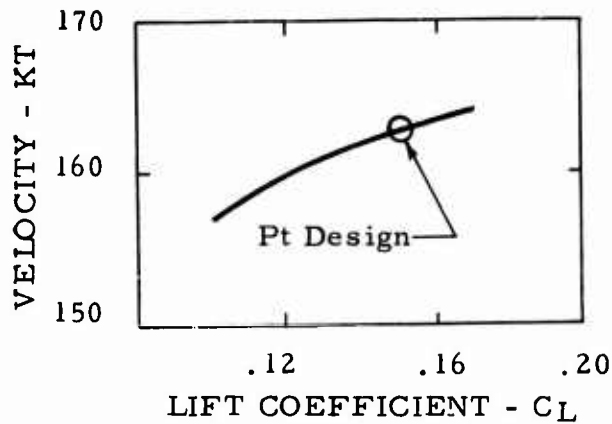


Figure 44. Maximum Velocity Sensitivity With Fin Lift Coefficient.

straight and level flight, trim forces must be supplied by the fan as the fin lift decreases. The cruise speed degradation with decreasing  $C_L$  is caused by the additional fan-induced drag and antitorque power required as the fan thrust is increased to supply the needed trim force. Only a positively loaded fan was considered in the curve of Figure 44. Thus, the lift coefficient had to be high enough for a given fin area to unload the fan for maximum performance. Increasing the lift coefficient by increasing angle of incidence or camber resulted in adverse autorotational characteristics. Therefore, the selection of lift coefficient was important for acceptable performance across the flight spectrum. A trim flap to vary fin lift would improve off-design performance.

### PERFORMANCE COMPARISONS

In this section, the performance of the basic SA 330 with conventional tail rotor was compared to the modified 330 with fan-in-fin in hover and in forward flight. Mission capabilities were also compared.

#### Hover

In previous discussions, it has been shown that the 6.4-ft-diameter fan does provide the same amount of thrust as the conventional 10.24-ft-diameter tail rotor for the same power absorbed (see Figure 34).

#### Forward Flight

The power required for the two systems was computed by the methods in Appendix II. The difference in parasite drag was taken into account. For the fan-in-fin, an equivalent fin with a mean chord of 6.57 ft and a wetted area of 194 sq ft was chosen. A factor of 1.5 was obtained from

Reference 10 to account for the interference drag caused by a duct through a fin. The equivalent flat plate drag was estimated to be 1.55 sq ft.

A drag area of 0.37 sq ft was estimated for the conventional tail rotor system's fin-pylon, and a drag area of 1.76 sq ft was obtained for the tail rotor head and shaft. The total drag of 2.03 sq ft for this system was 0.70 sq ft greater than that for the fan-in-fin system. Thus the antitorque system contribution to parasite drag was less for the fan-in-fin than for the conventional tail rotor system for this case.

The antitorque power required for both the conventional tail rotor (SA 330) and the fan-in-fin (modified SA 330) is shown in Figure 45 ratioed to the total power required as a function of speed. The fan, unloaded by the fin antitorque thrust contribution, requires less power for the antitorque role. A comparison of the total power required for both systems is

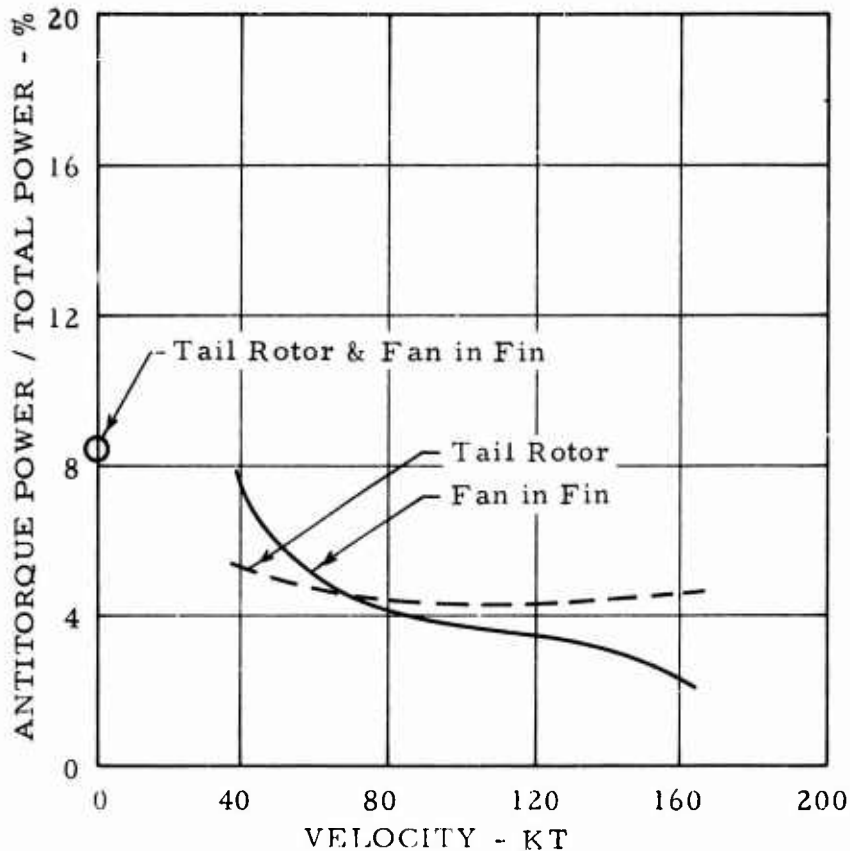


Figure 45. Comparison of Fan-in-Fin and Tail Rotor Antitorque Power Required in Forward Flight, SL STD, SA 330.

given in Figure 46 for a gross weight of 14,110 lb. Although the anti-torque power required by the fan at the higher speeds was less, a comparison of maximum speeds (defined by power required and the transmission power limit) shows (in Figure 47) diminished performance gains based on power considerations; this is caused by the induced effects of the fan and fin system. Taking into account structural limitations, the conventional tail rotor reached an estimated vibratory stress level of 3500 psi at about 150 kt for a gross weight of 14,110 lb. The fan, being rigid and lightly loaded, can achieve SA 330 VNE speeds without incurring the high stress levels. Thus a conventional tail rotor is limited due to structural considerations or requires increased structure with the accompanying weight penalty to attain the same higher speeds.

### Mission Performance

The relative merits of the fan-in-fin system versus the conventional tail rotor were analyzed with respect to mission requirements. Specific

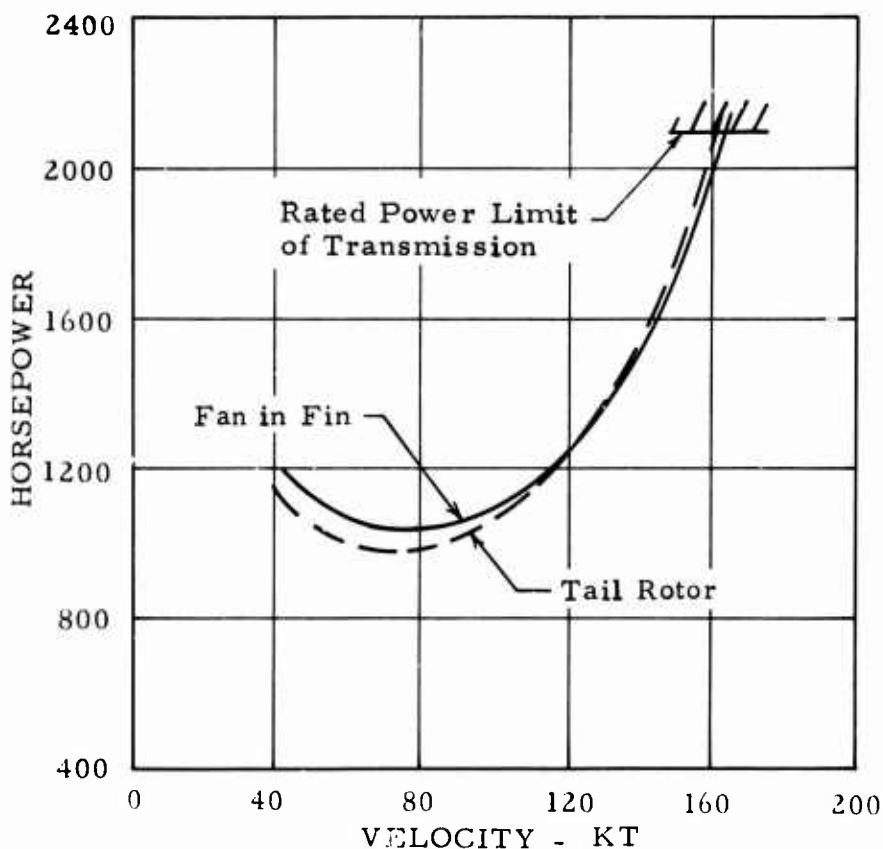


Figure 46. Comparison of Total Power Required for Fan-in-Fin and Tail Rotor Systems, SA 330.

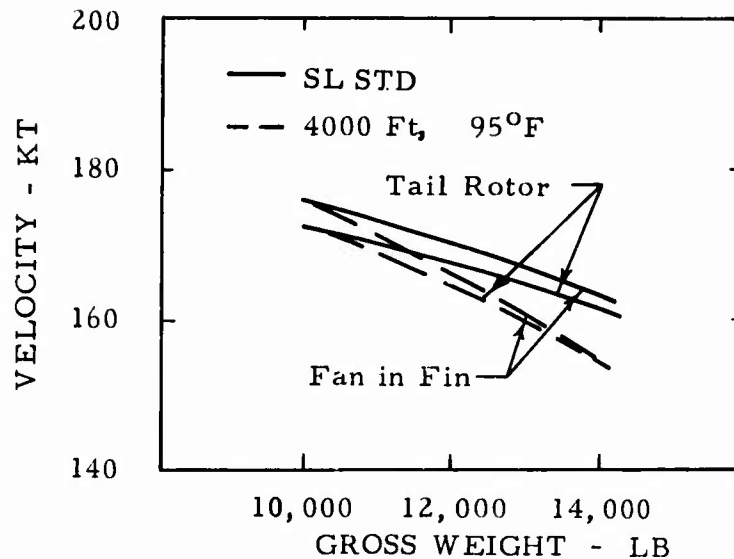


Figure 47. Maximum Speed Comparison for Fan-in-Fin and Tail Rotor Systems, SA 330.

ranges for the two systems are shown in Figures 48 and 49 at SL STD and 4,000 ft, 95°F. For mission performance calculations, specific fuel flow rates were reduced by 5 percent. The fan-in-fin system was shown to have equal or slightly better specific range. Figure 50, which compares best range speeds, defined as the speed for 99 percent maximum specific range, shows improved performance for the fan-in-fin.

A weight comparison between the fan-in-fin and tail rotor system showed no appreciable effect on the empty weight for this size helicopter. Thus the weight of the SA 330 and the modified 330 may be considered the same. The operational weight for the baseline aircraft complete with navigational aids, trapped fluids, and a crew of two was 8089 lb. For the maximum takeoff weight of 14,110 lb, the useful load was 6021 lb. The maximum fuel weight with standard tankage was 2686 lb. A payload-range comparison of the two systems computed from the above information is shown in Figure 51 for a sea level, standard day. A range increase of approximately 2 percent was noted for the maximum fuel load.

The fan-in-fin in this application has demonstrated slightly better range along with higher cruise speeds. Hover performance has been shown to be equal to the conventional tail rotor. Thus the fan-in-fin showed improved mission performance as compared to the tail rotor.

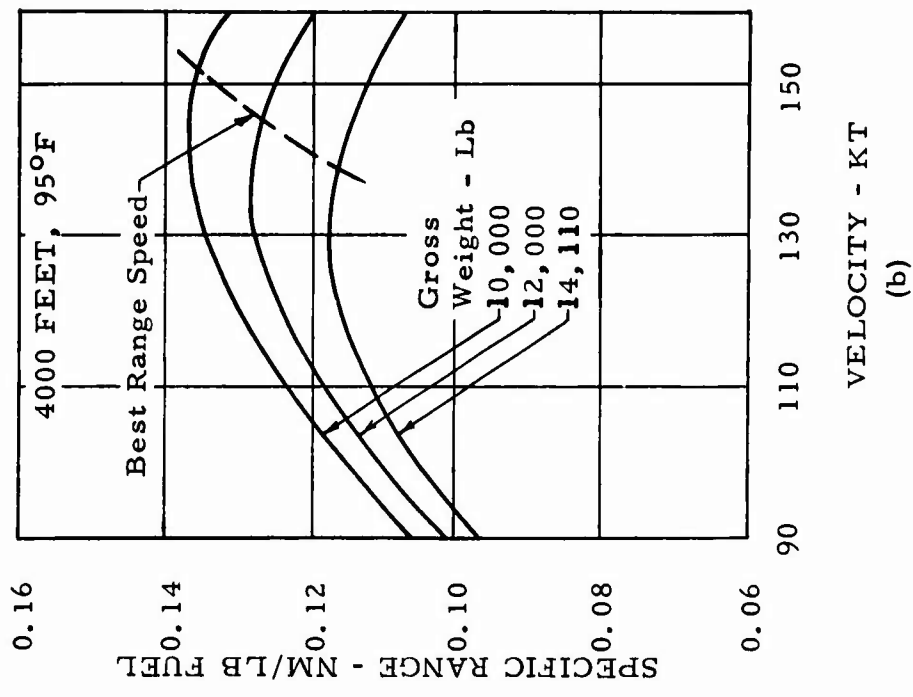
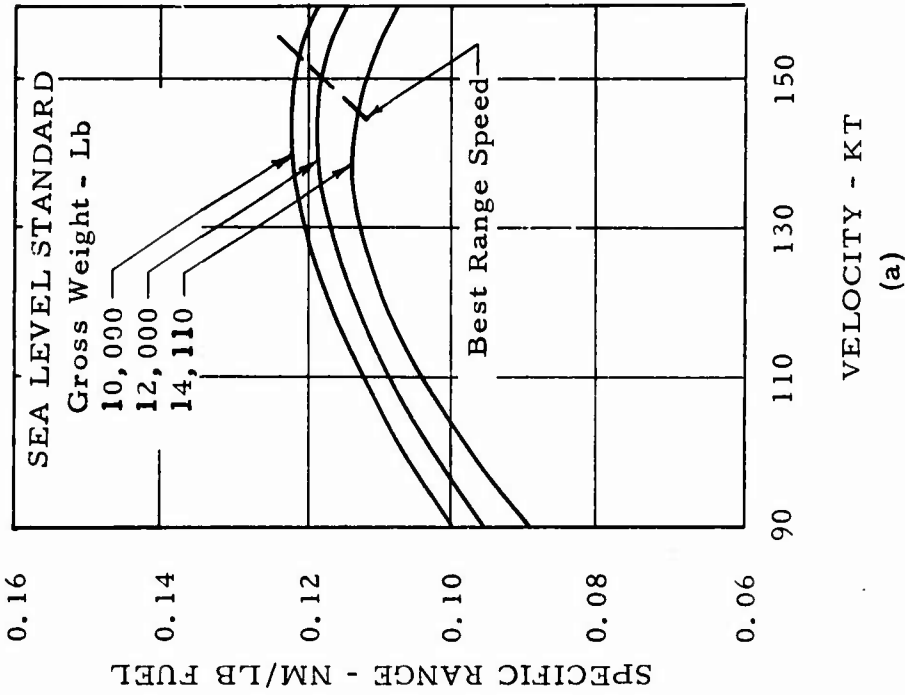


Figure 48. SA 330 Specific Range With Tail Rotor.

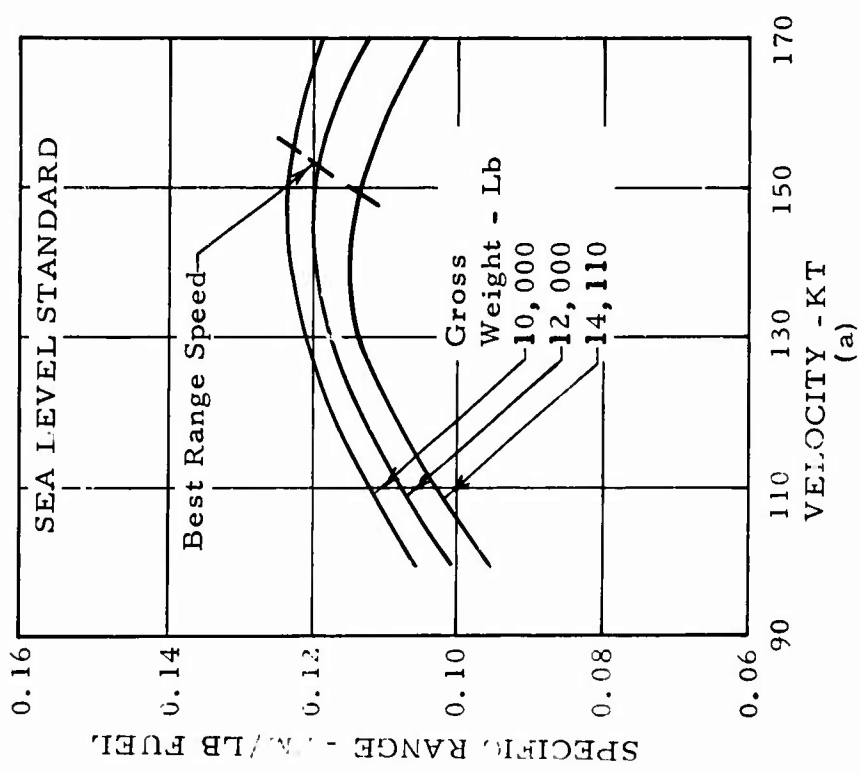
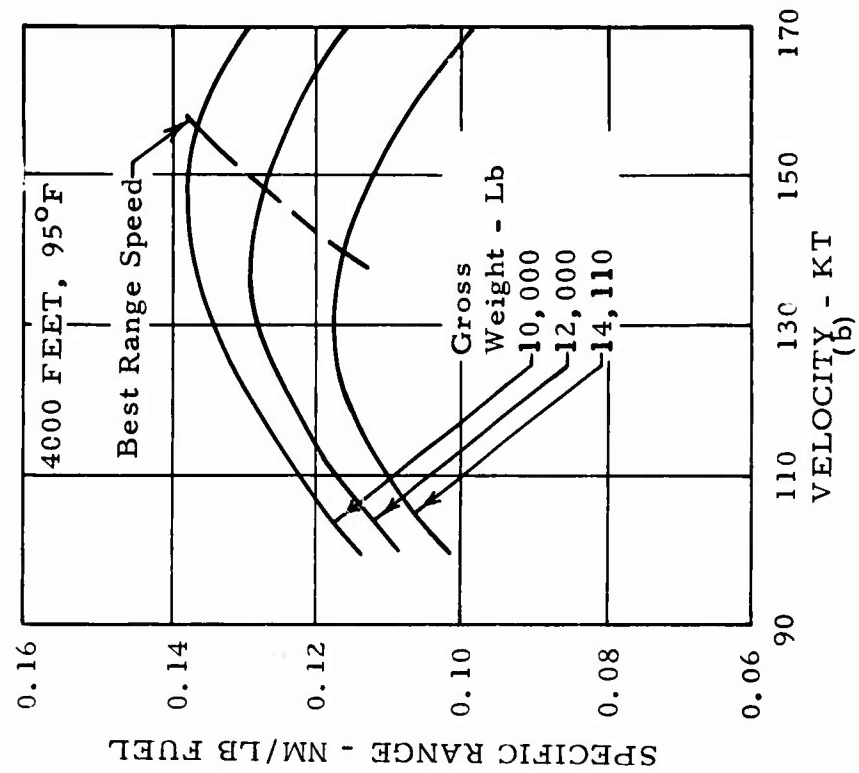


Figure 49. SA 330 Specific Range With Fan-in-Fin.

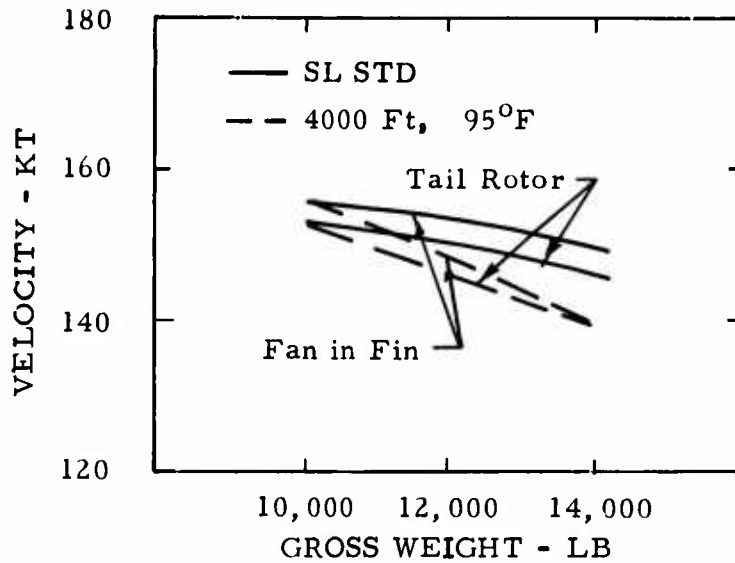


Figure 50. Best Range Speed Comparison for Fan-in-Fin and Tail Rotor Systems.

Of interest is the mission capability of this fan-in-fin system estimated for a design mission defined for this class of tactical transport. Specified mission requirements on a 4,000 ft, 95°F day are:

- 8 min. ground operation at idle power
- 20 min. operation at max. continuous power
- 80 min. at cruise speed
- 30 min. reserve at cruise speed

A mission takeoff weight of 12,600 lb was determined as the weight capable of achieving a 500 ft/min vertical rate of climb at 4,000 ft, 95°F and 95 percent of intermediate power. The fuel required to meet the mission was estimated to be 2859 lb, and an average mission cruise speed of 151 kt was determined. A payload of 1652 lb was then established for an operating weight of 8089 lb, including a 2-man crew.

#### MAINTAINABILITY AND RELIABILITY - FAN-IN-FIN VS. TAIL ROTOR

Application of the fan-in-fin design to replace the conventional tail rotor as the antitorque device on helicopters improves the reliability and maintainability to a considerable degree. This improvement is accomplished by elimination of components, reduced component stresses, and added protection from foreign object damage (FOD).

Fan blade retention is provided by tension-torsion straps, and the pitch change bearing is a plastic liner made of a low-friction nonlubricated

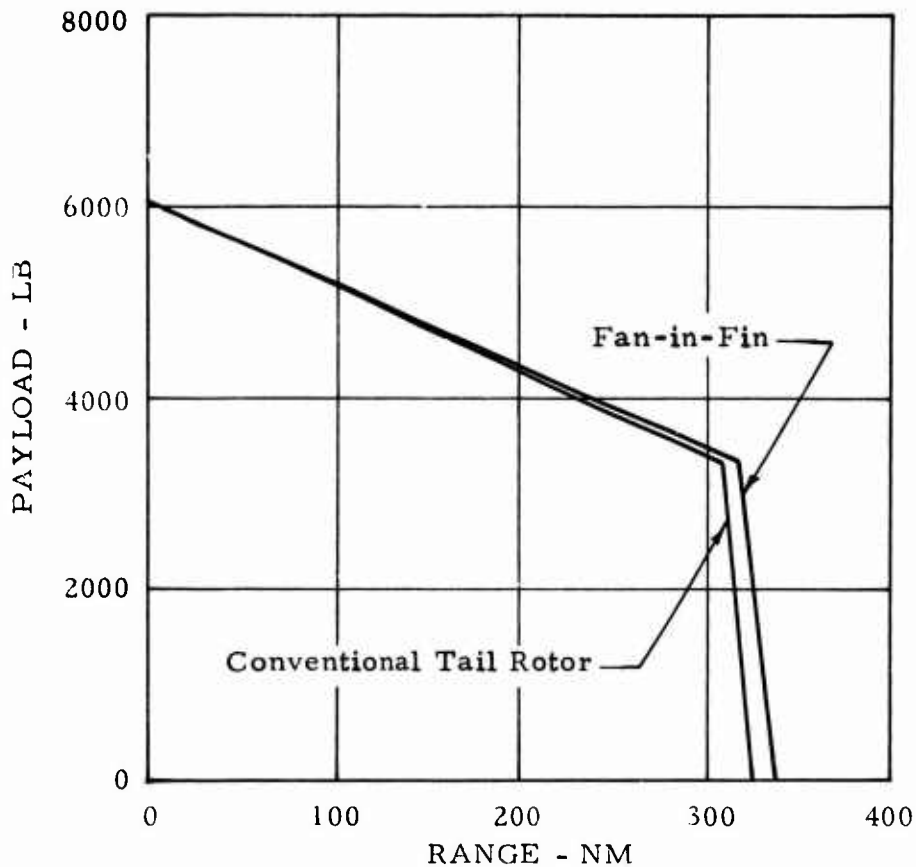


Figure 51. Comparison of Fan-in-Fin and Conventional Tail Rotor Payload-Range Performance, To GW=14,110 lb, SL STD.

material. This design eliminates the flapping hinge, thrust bearings, and pitch links that require frequent replacement due to limited service life.

Lower component fatigue stresses on the fan-in-fin, because of much lower power required in all flight conditions except hover, and elimination of stresses due to dynamic instabilities caused by the wake on a conventional tail rotor, provide for very long service life and allow much higher time between overhaul (TBO) with considerably improved mean time between failures (MTBF).

Another maintenance item is removed by elimination of the conventional tail rotor intermediate gearbox. Ability to complete a mission is provided by the fan-in-fin design even after a failure of the antitorque system. In forward flight, the fin provides the antitorque thrust. This

type of failure in a conventional tail rotor would necessitate an immediate autorotative landing.

ACOUSTICAL COMPARISON

Acoustics of the fan-in-fin antitorque device designed for the SA 330 are compared to the noise level of the conventional tail rotor presently used on the aircraft. Perceived noise levels for the fan-in-fin were calculated by a procedure adapted from Reference 12. The tail rotor noise levels were estimated using Reference 13. Table XIII gives a comparison of the results.

The table also shows the parameters used to predict the maximum noise levels for the two types of antitorque devices. The results of the comparison show that in general the fan-in-fin produces a higher maximum noise level than the conventional tail rotor. This comparison, however, does not show the effects of directivity, which appears to be more sensitive for the fan-in-fin.

TABLE XIII. SA 330 FAN-IN-FIN ACOUSTICAL COMPARISON		
	Conventional Tail Rotor	Fan-in-Fin
PNL @ 25M (82 ft) - PNdb	87	89
PNL @ 50 M (164 ft) - PNdb	81	83
Tip Speed - fps	690	850
Antitorque power - hp	152	152
Diameter - ft	10.2	6.4
No. Blades	5	13
Thrust - lb	1055	1055

## CONCLUSIONS

A fan-in-fin antitorque device has been shown to be feasible for a helicopter in the 14,000-lb to 15,000-lb gross weight range. A fan-in-fin designed for a representative vehicle in this weight class, the SA 330 Puma, showed equal or better performance compared to the conventional tail rotor presently installed on this helicopter both in hover and forward flight. Potential long service life and low maintenance associated with the fan-in-fin increase the attractiveness of this design.

A ducted propeller (fan) can be incorporated as an antitorque device with little or no power penalty.

No appreciable weight penalty is associated with installing a fan-in-fin on a Puma class vehicle considering the replacement of vertical pylon by a fin and the tail rotor, gearbox, and head with a fan and integrated gearbox. The incorporation of advanced lightweight technology blading could result in a small weight saving in the Puma over solid aluminum blades for the fan.

The reliability and maintainability of the fan-in-fin system are improved by the replacement of the flapping hinge, thrust bearings, and pitch links of a tail rotor with a blade retention system provided by tension-torsion straps and a pitch change bearing of a permanently lubricated material. Lower component fatigue stresses permit higher TBO's with greatly improved MTBF.

The fan-in-fin can sustain high-speed flight with low blade stress and vibration levels as contrasted to the conventional tail rotor.

The SA 341 Fenestron antitorque system has proven the feasibility of the fan-in-fin concept in light to medium helicopters. The power penalty associated with the Fenestron fan can be reduced by reducing the tip clearance and using blades with increased camber and twist.

The incorporation of a trim flap on the fin is desirable to insure the fan operation at low thrust levels in a range of cruise speeds. High drag penalties are incurred by fan operation at off-design conditions of the fin. Also, the trim flap could provide the means of counteracting the antitorque thrust of the fin in autorotational flight, thus increasing the safety of this system.

Application of fan-in-wing technology to a fan-in-fin antitorque device is limited because the technology was developed with either full span or perfectly end-plated models. The fan-in-fin is effectively (and

partially) end-plated by the action of the fan. Also, the adverse effect of the fan on fan-in-wing system thrust is associated with high fan thrust levels and should not be applicable when considering low-to-moderate fan thrust of a fan-in-fin system in forward flight. Therefore, wind tunnel tests are required to document the performance characteristics of basic fan-in-fin systems.

Foreign object damage should be reduced for the fan-in-fin concept since the normal tail rotor tip vortex is suppressed. This vortex is a major cause of foreign object ingestion.

Fenestron (fan-in-fin) wind tunnel tests showed trends similar to results obtained from fan-in-wing tests. These trends included forward shift of the device's thrust center with increase in speed and thrust. The power required to maintain a constant thrust level increased with speed in the lower ranges and then decreased significantly with higher speeds; or, for a given level of power, the thrust of the system decreased from static conditions at the low speeds and then increased markedly with increase in speed. The drag increment due to fan operation is significant and can be estimated from wind tunnel tests.

The fan-in-fin designed for the SA 330 will produce a higher maximum perceived noise level than the conventional tail rotor in use. However, the fan-in-fin noise level will be highly directional and will be significantly reduced at azimuth positions near the aircraft's longitudinal axis. Lower acoustic characteristics could be achieved for the fan-in-fin by reducing tip speed and disc loading, increasing the number of blades, and increasing the clearance between the mounting struts and the fan. The noise levels could also be reduced by treating the duct wall and support struts with acoustically absorbent material.

The simplified, low-maintenance features of the Fenestron integrated pitch change-gear drive system can be incorporated in larger fan-in-fin antitorque devices for helicopters in higher gross weight ranges.

## LITERATURE CITED

1. Grumm, Arthur W., and Herrick, Groves E., ADVANCED ANTITORQUE CONCEPTS STUDY, Sikorsky Aircraft, USAAMRDL Technical Report 71-23, Eustis Directorate, U.S. Army Air Mobility Research and Development Laboratory, Fort Eustis, Virginia, July 1971, AD 72960.
2. Velazquez, J. L., ADVANCED ANTITORQUE CONCEPTS STUDY, Lockheed California Co., USAAMRDL Technical Report 71-44, Eustis Directorate, U.S. Army Air Mobility Research and Development Laboratory, Fort Eustis, Virginia, August 1971.
3. Taylor, Robert T., EXPERIMENTAL INVESTIGATION OF THE EFFECTS OF SOME SHROUD DESIGN VARIABLES ON THE STATIC THRUST CHARACTERISTICS OF A SMALL-SCALE SHROUDED PROPELLER SUBMERGED IN A WING, NACA TN 4126, Jan. 1958.
4. Parlett, Lysle P., AERODYNAMIC CHARACTERISTICS OF A SMALL-SCALE SHROUDED PROPELLER AT ANGLES OF ATTACK FROM 0° to 90°, Langley Aeronautical Laboratory; Technical Note 3547, NASA, Langley Field, Virginia, November, 1955.
5. McNay, David E., STUDY OF THE EFFECTS OF VARIOUS PROPELLER CONFIGURATIONS ON THE FLOW ABOUT A SHROUD, Mississippi State University; Report No. 14, Office of Naval Research, February, 1958, AD 219121.
6. Pass, H.R., ANALYSIS OF WIND-TUNNEL DATA ON DIRECTIONAL STABILITY AND CONTROL, NACA TN 775, Sept. 1940.
7. Duvivier, J.F., and McCallum, R.B., INVESTIGATION OF TILTING DUCT AND FAN-WING IN TRANSITION FLIGHT, Massachusetts Institute of Technology, TREC Technical Report 61-19, U.S. Army Transportation Research Command, December 1960, AD 254847.
8. Kirk, Jerry V., Hickey, David H., and Hull, Leo P., AERODYNAMIC CHARACTERISTICS OF A FULL-SCALE FAN-IN-WING MODEL INCLUDING RESULTS IN GROUND EFFECT WITH NOSE-FAN PITCH CONTROL, NASA TN D-2368, July 1964.

9. Hickey, D. H., and Hall, L. P., AERODYNAMIC CHARACTERISTICS OF A LARGE-SCALE MODEL WITH TWO HIGH DISC-LOADING FANS MOUNTED IN THE WING, NASA TN D-1650, Ames Research Center, Moffett Field, California, Feb. 1963.
10. Hickey, David H., and Ellis, David R., WIND-TUNNEL TESTS OF A SEMISPAN WING WITH A FAN ROTATING IN THE PLANE OF THE WING, NASA TN D-88, Oct. 1959.
11. Hickey, David H., and Goldsmith, Robert H., CHARACTERISTICS OF AIRCRAFT WITH LIFTING-FAN PROPULSION SYSTEMS FOR V/STOL, IAS paper No. 63-27, Jan. 1963.
12. PRELIMINARY PROP-FAN GENERALIZED PERFORMANCE, WEIGHT AND NOISE DATA, Hamilton Standard Division, United Aircraft Corp., May 1970.
13. Brown, E. L., Cox, C. R., Halwes, D. R., A PRELIMINARY DESIGN STUDY OF A QUIET LIGHT OBSERVATION HELICOPTER, Bell Helicopter Company, USAAVLABS TR 69-99, U. S. Army Aviation Materiel Laboratories, Fort Eustis, Virginia, December 1969, AD 867010.
14. ACOUSTICAL STUDY OF THE FENESTRON, COMPARISON WITH THE CLASSICAL TAIL ROTOR, H-DE-ER 350/70, Aerospatiale, Marignane, France, June 1970.
15. Lynn, R. R., Robinson, F. D., Batra, N.N., Duhon, J. M., TAIL ROTOR DESIGN PART I: AERODYNAMICS, Journal of the American Helicopter Society, Vol. 15, No. 4, Oct. 1970, pp. 2-15.
16. GENERALIZED METHOD OF SHROUDED PROPELLER PERFORMANCE ESTIMATION, Hamilton Standard, Report No. PDB 6220, United Aircraft Corp., Windsor Locks, Connecticut, Sept. 1962.
17. Pope, Alan, WIND TUNNEL TESTING, New York, John Wiley & Sons, Inc., 1947, pp 41-57.

APPENDIX I  
BIBLIOGRAPHY OF LITERATURE  
ON FAN-IN-FIN RELATED WORK

Grumm, Arthur W., and Herrick, Groves E., ADVANCED ANTITORQUE CONCEPTS STUDY, Sikorsky Aircraft, USAAMRDL Technical Report 71-23, Eustis Directorate, U.S. Army Air Mobility Research and Development Laboratory, Fort Eustis, Virginia, July 1971, AD 729860.

Rubbert, P.E., et al., A GENERAL METHOD FOR DETERMINING THE AERODYNAMIC CHARACTERISTICS OF FAN-IN-WING CONFIGURATIONS, USAAVLABS Technical Report 67-61B, Dec. 1967.

Hickey, David H., and Hall, Leo P., AERODYNAMIC CHARACTERISTICS OF A LARGE SCALE MODEL WITH TWO HIGH DISC-LOADING FANS MOUNTED IN THE WING, NASA TN D-1650, Feb. 1963.

Mendenhall, M.R., THEORETICAL STUDY OF DUCTED FAN PERFORMANCE, CR-1494, Jan. 1970.

Hickey, David H., and Ellis, David R., WIND-TUNNEL TESTS OF A SEMISPAN WING WITH A FAN ROTATING IN THE PLACE OF THE WING, NASA TN D-88, Oct. 1959.

Hickey, David H., and Goldsmith, Robert H., CHARACTERISTICS OF AIRCRAFT WITH LIFTING-FAN PROPULSION SYSTEMS FOR V/STOL, IAS Paper No. 63-27, Jan. 1963.

Ham, Norman D., and Moses, Herbert H., PRELIMINARY INVESTIGATION OF A DUCTED FAN IN LIFTING FORWARD FLIGHT, IAS Preprint No. 827, Jan. 1958.

Martin, Eugene E., THE LIFT PRODUCED BY A WING MOUNTED LIFT FAN AT FLIGHT SPEEDS BELOW TRANSITION, MIT, M.S. Thesis, June 1963.

Norland, Sven-Anders, AN INVESTIGATION OF THE LIFT PRODUCED BY A FAN IN A TWO-DIMENSIONAL WING, MIT, M.S. Thesis, Feb. 1962.

Duvivier, J.F., and McCallum, R.B., INVESTIGATION OF TILTING DUCT AND FAN-WING IN TRANSITION FLIGHT, Massachusetts Institute of Technology, TREC Technical Report 61-19, U.S. Army Transportation Research Command, Fort Eustis, Virginia, Dec. 1960, AD 254847.

Chambers, Joseph R., and Grafton, Sue B., STATIC AND DYNAMIC LONGITUDINAL STABILITY DERIVATIVES OF A POWERED 0.18-SCALE MODEL OF A FAN-IN-WING VTOL AIRCRAFT, NASA TN D-4322, Feb. 1968.

Kirk, Jerry V., Hickey, David H., and Hull, Leo P., AERODYNAMIC CHARACTERISTICS OF A FULL-SCALE FAN-IN-WING MODEL INCLUDING RESULTS IN GROUND EFFECT WITH NOSE-FAN PITCH CONTROL, NASA TN D-2368, July 1964.

Prezedpelski, Zygmunt J., LIFT FAN TECHNOLOGY STUDIES, NASA CR-761.

Platt, Robert J., Jr., STATIC TESTS OF A SHROUDED AND AN UNSHROUDED PROPELLER, NACA RM L7H25, Feb. 1948.

Taylor, Robert T., EXPERIMENTAL INVESTIGATION OF THE EFFECTS OF SOME SHROUD DESIGN VARIABLES ON THE STATIC THRUST CHARACTERISTICS OF A SMALL-SCALE SHROUDED PROPELLER SUBMERGED IN A WING, NACA TN 4126, Jan. 1958.

Hesselgreaves, J. E., A CORRELATION OF TIP-CLEARANCE/EFFICIENCY MEASUREMENTS ON MIXED FLOW AND AXIAL-FLOW TURBOMACHINES, NEL Report No. 423, July 1969.

Rosen, George, PROP-FAN - A HIGH THRUST, LOW NOISE PROPULSOR, SAE Paper No. 710470, May 1971.

Theodorsen, Th., THEORETICAL INVESTIGATION OF DUCTED PROPELLER AERODYNAMICS, Vol. I and II., U.S. Army Transportation Research Command, Technical Report crd 3860, Aug. 1960.

Theodorsen, Th., THEORETICAL INVESTIGATION OF DUCTED PROPELLER AERODYNAMICS, Vol. III, U.S. Army Transportation Research Command, Technical Report 61-119, Sept. 1961.

Turner, R.C., NOTES ON DUCTED FAN DESIGN, National Gas Turbine Establishment Memo No. M 386, Aug. 1964.

Grose, Ronald M., WIND TUNNEL TESTS OF SHROUDED PROPELLERS AT MACH NUMBERS FROM 0 TO 0.60, USAF WADC Technical Report 58-604, Dec. 1958.

Statler, I. C., Kurylowich, G., Erickson, J. C., Jr., and Jowyrda, A., PREDICTIVE METHODS FOR THE DYNAMIC RESPONSE OF A QUAD TILT-DUCT V/STOL AIRCRAFT IN TRANSITION, AFFDL/FGC Technical Report AFFDL-TR-70-140, Dec. 1970.

Gulianetti, Demo J., Biggers, James C., and Maki, Ralph L., LONGITUDINAL AERODYNAMIC CHARACTERISTICS IN GROUND EFFECT OF A LARGE-SCALE, V/STOL MODEL WITH FOUR TILTING DUCTED FANS ARRANGED IN A DUAL TANDEM CONFIGURATION, NASA TN D-4218, Oct. 1967.

Mouille, Rene', THE "FENESTRON," SHROUDED TAIL ROTOR OF THE SA 341 "GAZELLE," Sud Aviation Document GIR 3530, April 1970.

Lecarme, M., SA 340D SHROUDED ROTOR, Sud Aviation Wind Tunnel Report 210, Dec. 1966.

Lecarme, M., SA340D SHROUDED ROTOR, Sud Aviation Wind Tunnel Report 214, Dec. 1966.

Vidal, J. P., SA 341 SHROUDED ROTOR, Sud Aviation Wind Tunnel Report 236, March 1969.

Foudral, J., SA 341 FENESTRON EFFICIENCY, Aerospatiale Wind Tunnel Report 246, Sept. 1970.

Alenne, G., and Gendre, M., SHROUDED ROTOR AERODYNAMIC CHARACTERISTICS, Sud Aviation Document SA 340D-02-2202, Sept. 19, 1966.

Alenne, G., SHROUDED ROTOR AERODYNAMIC CHARACTERISTICS (AT INCIDENCE AND ZERO SIDESLIP) WITH BLADE PROFILES OF THE NACA OXY FAMILY, Sud Aviation Document SA 340D-02-22-03, Dec. 20, 1966.

Fabre, P., "FENESTRON" LATERAL LIFT AT LOW PITCHES AND SIDESLIP, Sud Aviation Document SA 340D-02-22-05, Feb. 3, 1969.

Gallot, J., SHROUDED ROTOR, AERODYNAMIC CHARACTERISTICS FOR HIGH SIDESLIP AT LOW SPEEDS, Sud Aviation Document SA 341-02-22-06, Oct. 14, 1970.

Chabert, J., DYNAMIC CHARACTERISTICS OF THE "FENESTRON" ASSEMBLY, Sud Aviation Document 340A-06-1007, June 24, 1968.

Chabert, J., and Mens, J., CHARACTERISTICS OF THE FENESTRON ROTOR EQUIPPED WITH SHORTENED BLADES, Sud Aviation Document 340A-06-1012, July 31, 1968.

Fabre, P., SUMMARY OF THE FENESTRON DEVELOPMENT, Sud Aviation Document SA 340D-02-52-19, May 14, 1969.

Allenne, G., SHROUDED ROTOR IN NON-AXIAL TRANSLATION, Sud Aviation Document CAL-01-034, Dec. 10, 1969.

Allenne, G., COMPARISON OF ANTITORQUE BY A SHROUDED ROTOR AND CLASSICAL ANTITORQUE AT FIXED POINT, Aerospatiale Document SA 341-02-52-22, June 17, 1970.

Bourquardez, G., ACOUSTIC STUDY OF THE FENESTRON, COMPARISON WITH A CLASSICAL TAIL ROTOR, Sud Aviation Document H-DE-ER 350/70, June 18, 1970.

Wardlaw, R. L., and Templin, R. J., PRELIMINARY WIND TUNNEL TESTS OF A LIFTING FAN IN A TWO-DIMENSIONAL AEROFOIL, National Aeronautical Establishment Lab Report LR-207, Sept. 1957.

Cullom, Richard R., Montgomery, John C., and Yasaki, Paul T., EXPERIMENTAL PERFORMANCE OF A 0.35 HUB-TIP RADIUS RATIO TRANSONIC AXIAL-FLOW-COMPRESSOR STAGE DESIGNED FOR 40 POUNDS PER SECOND PER UNIT FRONTAL AREA, NACA RM E58DO4a, Sept. 1958.

Montgomery, John C., and Yasaki, Paul T., DESIGN AND EXPERIMENTAL PERFORMANCE OF A 0.35 HUB-TIP RADIUS RATIO TRANSONIC AXIAL-FLOW-COMPRESSOR ROTOR DESIGNED FOR 40 POUNDS PER SECOND PER UNIT FRONTAL AREA, NACA RM E58D17, Sept. 1958.

Gregory, N., Raymer, W. G., and Love, Edna M., THE EFFECT OF FORWARD SPEED IN THE INLET FLOW DISTRIBUTION AND PERFORMANCE OF A LIFTING FAN INSTALLED IN A WING, Aeronautical Research Council R & M No. 3388, 1965.

Hoehne, Vernon O., and Wattson, Robert K., Jr., SHROUDED PROPELLER INVESTIGATIONS: WIND-TUNNEL TESTS OF A SHROUDED PROPELLER WITH A 17-BLADED ROTOR INLET AND EXIT STATORS, AND A LONG SHROUD WITH HIGH-SPEED INLET AND NO EXIT DIFFUSION, The University of Wichita Report Nos. 213-1, 2, 3, 4, 5, 6, 7, 9, and 10, June 1958.

Velazquez, J. L., ADVANCED ANTITORQUE CONCEPTS STUDY, Lockheed California Co., USAAMRDL Technical Report 71-44, Eustis Directorate, U.S. Army Air Mobility Research and Development Laboratory, Fort Eustis, Virginia, Aug. 1971.

V/STOL AIRCRAFT FANS, Hamilton Standard, Report No. PDB 6517.

GENERALIZED PERFORMANCE AND WEIGHT DATA FOR VARIABLE PITCH FANS, Hamilton Standard, Report No. PDB 6605, Jan. 25, 1966.

GENERALIZED METHOD OF SHROUDED PROPELLER PERFORMANCE ESTIMATION, Hamilton Standard, Report No. PDB 6220.

APPENDIX II  
PERFORMANCE PREDICTION METHODS

The symbols used in this appendix are given below along with definitions

A	Rotor disc area, sq ft
$C_{xe}$	Total equivalent blade profile coefficient
$C_{x0}$	Basic blade profile drag coefficient
$\Delta C_{xMN}$	Increment of blade drag due to compressibility
$\Delta C_{xs}$	Increment of blade profile drag due to stall effects
$\overline{C_L}$	Mean blade lift coefficient
$f_e$	Equivalent helicopter flat plate area based on disc area, sq ft
$K_1$	Rotor-induced flow correction factor
$l$	Moment arm length, ft
$K_p$	Profile power correction factor
$P_{AT}$	Antitorque power, hp
$P_i$	Induced power, hp
$P_{MR}$	Main rotor power, hp
$P_p$	Profile power, hp
$P_{PAR}$	Parasite power, hp
$P_T$	Total engine power required, hp
Q	Torque, ft-lb
$RN_{.7}$	Rotor blade Reynolds No. at 70% of blade radius
T	Rotor thrust required (includes download or interference when applicable) lb
$T_{AT}$	Antitorque thrust, lb

$T_M$	Tail rotor maneuver thrust, lb
$V$	Freestream velocity along the flight path, ft/sec
$V_T$	Rotor tip speed, ft/sec
$\mu$	Advance ratio, $v/V_T = V/\omega R$
$\rho$	Air Density, slugs/cu ft
$\sigma$	Rotor solidity
$\omega$	Rotor rotational speed, rad/sec

### ESTIMATION OF TOTAL POWER REQUIRED

The total power required for a helicopter is estimated as the sum of the main rotor power, antitorque power, and power due to mechanical losses. Main rotor power is composed of induced power, profile power, and parasite power,  $P_{MR} = P_i + P_p + P_{PAR}$

#### Main Rotor Induced Power

From simple momentum theory, the induced power in forward flight is:

$$P_i = (K_1 T/550) \left\{ 1/2(-V^2 + \sqrt{V^4 + (T/\rho A)^2}) \right\}^{1/2}$$

which in hover reduces to:

$$P_i = (K_1 T/550) \sqrt{T/2\rho A}$$

#### Main Rotor Profile Power

Rotor profile power, determined from blade element theory, is:

$$P_p = \rho A V_T^3 \sigma C_{x_e} / 4400$$

where the equivalent blade profile drag coefficient is:

$$C_{x_e} = C_{x_0} (1 + 4.65\mu^2) + 3/8\mu^4 + \Delta C_{x_{MN}} + \Delta C_{x_s}$$

The basic blade profile drag coefficient for an NACA 0012 airfoil section is:

$$C_{x_0} = K_p [0.00842 - (0.00022 \times RN_{.7} \times 10^{-6}) + \{0.0073 + (0.014/RN_{.7} \times 10^{-6})\} \overline{C_L}^2]$$

with the mean blade lift coefficient defined as:

$$\overline{C_L} = 6T/\rho AV_T^2 \sigma$$

Whenever conditions warrant, an increment in drag due to compressibility,  $\Delta C_{xMN}$ , is estimated as a function of the amount by which the drag-divergence Mach number is exceeded at the tip of the advancing blade. Retreating blade stall,  $\Delta C_{xs}$ , is accounted for as a function of the rotor blade angle of attack at 75% blade radius and 270° azimuth position in excess of the blade angle of attack for lift and moment divergence.

#### Parasite Power Including Fan/Fin Effects

The parasite power due to the parasite drag of the helicopter is:

$$P_{PAR} = \rho V^3 f_e / 1100$$

where  $f_e$  is the equivalent flat plate drag coefficient of the fuselage and its appendages. The helicopter drag component due to a fan-in-fin is the sum of the minimum drag of the fin, the fin-induced drag, and the fan-induced drag. The fin contribution is estimated from an equivalent fin similar in dimension to the fan/fin configuration. At a representative Reynolds number, the basic skin friction drag of this fin at zero angle of attack, adjusted for thickness-to-chord ratio, fuselage interference, and interference effects associated with a duct through it, is considered to be the drag of the fan/fin with the fan operating at zero thrust. The fin lift-induced drag is estimated from conventional wing theory as  $C_{Di} = C_L^2 / \pi AR$  where AR is an equivalent aerodynamic aspect ratio. The fan-induced drag is determined from empirical relationships obtained from the Fenestron wind tunnel tests. Any additional power required due to fan-induced effects is then computed.

#### Antitorque Power

The antitorque power is the power required to provide sufficient thrust to counteract the main rotor torque and any additional thrust required for maneuvers.

The main rotor torque determined from the main rotor power is:

$$Q = P_{MR}^{550/\omega_{MR}}$$

and the antitorque thrust is:

$$T_{AT} = (Q/\lambda) + T_M$$

where  $\lambda$  is the distance from the main rotor hub to the center of thrust of the antitorque device. Depending on the flight condition being evaluated, the maneuver thrust needed to achieve the MIL-H-8501A specified yaw requirements or to achieve sideward flight is computed. The sum of these thrusts makes up the total thrust required from the antitorque device. Any antitorque contribution from a fin is subtracted from that required. The remainder is supplied by the rotor. In the case of a conventional tail rotor, the thrust required is adjusted to include interference effects due to the proximity of a fin or tail boom. The antitorque power required is then computed from the previously described methods as  $P_{AT} = P_i + P_p$ . For a fan-in-fin, the fin contribution to the antitorque thrust is subtracted, establishing the required fan thrust, and the power required to obtain this thrust is estimated using test data.

#### Losses and Total Power Required

An evaluation is made of mechanical losses such as gear meshes and power takeoffs in the power transmission system. For preliminary design these losses are considered a percentage of the total power required. Summing the main rotor power and antitorque power and adding an increment for mechanical losses gives the total power required. Thus the power required in hover and in forward flight can be estimated for any weight, speed, altitude or temperature condition. This method has been checked against test data from other conventional helicopters and found to give good agreement. Although not a rigorous analytical procedure, this approach is an effective means of predicting overall performance.

#### MISSION PERFORMANCE CALCULATIONS

The estimated total power required is then matched with the power available at the main gearbox. Maximum speeds, hover ceilings, and rates of climb can then be obtained. Specific range is computed from the fuel consumption of the engine, and economic cruise speeds and loiter speeds are determined. Mission performance and payload vs. range is then computed, adjusting the empty weight for any weight differences due to a fan-in-fin. Thus the performance of a helicopter using either a conventional tail rotor or a fan-in-fin can be analyzed and the relative merits of the total systems established.

**APPENDIX III**  
**EXCERPTS FROM AEROSPATIALE NOISE TESTS**

The figures on the following pages are excerpted from Reference 14 and other unpublished French data to aid in the interpretation of the Fenestron noise data. These excerpts are presented without comment.

Figures 52 and 53 show the location of instrumentation elements during the noise testing of the SA 341-02 (Gazelle) and the SA 3180-03 (Alouette II) respectively. The directionality of the Fenestron noise is shown in Figure 54, while the nondirectional characteristics of the conventional tail rotor are shown in Figure 55. A perceived noise level comparison of the two types of antitorque devices as a function of distance is shown in Figure 56.

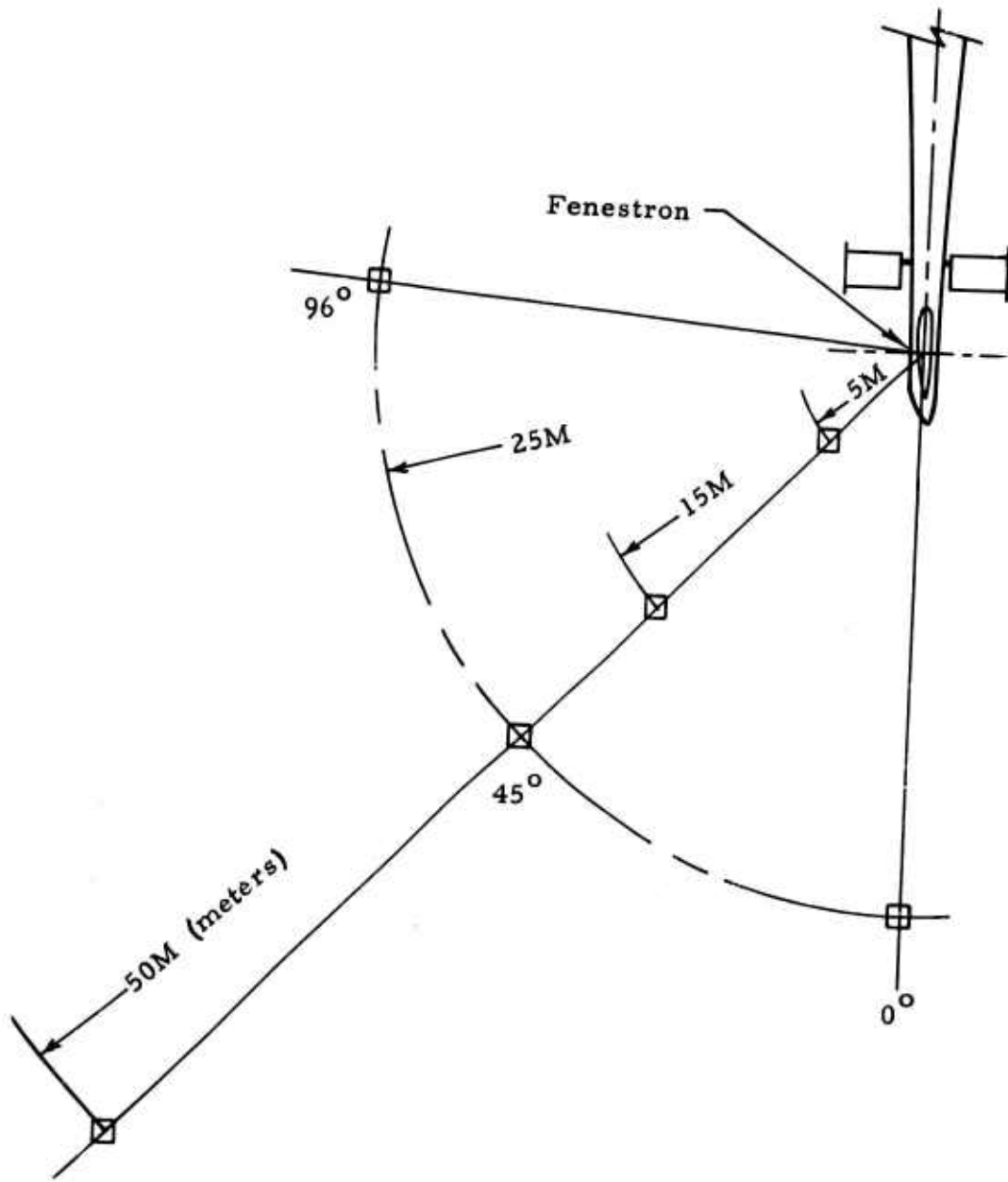


Figure 52. Location of Instrumentation; SA 341-02 (Gazelle).

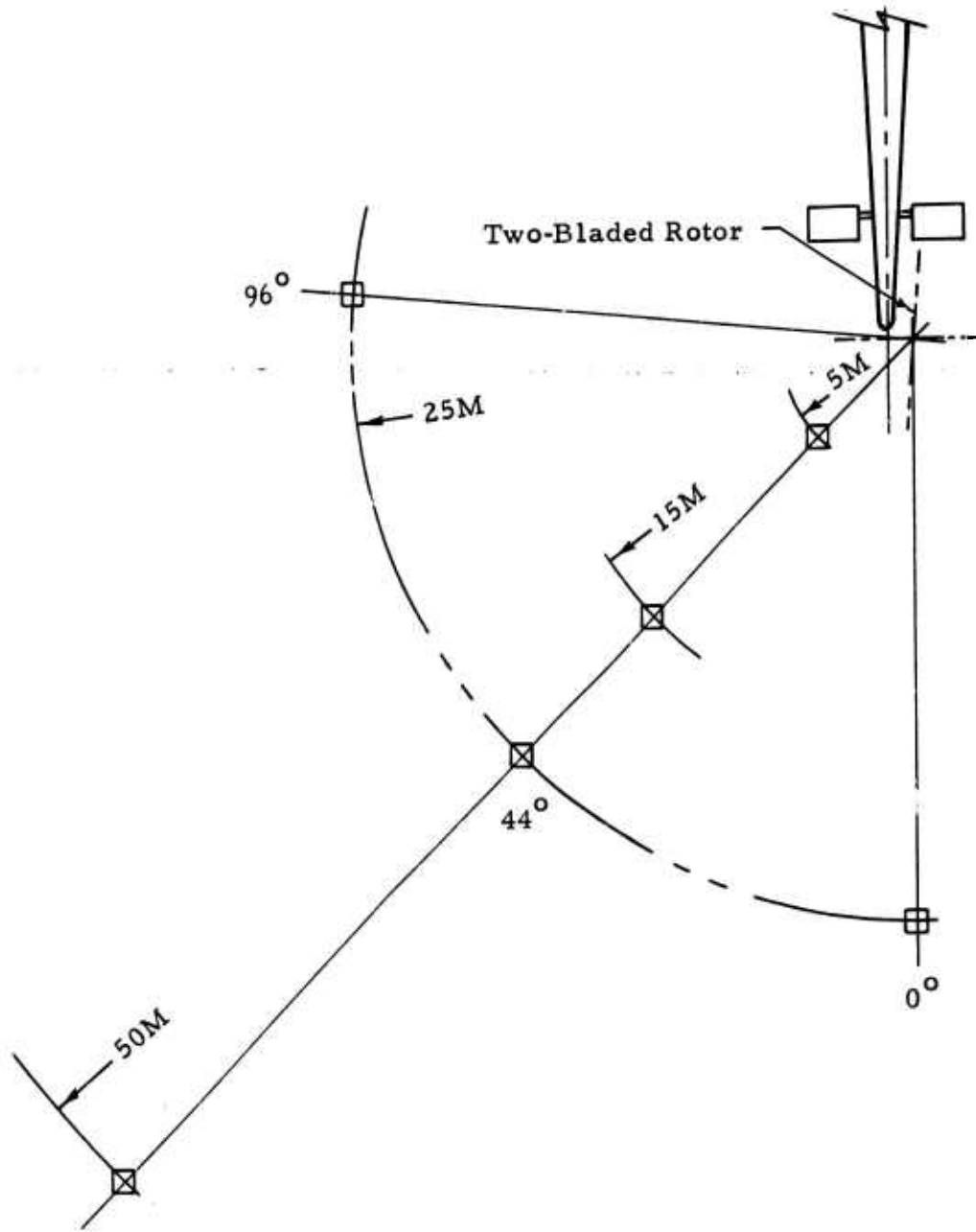


Figure 53. Location of Instrumentation; SA 3180-03 (Alouette II).

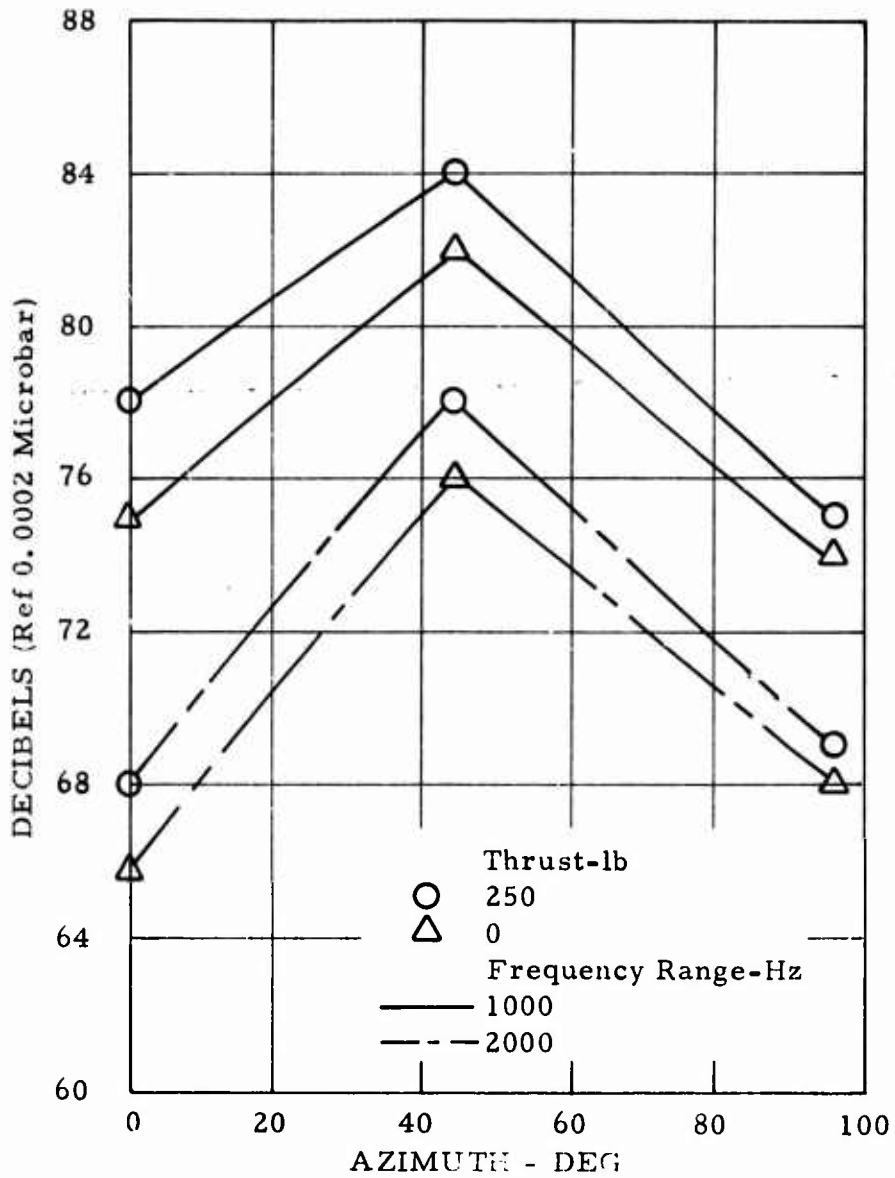


Figure 54. Directional Effects of the SA 341-02 Fenestron at 25M.

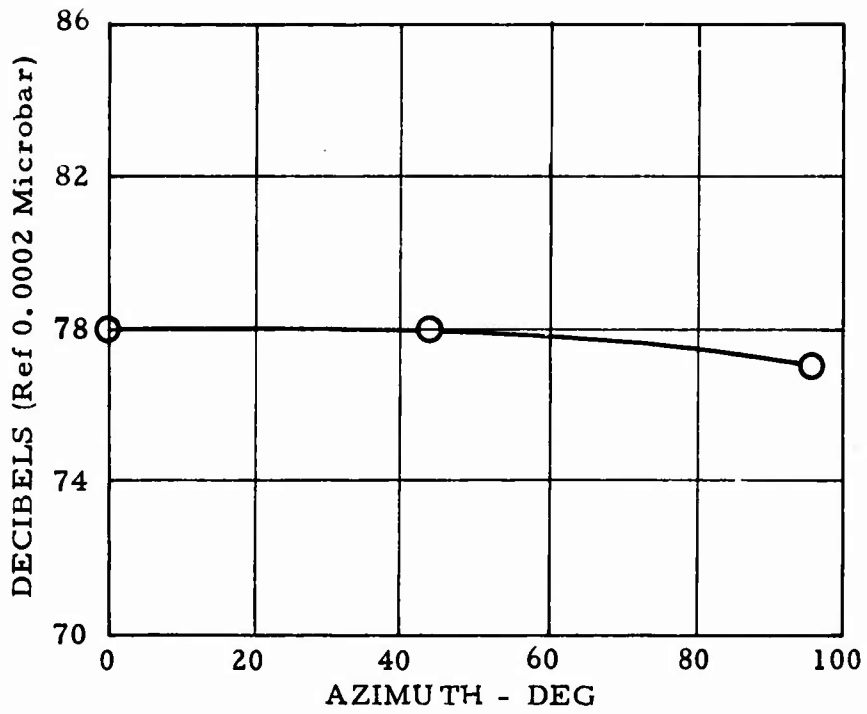


Figure 55. Directional Effects of the SA 3180-03 Two-Bladed Rotor at 25M With an Average Frequency of 63 Hz.

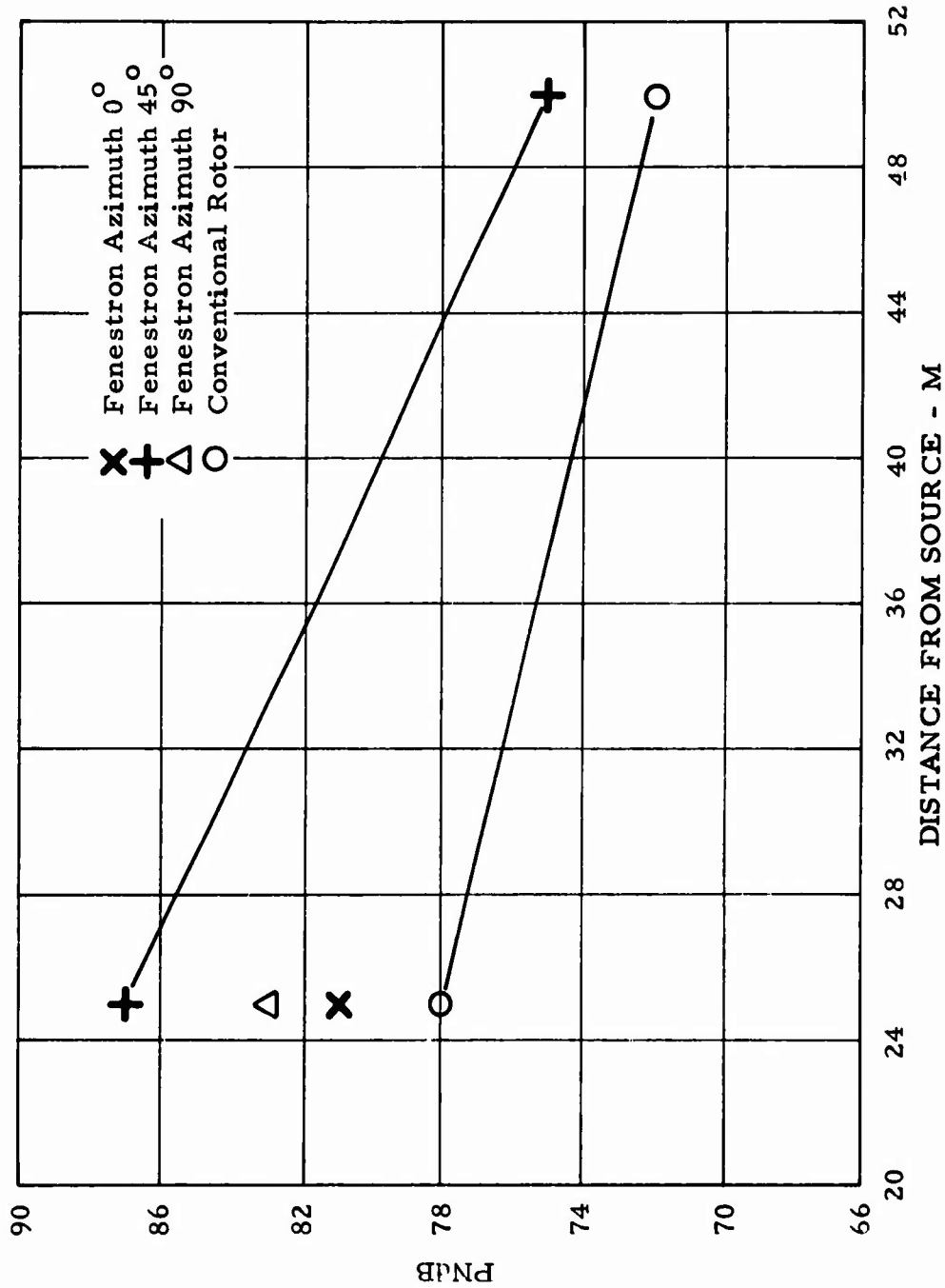


Figure 56. Comparison of Perceived Noise Levels Between the SA 341-02 (Gazelle) Fenestron and the SA 3180-03 (Alouette II) Two-Bladed Conventional Tail Rotor.